

9-2 FLUID FLOW IN REACTOR SYSTEMS

BY

Charles F. Bonilla

PRINCIPAL NOMENCLATURE

- A = wall area
 C = volume fraction of solids in a suspension [Eqs. (11) to (13)]
 c = specific heat, when c_p substantially = c_v
 C_C = coefficient of stream-area contraction
 C_D = orifice discharge coefficient
 c_p = specific heat at constant pressure
 c_v = specific heat at constant volume
 D = pipe diameter
 E = total energy per unit mass
 \mathbf{E} = pump efficiency
 e = wall roughness
 F = energy lost as friction
 \mathbf{F} = force
 f_F = Fanning friction factor
 G = mass velocity, w/S
 g = acceleration due to gravity
 g_c = dimensionless ratio F/ma for units employed
 h = enthalpy per unit mass
 i = internal energy per unit mass
 K = number of pipe average-velocity heads lost in a fitting
 m = mass; hydraulic radius
 L = length
 L_e = length of straight pipe having same friction loss as a fitting
 n = rotational speed of pump or blower, revolutions
 P = pressure
 \mathbf{P} = pump shaft power
 Q = rate of flow of volume [except heat absorbed from surroundings in Eqs. (17) and (58)]
 q = rate of heat flow
 R = pipe radius
 R' = gas constant
 S = cross-sectional area of coolant stream
 T = absolute temperature
 t = thermometric temperature
 u = velocity
 \bar{u} = average velocity in a channel
 \bar{u}_s = superficial velocity in a porous body, based on total cross section
 u^+ = dimensionless local velocity
 V = specific volume = $1/\rho$
 W = work done by surroundings
 w = rate of flow of mass
 x = fraction of vapor in vapor-liquid mixture

- y^+ = dimensionless wall distance
 z = elevation above horizontal datum plane
 α = ratio between actual kinetic energy of a stream and that at \bar{u}
 β = volumetric coefficient of thermal expansion
 δ = thickness of a boundary layer
 δ' = thickness of layer equivalent to wall slippage
 ϵ = eddy diffusivity [except Eq. (21)]
 η = coefficient of rigidity
 θ = time
 μ = viscosity
 ν = kinematic viscosity
 ρ = density
 τ = shear stress

All nuclear reactors are cooled by one or more fluids in motion. In order to maintain proper cooling and safe operation at high powers it is necessary that the coolant distribute itself appropriately throughout the core, shields, and blankets under all conditions. It is also desirable that the coolant circuit be designed to achieve optimum over-all economy. Accordingly, fluid-flow principles and design methods are very pertinent in reactor design.

1 VISCOSITY

Viscosity μ defines the capacity of a fluid to transmit shear stress through the relative motion of individual molecules or atoms. Under shear stress τ a velocity gradient du/dy will be obtained normal to the plane of the shear. These quantities are related by

$$\tau g_c = \mu(du/dy) \quad (1)$$

If μ is constant over a wide range of τ , the fluid is designated *Newtonian*. This includes all gases; most liquids, in particular all proposed reactor coolants except slurries and other two-phase mixtures; and solid particles. Equation (1) is valid only in the absence of turbulence, namely, for streamline (i.e., laminar or viscous) flow (see Art. 3).

The cgs unit of viscosity is the poise (grams per centimeter per second), which requires τ in Eq. (1) in dynes per square centimeter, du/dy in sec^{-1} , and g_c , as in all absolute systems, to equal unity. Viscosity in poises must be multiplied by 0.0672 to convert it to pounds per foot-second, by 242 for pounds per foot-hour, and by 0.00209 for slugs per foot-second. For other conversions see Table 17 of Sec. 1-3.

1.1 Viscosity of Gases

The viscosity of gases is independent of pressure at normal pressures (such as up to 10 per cent of the critical pressure) while above the critical temperature and is also independent of shear stress.

Values of viscosity are tabulated in Sec. 9-1. For higher temperatures and atmospheric pressure the following formulas are suitable. μ' is in micropoises and T in degrees centigrade + 273.1.

$$\text{Nitrogen:}^1 \quad \mu' = 14.05T^{3/2}/(T + 109.1) \quad (2)$$

$$\text{Air:}^1 \quad \mu' = 14.60T^{3/2}/(T + 109.6) \quad (3)$$

$$\text{Argon:}^{1,2} \quad \mu' = 19.07T^{3/2}/(T + 135.4) \quad (4)$$

$$\text{Carbon dioxide:}^1 \quad \mu' = 15.24T^{3/2}/(T + 219.4) \quad (5)$$

$$\text{Oxygen:}^1 \quad \mu' = 17.00T^{3/2}/(T + 126.8) \quad (6)$$

$$\text{Helium:}^1 \quad \mu' = 4.23T^{3/2}/(T^{0.326} - 0.409) \quad (7)$$

$$\text{H}_2\text{O (steam):}^2 \quad \mu' = 24.40T^{3/2}/(T + 1137) \quad (8)$$

$$\text{D}_2\text{O vapor:}^2 \quad \mu' = 25.13T^{3/2}/(T + 1142) \quad (9)$$

$$\text{Hydrogen:}^1 \quad \mu' = 6.42T^{3/2}/(T + 71.7) \quad (10)$$

The effect of pressure on μ will generally be negligible at practical reactor pressures. However, correction can be applied if desired.*⁵

The viscosity of a mixture of gases of similar molecular weight, such as oxygen and nitrogen, may be accurately obtained by interpolation by mole fraction between the viscosities of the pure components at the same temperature and pressure as the mixture. With other gases the viscosity of the mixture may range up to 25 per cent or more higher than the interpolated value and may roughly be estimated graphically³ or calculated by available formulas.⁴

1.2 Viscosity of Liquids

The viscosities of liquids are much higher than those of gases, as shown in Sec. 9-1, on account of their greater density and, thus, molecular interactions. Among the methods of interpolating or extrapolating to other temperatures, the following are most used: (1) A plot of μ versus t yields a smooth curve with a maximum deviation from a straight line of the order of 1 per cent per 20°C interval over useful ranges. Thus linear interpolation over short intervals is permissible. (2) A plot of fluidity $1/\mu$ versus t is closely linear over fairly long temperature intervals and thus suitable for reasonably long interpolations or extrapolations. (3) A plot of $\log \mu$ versus $1/T$ is straight over temperature ranges having a constant energy of activation E and is useful for interpolation or extrapolation with two or more known values of μ and T . If viscosity is known at only one temperature, it can be extrapolated by a line parallel to the $\log \mu$ versus $1/T$ plot for a similar compound.

The effect on liquid viscosities of pressures that are appropriate for nuclear reactors is generally negligible at the (low) temperatures employed.

1.3 Flow Properties of Suspensions

The properties of suspensions are of interest in nuclear engineering in view of the possibility of the use of finely divided fuel and/or fertile elements, alloys, and compounds suspended in a liquid. Dilute suspensions of solid particles tend to be Newtonian, following the Einstein equation:

$$\mu_s/\mu_m = 1 + 2.5C \quad (11)$$

up to a volume fraction C of solid of the order of 0.05. μ_s and μ_m are the viscosities of the suspension and medium, respectively. The coefficient 2.5 holds for any reasonably equiaxed shape and is constant or increases only slightly in going to the smallest sizes or the most irregular shapes.

A straight line through the origin on a plot of du/dy versus τ indicates Newtonian behavior [Eq. (1)], the slope of the line being the fluidity $1/\mu_s$. Suspensions with equiaxed particles that interfere more with each other the higher the shear rate show a downward concavity in Fig. 1 and are *dilatant*, or *inverted, plastics*. Long particles that line up more closely parallel with each other the higher the shear show the opposite curvature and are *pseudoplastic*; the shear diagram usually becomes straight at high shear. If the lining-up requires an appreciable amount of time or work, the substance is *thixotropic*. In Fig. 1 the line D represents a rapid increase in shear and G the infinitely slow or equilibrium increase or decrease. If the rate of shear is held constant after a rapid increase, the shear stress will gradually decrease along a line such as E , reaching F and finally G .

Solids and some concentrated suspensions require a definite yield shear stress τ_y before any motion occurs. These materials are not therefore fluids and are designated plastic substances. Many plastic suspensions approach an idealized straight-line behavior, that of the "Bingham body."

The ratio of the shear stress to the velocity gradient at any point on the shear curve of a substance is the *effective viscosity* μ'' at that point. For instance, the slope of

* Superscript numbers refer to References at end of subsection.

line A is $1/\mu''$ for point B. The reciprocal of the local slope at any point, such as B, is designated the rigidity η at that point.

Several equations are available for predicting the effective viscosity of suspensions at practical shear stresses. For volume concentrations up to the order of 25 per cent, reasonable agreement with equiaxed particles is obtained by retaining more terms in Einstein's derivation, as in Vand's equation:

$$\mu''_s/\mu_m = 1 + 2.5C + 7.17C^2 + 16.2C^3 \tag{12}$$

Orr has found substantially Newtonian behavior in suspensions of different types and sizes of particles with 10 to 20 per cent solids by volume. In streamline flow

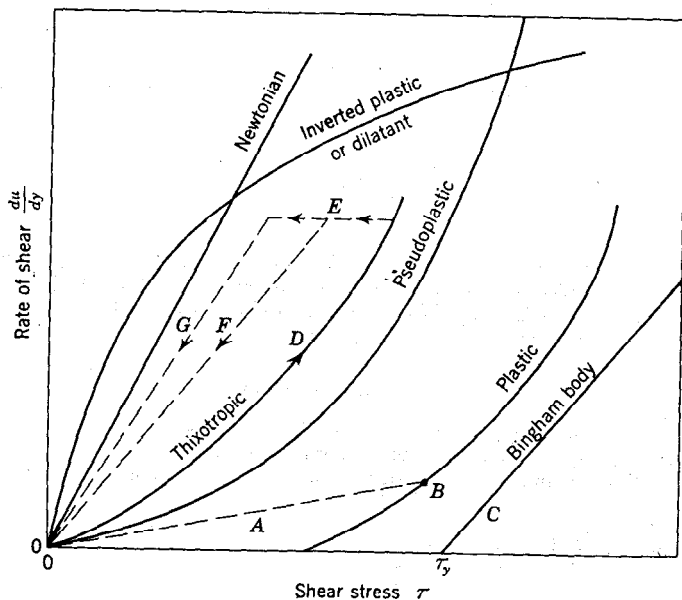


FIG. 1. Types of shear diagrams in streamline flow. (From C. F. Bonilla, Ref. 1.)

they roughly follow Eq. (13) up to the fraction of solids by volume, C_∞ , to which the particles settle in infinite time.

$$\mu''_s/\mu_m = [(1 - C)/C_\infty]^{-1.8} \tag{13}$$

Many other equations have been proposed for high concentrations, but it is not safe in general to rely on such relations without experimental confirmation at the identical conditions.

2 MATERIAL AND MECHANICAL BALANCES

2.1 Material or Mass Balances

Applying the law of conservation of mass to a flow process yields a material balance, or "continuity equation." The steady-state flow w in mass per unit time is the same through any surface S , completely cutting the stream. Standard methods of computation are

$$w = Q\bar{\rho} = \bar{u}\rho S = \bar{G}S = \sum_0^S (\bar{u}\rho \Delta S) = \int_0^S u\rho dS \tag{14}$$

The bars designate averages over S . The summation is commonly employed to evaluate w in a test when velocity and temperature vary irregularly over a large duct. The integral is useful for radially symmetrical flow in a pipe.

2.2 Pressure of Force Balances

Fluid pressure forces may be very large in high-pressure or large reactors. If z is the elevation above a datum surface at which the pressure is constant, the difference in pressure between elevations z_2 and z_1 in a static fluid (no friction or acceleration) is

$$P_2 - P_1 = \int_{z_2}^{z_1} \rho g dz / g_c = \bar{\rho} g (z_1 - z_2) / g_c \quad (15)$$

This expression is useful in computing free-convection driving pressures, nonisothermal manometer lead corrections, etc. Integrating completely around a closed circuit gives

$$\Delta P_B = \frac{g}{g_c} \left(\int_{z_2}^{z_1} \rho_a dz + \int_{z_1}^{z_2} \rho_b dz \right) = \frac{g}{g_c} \int_{z_2}^{z_1} (\rho_a - \rho_b) dz = \frac{g \rho_0 \bar{\beta}_0}{g_c} \int_{z_2}^{z_1} (t_b - t_a) dz \quad (16)$$

where a and b represent the two sides and $\bar{\beta}_0$ is the average value of the coefficient of thermal expansion over the temperature range, based on ρ_0 . With a stationary fluid the buoyant pressure $\Delta P_B = 0$. If the fluid is moving, ΔP_B equals the pressure spent in losses, plus acceleration if not in steady state.

2.3 Total Energy Balances

The law of conservation of energy is particularly useful in cases in which the velocity, expansion, and heat flow are all high, as in many optimized nuclear-reactor designs. Following unit mass of a stream in steady flow along a differential length of its path,

$$di + d \left(\frac{P}{\rho} \right) + \frac{g dz}{g_c} + \frac{\alpha d(\bar{u}^2)}{2g_c} = dh + \frac{g dz}{g_c} + \frac{\alpha d(\bar{u}^2)}{2g_c} = dQ + dW \quad (17)$$

All terms must be in the same units of energy per unit of mass. dQ is heat gained from the outside, and dW is work done on the fluid from the outside in addition to the "flow work" $d(P/\rho)$. α is a factor to obtain the average kinetic energy from the average velocity \bar{u} . Tables of i and h are available for many fluids, and generalized plots of h versus reduced temperature and pressure for gases. c_v and c_p are reasonably constant over a limited ΔT , except near the critical point, and $\Delta i = c_v \Delta T$ and $\Delta h = c_p \Delta T$. Equation (17) may be integrated between any two positions by merely replacing each differential by the finite increment.

2.4 Mechanical Energy Balances

Applying Newton's law $F = ma$ to a steady stream yields the mechanical energy balance, or Bernoulli's principle.²⁸ This relation is more convenient than the total energy balance when thermal effects are small and is necessary in evaluating the friction in a test, predicting coolant pressure drop in a reactor, etc. However, the relation between ρ and P must be known before it can be integrated. It may be written:

$$g dz / g_c + (dP) / \rho + \alpha d(\bar{u}^2) / 2g_c = dW - dF \quad (18)$$

dF is the energy lost as friction.

These energy balances simplify in many applications. For instance, in stationary fluid the last three terms are zero, and in horizontal flow $dz = 0$. If ρ is constant, the

integral of the second term is $\Delta P/\rho$, and if in addition the stream cross section is constant, $d(\bar{u}^2) = 0$. If ρ varies only moderately, it is usually sufficiently accurate to replace it by its average $\bar{\rho}$. $W = 0$ unless there is a pump or fluid motor in the system between the limits of integration.

For constant or moderately changing ρ or for isothermal gas flow Eq. (18) can be integrated analytically. For flow through a nozzle or orifice dF may be neglected and Eq. (18) integrated by obtaining the relation between P and ρ from Eq. (17) or the adiabatic expansion relation. For the general case in a reactor of heat generation and a considerably expanding fluid, it is convenient to proceed in succession over short sections of the channel such that ρ does not vary much. When the conditions at one end of a section are known, Eqs. (17) and (18) are solved simultaneously for P and ρ at the other end. This is continued over the whole channel. If stated conditions at the second end of the channel are not matched, the process is repeated with a different flow or different assumed first end conditions. Some 10 to 20 increments usually yield an accuracy comparable to that of the friction calculation. The method is evidently also applicable to adiabatic flow on setting $\Delta Q = 0$ and to isentropic flow on setting $\Delta F = 0$.

2.5 Momentum Balances

Applying Newton's law over an interval of time $\Delta\theta$ yields the equality between impulse and momentum change, $F\Delta\theta = m\Delta u$, where F is the net or resultant force and Δu is the vectorial change in velocity. Dividing by $\Delta\theta$ for a steady flow process

$$Fg_c = \Delta u(m/\Delta\theta) = \Delta u(dm/d\theta) = w\Delta u \quad (19)$$

In certain problems requiring the calculation of a force or pressure due to a change in direction or magnitude of the velocity of a stream, the momentum balance is more convenient than an energy balance. Equations (18) and (19) both hold for any steady flow process. Some cases exhibit an apparent discrepancy between the two methods, but this is the result of an incorrect application.

3 STREAMLINE FLOW

3.1 Isothermal Streamline Flow

3.11 Isothermal Newtonian Streamline Flow in Ducts of Regular and Constant Cross Section. Streamline flow in symmetrical channels, such that the relation between the shear stress and the distance y from the wall is known, may be analyzed directly by Eq. (1). The principal results are given under streamline flow in Table 1. To illustrate the use of the table, for the average velocity in circular pipe

$$\frac{\bar{u}\mu L}{\Delta P g_c} = \frac{R^2}{8}$$

or

$$\Delta P = \frac{8\bar{u}\mu L}{R^2 g_c} \quad (20)$$

The relations for mean momentum and mean kinetic energy of the streams per unit time are used in unsteady-state or start-up and coast-down calculations.

In short channels with a smooth inlet nozzle, extra pressure drop is required near the inlet to convert the uniform velocity so obtained to the parabolic velocity distribution characteristic of laminar flow. This is given for pipes and wide flat channels in Table 2.

3.12 Streamline Flow in Irregular Channels. For channels of irregular cross section (i.e. triangular) such that the spatial distribution of τ is not known, numerical methods of computation are available.¹ Certain cases are already in the literature.⁵ For a narrow annulus with an eccentricity, or distance between the two axes, of ϵ , an approximate flow equation is obtained by taking the annular width as $(R_2 - R_1 + \epsilon \cos \theta)$, substituting into the relation for flow in a parallel wall channel, and inte-

Table 1. Flow at Constant Density in Long Horizontal Channels*

	f_F	Circular pipe, radius = R	Concentric annulus, radii = R_1, R_2			Wide flat channel, spacing = b	Square channel, side = b
Streamline flow:							
Average velocity, $\frac{\bar{u}L}{\Delta P g_c}$		$\frac{R^2}{8}$	$\frac{1}{8} \left(R_2^2 + R_1^2 - \frac{R_2^2 - R_1^2}{\ln R_2/R_1} \right)$			$\frac{b^2}{12}$	$\frac{b^2}{28.6}$
Local velocity, $\frac{u\mu L}{\Delta P g_c}$		$\frac{R^2 - r^2}{4}$	$\frac{1}{4} \left(R_1^2 - r^2 + \frac{R_2^2 - R_1^2}{\ln R_2/R_1} \ln \frac{r}{R_1} \right)$			$\frac{yb - y^2}{2}$	See Ref. 1
			R_2/R_1				
		(∞)	(3)	(2)	(1.2)	(1)	
Maximum velocity, $\frac{u_{max}}{\bar{u}}$		2	1.5180	1.5077	1.5019	1.500	2.07
γ		1.333	1.207	1.204	~ 1.2	1.200	1.36
α		2	1.568	1.552	~ 1.543	1.543	2.22
Turbulent flow:							
Maximum velocity, $\frac{u_{max}}{\bar{u}}$	0.01	1.286					
	0.005	1.202					
	0.0025	1.143					
γ	0.01	1.055			~ 1.035	1.035	1.078
	0.005	1.030			~ 1.018	1.018	1.038
	0.0025	1.017			~ 1.010	1.010	1.02
α	0.01	1.135				1.229	
	0.005	1.073				1.055	
	0.0025	1.040				1.022	

Momentum per unit time = kinetic energy per unit length
 Momentum per unit time at \bar{u} = kinetic energy per unit length at \bar{u} = γ
 Momentum per unit length = 1 Kinetic energy per unit time = α
 Momentum per unit length at \bar{u} = 1 Kinetic energy per unit time at \bar{u} = α

* SOURCE: C. F. Bonilla, "Nuclear Engineering," Ref. 1.

Table 2. Excess Streamline Pressure Drop in Short Tubes and Wide Slots Due to Uniform Inlet Velocity*

(To be added to pressure drop by Table 1 to obtain total pressure drop from start of tube or slot. Does not include pressure drop across the nozzle.)

Pipe diameters or slot widths downstream of nozzle outlet	Excess velocity pressures $\Delta P_{ex}/(\rho \bar{u}^2/2g_c)$	
	Pipe	Slot
0 Re	0	0
0.000125 Re	0.14	0.104
0.00025 Re	0.20	0.148
0.0005 Re	0.288	0.208
0.0010 Re	0.396	0.290
0.0015 Re	0.464	0.339
0.0020 Re	0.522	0.370
0.0025 Re	0.570	0.39
0.0050 Re	0.74	0.448
0.010 Re	0.99	0.522
0.015 Re	1.14	0.560
0.030 Re	1.32	0.601
0.040 Re	1.37	0.601
> 0.060 Re	1.41	0.601
Total ΔP in long channel (parabolic velocity distribution, first line, Table 1):		
Each 1.0 Re	64.00	48.00

* SOURCE: C. F. Bonilla, "Nuclear Engineering," Ref. 1.

grating around the semicircle. If $R_2/R_1 < 1.5$, the formula obtained

$$\bar{u} = (g_c/12\mu)(dP/dL)[(R_2 - R_1)^2 + \frac{1}{2}\epsilon^2] \quad (21)$$

is correct to 1 per cent or better.

For a flat wide channel of nonparallel walls and constant cross section, integrating across the channel from b_1 to b_2 gives

$$\bar{u} = (g_c/24\mu)(dP/dL)(b_1^2 + b_2^2) \quad (22)$$

Wall roughness generally has negligible effect in streamline flow. It has been shown⁶ that the minimum height e of roughness necessary to disturb the flow is $(4D\mu/\bar{u}\rho)^{1/2}$ in a pipe or $(9b\mu/2\bar{u}\rho)^{1/2}$ in a wide channel with parallel walls a distance b apart.

Two-dimensional plane flow problems, such as coolant distribution through narrow channels between thermal shields (neglecting thermal buoyancy and inertia effects), can be attacked by several methods.

For streamline flow the same general methods of solution are available as for heat conduction. Analytical solution by complex variable⁷ or numerical solution by actual and fictitious sources and sinks⁸ is rigorous for the assumed conditions.

For many cases an adequate and quick solution is obtainable by trial-and-error drawing of the "flow net." A system of curved streamlines between source and sink estimated to divide up the flow equally is first drawn. A second system of curved isobars is then sketched in, of which the source is the first, so as to be perpendicular to the assumed streamlines at every intersection and so spaced as to form curvilinear squares with the streamlines. When these conditions of perpendicularity and squareness can be maintained and the last isobar fits the sink or is parallel to it, the correct flow net has been obtained. For flow between parallel planes the total pressure drop is then¹ equal to $12s\mu Q/pgcb^3$, where Q is the total volumetric flow, b the spacing of the planes, and s and p the number of squares in series and parallel, respectively. For a porous slab the quantity $12\mu/gcb^2$ is replaced by $(dP/dL)/\pi\bar{u}$, where dP/dL is the pressure gradient caused by average or "superficial" velocity \bar{u} .

Electrical analogues are also readily applicable to streamline flow problems. A continuous conductor or semiconductor may be used having the same shape as the flow field, or a set of discrete "nodes" covering the field (usually in a square lattice) and connected with adjacent nodes by appropriate resistors.¹ Flow is conveniently measured as electrical current, and pressure difference as voltage difference.

3.2 Nonisothermal Streamline Flow

If the viscosity at the wall of a pipe μ_w is higher than that at the average temperature of the stream $\bar{\mu}$, as in cooling a liquid or heating a gas, the pressure gradient $-dP/dL$ will be higher than that computed for isothermal flow at the average stream temperature t_b and vice versa. Theoretical calculation of the correction is difficult, but empirically it is found satisfactory⁹ to divide the isothermal pressure drop by $(\mu_b/\mu_w)^{0.23}$ when cooling the stream and by $(\mu_b/\mu_w)^{0.32}$ when heating, or by $1.1(\mu_b/\mu_w)^{0.28}$ for either case, though with less accuracy.

Another method is to employ the isothermal formula with the viscosity at a temperature t' intermediate between t_b and the wall temperature t_w . For oils

$$t' = 0.25t_w + 0.75t_b$$

is used. For gases $t' = 0.58t_w + 0.42t_b$ has been recommended,⁹ and for liquid metals $t' = 0.54t_w + 0.46t_b$.

4 TURBULENT FLOW IN DUCTS

4.1 Dimensionless Ratios

All fundamental laws are dimensionally consistent. Thus all derived laws must also be, whether obtained theoretically or empirically. For maximum compactness

and generality, the variables involved in any phenomenon are best grouped into the simplest and fewest possible dimensionless ratios. This is particularly true of turbulent flow, the knowledge of which is mainly empirical. The most used dimensionless ratios in fluid and heat flow are listed in Table 3.

Table 3. Common Dimensionless Ratios*

Name	Symbol	Definitions
Reynolds No.	Re	$D_e \bar{u} \rho / \mu$
Fanning† friction factor	f_F	$\Delta P f_F g_c D_e / 2 L \rho \bar{u}^2$
von Karman No.	Ka	$\Delta P f_F g_c D_e^3 \rho / L \mu^2 = \text{Re}^2 2f_F$
Diameters.		L/D
Relative roughness.		e/D
Mach No.†.	M	u/c
Drag coefficient.	C_d	$2 \Delta P f_F g_c / \rho u^2$
Nusselt No.‡.	Nu	$hD/k, hL/k$
Prandtl No.	Pr	$c_p \mu / k$
Stanton No.§.	St	$h/cG = \text{Nu}/(\text{Re Pr})$
Graetz No.	Gz	wc/kL
Grashoff No.	Gr	$(D^3 \rho^2 g) / \mu^2 (\beta \Delta t)$
Peclet No.	Pe	$DGc/k = \text{Re Pr}$
Fourier No.	Fo	$k\theta/c\rho L^2, \alpha\theta/L^2$
j factor.	j_H	$\text{St Pr}^{3/4}$

* Source: C. F. Bonilla, "Nuclear Engineering," Ref. 1.

† The Weisbach friction factor, also widely used, is $4f_F$.

‡ The symbol c here represents velocity of sound rather than specific heat.

§ The symbol h here represents the heat-transfer coefficient rather than enthalpy.

4.2 Turbulent Flow Friction

Many turbulent pressure-drop results have been accumulated for widely different fluids and conditions, including wetting and nonwetting liquid metals. For any one pipe, results plotted as f_F versus Re invariably lie in a narrow band. With rougher pipes f_F is higher and levels off sooner, as shown in Fig. 2. The roughness e in the parameter in Fig. 2 is the diameter of sand particles glued to cover uniformly the inner wall of the pipe. Commercial pipe must be tested for pressure drop to evaluate the equivalent e . Recommended values¹⁰ of equivalent e are as follows: drawn tubing 0.000,005 ft, commercial steel pipe 0.00015 ft, galvanized iron 0.0005 ft, cast iron 0.00085 ft, and riveted pipe 0.003 to 0.03 ft.

Figure 2 is based¹⁰ on the Colebrook relation for the transition and turbulent regions:

$$1/\sqrt{f_F} = -4 \log_{10} \left(\frac{e}{3.7D} + \frac{1.255}{\text{Re} \sqrt{f_F}} \right) \quad (23)$$

Setting $e = 0$, this agrees with Prandtl's original equation for hydraulically smooth pipes:

$$1/\sqrt{f_F} = 4 \log_{10} (\text{Re} \sqrt{f_F}) - 0.4 \quad (24)$$

For full turbulence, setting $\text{Re} = \infty$ in Eq. (23):

$$f_F = \left(2.28 - 4 \log \frac{e}{D} \right)^{-2} \quad (25)$$

Most nuclear-reactor channels will have smooth walls. The following relations are equivalent to but more convenient than Eq. (24):

$$\text{Whole turbulent range: } f_F = 0.00140 + 0.125(\text{Re})^{-0.32} \quad (26)$$

$$5,000 < \text{Re} < 200,000: f_F = 0.046(\text{Re})^{-0.20} \quad (27)$$

The walls are usually rougher in other industrial applications. The curve so labeled in Fig. 2 is typical of commercial operation.

By whatever method f_F is obtained, friction pressure gradient is then computed, as in Table 3, by

$$\frac{dP_F}{dL} = \rho \frac{dV}{dL} = \frac{2f_F \bar{u}^2 \rho}{g_c D} = \frac{2f_F \bar{G}^2}{g_c D \rho} = \frac{2f_F w^2}{g_c D \rho S^2} \tag{28}$$

In substantially equiaxed cross sections and in rectangular cross sections or concentric annuli in which the turbulence in the main stream would extend almost

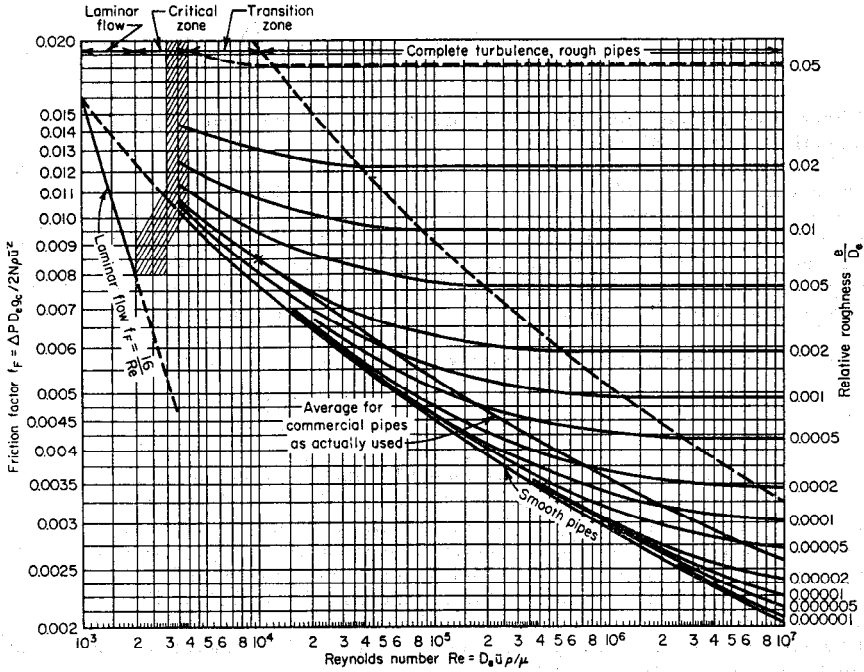


FIG. 2. Fluid friction in pipes. (From C. F. Bonilla, Ref. 1.)

equally over the cross section, the pressure gradient for a given fluid and average velocity will be substantially the same as for a circle having the same ratio of (cross section)/(wetted perimeter), or hydraulic radius m . Since a circle has

$$m = \pi D^2 / 4\pi D = D/4$$

the equivalent diameter D_e for any section to use Fig. 2 is $4m$. D_e equals the side of a square section, the difference in outer and inner diameters for an annulus, and twice the spacing b for a wide duct with parallel walls. For a concentric annulus, however, if the inner diameter is less than some two-thirds of the outer diameter, the pressure drop starts to exceed that given by the usual hydraulic radius.¹¹ When

$$D_e = 2R_2 - \frac{R_2^2 - R_1^2}{R_2 \ln (R_2/R_1)}$$

is used, agreement with Fig. 2 is obtained. For flow parallel to uniform tube and rod bundles, Fig. 2 is some 40 per cent low.

4.21 Nonisothermal Turbulent Flow. Isothermal flow and small temperature gradients are minimized in nuclear power plants, as they represent unproductive

weight, space, cost, and pumping power. Thus highly nonisothermal flow is important for gases in pipes. Figure 2 holds¹² if μ and ρ are used at $t' = (t_b + t_w)/2$ or¹³ μ at $t' = 0.4t_b + 0.6t_w$ and ρ at t_b . For liquids⁵ μ and ρ may be taken at t_b and the computed pressure drop divided by $1.02(\mu_b/\mu_w)^{0.13}$. In high-speed flow¹⁴ the pipe walls will heat up by an additional amount $\gamma' \bar{u}^2/2g_c c_p J$ because of frictional heat. J is the mechanical equivalent of heat, and γ' , the "recovery factor," approximately equals $Pr^{1/2}$.

4.22 Turbulent Flow of Compressible Fluids. In isothermal or substantially isothermal flow of gases, Eqs. (18) and (28) can be combined to eliminate dF and integrated analytically. Setting dW and $dz = 0$,

$$P_1^2 - P_2^2 = \frac{2R'G^2}{g_c} \left(\alpha \bar{T} \ln \frac{\rho_1}{\rho_2} + \frac{2\bar{f}_F \bar{T} L}{D_e} \right) \quad (29)$$

Either unknown pressure is usually obtainable on the second trial by substituting for ρ_1/ρ_2 the first trial value of P_1/P_2 .

Equation (29) is also applicable in spite of large temperature variation provided the friction term considerably exceeds the expansion term. In this case the average of $f_F T$ over L is employed. Normally μ and therefore Re do not vary with P and only with about the three-fourth power of T . By Eq. (27) f will thus vary only as the one-seventh power of T , approximately, and may be taken, for simplicity, as constant at an average value \bar{f} . \bar{T} then is averaged over L , and thus is the midplane temperature for a nuclear reactor with symmetrical heat generation and a coolant of constant specific heat.

Multiplying through by V before integrating yields, for any fluid,

$$P_1 - P_2 = \frac{G^2}{g_c} \left[(V_2 - V_1)\alpha + \frac{\bar{f}_F L(V_2 + V_1)}{D_e} \right] \quad (30)$$

The quantity $2g(z_2 - z_1)/(V_2 + V_1)g_c$ should be added outside the brackets if appreciable. This relation is usually sufficiently accurate if $2 > (V_2/V_1) > 0.5$ and is particularly useful in an integration by finite increments of channel length. Special methods are available for adiabatic flow.⁵ Equations (29) and (30) apply to streamline flow as well as turbulent if f does not vary too much to permit the use of \bar{f} .

4.23 Velocity Distribution and Eddy Diffusivity in Turbulent Streams. The velocity distribution that is obtained in turbulent flow in pipes and flat channels has been correlated in various ways¹ in terms of the dimensionless local velocity u^+ and distance from the wall y^+ , where

$$u^+ = u \left(\frac{\rho}{\tau_w g_c} \right)^{1/2} \quad y^+ = \frac{y}{\mu} (\tau_w \rho g_c)^{1/2} \quad (31)$$

τ_w is $(D/4)(dP/dL)$ in a pipe and $(b/2)(dP/dL)$ in a flat channel. Von Karman's velocity distribution is given by

$$0 < y^+ < 5 \quad u^+ = y^+ \quad (32)$$

$$5 < y^+ < 30 \quad u^+ = -3.05 + 5.0 \ln y^+ \quad (33)$$

$$30 < y^+ \quad u^+ = 5.5 + 2.5 \ln y^+ \quad (34)$$

Equation (34) is normally used all the way to the axis or midplane. However, there it yields a definite velocity gradient instead of zero. Accordingly Eq. (34) is at times¹⁵ only used halfway to the axis, from which point u^+ is continued constant to the axis.

One application of Eqs. (32) to (34) is in the calculation of mean and maximum stream velocity in turbulent flow, also mean momentum and kinetic energy. Values are listed in Table 1.

Another important application is in the prediction of heat- and mass-transfer coefficients, temperature distributions, etc., in channels of the shapes to which they apply and for conditions not so far investigated experimentally. For this purpose the

eddy diffusivity of shear force ϵ_F is computed for each region from Eqs. (32) to (34) by means of

$$\epsilon_F = \frac{\tau_w g_c}{\rho} \left(1 - \frac{y}{R}\right) \quad (35)$$

ϵ_F is then taken as equal to the eddy diffusivity* of heat ϵ_H or the eddy diffusivity of mass ϵ_M and employed in the equations

$$\frac{q}{A} = (k + \rho c_p \epsilon_H) \frac{dt}{dy} \quad (36)$$

$$N_M = (D_V + \epsilon_M) \frac{dC}{dy} \quad (37)$$

When these are integrated over the radius or thickness of the channel, the desired local and average temperature or concentration relations are obtained.

4.24 Wall Boundary Layers. At the inlet of channels, leading edges of strips, etc., "boundary layers" of slowed-down fluid begin to form. They progressively thicken, finally for long channels becoming the steady velocity distribution of Eqs. (32) to (34). If the thickness δ of the boundary layer is less than the available space, boundary-layer relations rather than long-channel relations will apply in the calculation of wall shear forces. These are as follows:

Laminar boundary layer (for $Lu\rho/\mu < \text{about } 400,000$):

$$\frac{\delta}{L} = 5 \left(\frac{Lu\rho}{\mu}\right)^{-1/2} \quad (38)$$

$$(\tau_w)_L = 0.332 \frac{\rho u^2}{g_c} \left(\frac{Lu\rho}{\mu}\right)^{-1/2} \quad (39)$$

$$(\bar{\tau}_w)_{0 \text{ to } L} = 0.664 \frac{\rho u^2}{g_c} \left(\frac{Lu\rho}{\mu}\right)^{-1/2} \quad (40)$$

Turbulent boundary layer (for $Lu\rho/\mu > \text{about } 400,000$):

$$\frac{\delta}{L} = 0.377 \left(\frac{Lu\rho}{\mu}\right)^{-1/5} \quad (41)$$

$$(\tau_w)_L = 0.0295 \frac{\rho u^2}{g_c} \left(\frac{Lu\rho}{\mu}\right)^{-1/5} \quad (42)$$

$$(\bar{\tau}_w)_{0 \text{ to } L} = 0.0369 \frac{\rho u^2}{g_c} \left(\frac{Lu\rho}{\mu}\right)^{-1/5} \quad (43)$$

u is the relative velocity of the wall and the approaching stream. At high velocity or with simultaneous heat transfer, ρ and μ may be evaluated¹⁶ at $0.75t_w + 0.25t_b$.

4.25 Initiation of Turbulence in Channels. From visual observation of threads of dye solution in pipes¹⁷ turbulence seems to occur first at the axis and at $Re = 900$, though with a smooth trumpet-shaped inlet much higher flow may remain streamline. An over-all phenomenon such as friction pressure drop (Fig. 2) generally first shows in long pipes observable departure from streamline flow at about $Re = 2,100$. In the "critical region," approximately $2,100 < Re < 3,500$ if flow rate is given or $70,000 < Ka < 270,000$ if pressure drop is given, flow is irregular, specially in short pipes. It is generally desirable to avoid this region in nuclear reactors and heat exchangers, since pulsing may develop in which flow alternates between streamline and turbulent, the velocity of the stream controlling the period of the pulses. Such flow irregularities would cause undesirable temperature and thermal-stress cycling. In other cross sections, such as annuli and square or flat ducts, turbulence initiates less abruptly and a pulsing is less likely to be encountered.

* This is inaccurate for Prandtl numbers much smaller than unity, namely, for liquid metals.

4.3 Pressure Losses in Fittings

Pressure and energy losses in fittings cannot be reliably predicted, since fittings are not highly reproducible, differ widely among different brands, and affect one another unless widely separated. However, approximate rules have been developed to estimate the losses for rough design purposes.

In turbulent flow, the irregularities in most fittings are analogous to large values of e in Fig. 2, and the friction loss is thus generally proportional to \bar{u}^2 . A convenient measure is the number K of pipe average-velocity heads or pressures lost in the fitting. Another convenient unit is the length of straight pipe expressed in pipe internal diameters L_e/D having the same friction loss as the fitting.

These quantities are related by $K = 4f_F(L_e/D)$. An average value of $f_F = 0.0055$ may be used to compute L_e/D approximately from K instead of the actual f_F in the pipe. The friction computed from Table 4 is added to that for the same actual total distance as if it were straight pipe. Screwed and flanged fittings give similar K values. The computed drop in pressure is in addition to any drop or rise by Bernoulli's principle.

When the discharge coefficient C_D is provided, the pressure drop can be calculated by Eq. (60). Losses at an expansion may be estimated by

$$K_{exp} = 1 - 2\gamma_1 A_1/A_2 + (A_1/A_2)^2(2\gamma_2 - 1)$$

where γ_1 and γ_2 are the momentum ratios from Table 1, based on f_F for the upstream and downstream pipes, respectively. At a contraction,

$$K_{con} = (1/C_c) - 2 + C_c(2\gamma_2 - 1)$$

where C_c is the coefficient of stream-area contraction.* In streamline flow these calculated values may average 19 per cent high, and in turbulent flow 11 per cent high.¹⁸ K_{exp} and K_{con} are used in Eq. (60) with the smaller area.

When many fittings are near one another, as frequently occurs in reactor designs, the pressure drop may be up to several times that calculated by Table 4, which is for isolated fittings.

4.4 Optimum Size of Pipes

To compute the optimum pipe or channel to conduct a given stream it is necessary to reduce all the factors involved to a common unit, preferably net cost per unit of total time, and determine the size at which the total cost is a minimum. Ideally, every cost item should include all advantages and disadvantages, such as space, weight, availability, probability of unexpected troubles, etc., in terms of money as well as the actual money cost.

The total annual fixed charge per unit length for pipe and fittings, completely installed, is generally approximately proportional to D^2 , or, say, equal to XD^2 dollars/(year)(ft). The total annual fixed charge on the fluid in the pipes is generally negligible, relatively. However, for D_2O , an expensive liquid metal, or a fuel solution, it may be important, say equal to YD^2 dollars/(year)(ft).

The total annual net cost of the required pumping energy is inversely proportional to a high power of D , say equal to ZD^{-n} dollars/(year)(ft). The exponent

$$n = 5 + d(\log f)/d(\log Re)$$

from Fig. 2, ranging from 4 for streamline flow to 5 for full turbulence (likely in many nuclear-power-reactor applications).

The optimum diameter from the standpoint of these costs is obtained by adding

* C_c = minimum cross section of the jet downstream of the orifice or slot, divided by the cross section of the orifice or slot.

Table 4. Friction in Typical Pipe Fittings, etc. *

Fitting	$K†$	L_e/D	C_D	Convergence ratio, D_2/D_1 or b_2/b_1	$C_c + C_D$
Turbulent Flow‡					
One average-velocity head.....	1	45 (pipe)			
Pipe fittings:					
Elbow, 45° standard.....	0.35	15			
Elbow, 45° long radius.....	0.2	10			
Elbow, 90° standard.....	0.82	35			
Elbow, 90° long radius.....	0.53	25			
Elbow, 90° square.....	1.3	60			
Return bend, 180° close.....	2.0	90			
Return bend, 180° medium.....	1.2	55			
Tee, 0° through.....	0.4	20			
Tee, 90° side outlet.....	1.3	60			
Tee, 90° side inlet.....	1.5	70			
Coupling, union, 0° through.....	0.04	2			
Valves:					
Valve, open, 0° gate.....	0.16	7			
Valve, open, 0° globe.....	6	270			
Valve, open, 90° angle.....	3	135			
Valve, open, 0° swing check.....	2	90			
Pipe bends:					
Bend, 90°; $r/D = 0.5$	0.8	35			
Bend, 90°; $r/D = 1$	0.35	16			
Bend, 90°; $r/D = 4$	0.16	7			
Bend, 90°; $r/D = 10$	0.16	7			
Coil, each turn, 360°; $r/D = 1$	2.2	100			
Coil, each turn, 360°; $r/D = 4$	0.55	25			
Coil, each turn, 360°; $r/D = 10$	0.3	14			
Contraction and expansion:					
Sudden contraction, $D_1/D_2 = 1.33$	0.19	9			
Sudden contraction, $D_1/D_2 = 2$	0.33	15			
Sudden contraction, $D_1/D_2 = 4$	0.42	19			
Sudden expansion, $D_2/D_1 = 1.33$	0.19	9			
Sudden expansion, $D_2/D_1 = 2$	0.56	25			
Sudden expansion, $D_2/D_1 = 4$	0.92	42			
Gradual conical expansion in pipe.....	0.2-0.5				
Gradual conical convergence in pipe.....	0.06-0.15				
Gradual conical converging inlet.....	0.13-0.4		0.35-0.94		
Orifices and nozzles:¶					
Small square-edged orifice.....	0.05	2	0.60		
Rounded nozzle.....	0.05	2	0.98		
Excess in tube below nozzle.....	0.02	1			
Short tube downstream of plate ($L < 3D$).....	0.05	2	0.60		
Long tube downstream of plate ($L > 3D$).....	0.5	23	0.82		
Short tube upstream of plate ($L < 3D$).....	0.06	3	0.53		
Long tube upstream of plate ($L > 3D$).....	0.8	35	0.72		
Streamline Flow					
Conical or straight slot convergence (135°)				0	0.746
				0.4	0.749
				0.8	0.789
				1.0	1.0
Sharp-edged orifice or slot (90°)				0	0.611
				0.4	0.631
				0.8	0.722
				1.0	1.0

* SOURCE: C. F. Bonilla, "Nuclear Engineering," Ref. 1.

† Where there is a change in cross section, K applies to the velocity in the smaller cross section.

‡ For additional data see particularly M. P. O'Brien and G. H. Hickox, "Applied Fluid Mechanics," p. 350, McGraw-Hill Book Company, Inc., New York, 1937.

¶ K does not include downstream losses, which can be calculated as for an expansion.

them and differentiating with respect to D . Thus is obtained

$$D_{opt} = \left[\frac{nZ}{2(X+Y)} \right]^{1/(n+2)} = 1.12 \left(\frac{Z}{X+Y} \right)_{\text{(streamline)}}^{1/6} = 1.12 \left(\frac{Z}{X+Y} \right)_{\text{(turbulent)}}^{1/4} \quad (44)$$

Since X , Y , and Z normally vary somewhat with D , after a preliminary calculation of D_{opt} they should be recomputed from the data for the problem and a second approximation of D_{opt} computed. D may be changed somewhat (roughly ± 25 per cent) from D_{opt} without making a large change in total annual cost, since at D_{opt} the rate of change of fixed costs with increasing D is exactly equal and opposite to the rate of change of operating costs with D .

4.5 Flow in Complex Circuits

Complex circuits and networks in steady-state flow in reactors can be solved by principles analogous to Kirchhoff's laws for electrical circuits. Thus, the net flow to any location is zero, and the pressure change when integrated around any closed path is zero. With streamline flow at known temperatures, the simultaneous equations are all linear in mass-flow rate w , and enough can be written to solve any network directly. In the more common case of turbulent flow, the net-flow equations are linear in w but the pressure-drop equations are not. Thus in the general case simultaneous solution is not possible, though trial and error may be satisfactory.

Alternatively, and particularly where the direction of all flows is evident, the concept of summation of series resistances and parallel conductances is useful for computing total effective resistance of a network. From Eq. (20) in streamline flow, the resistance $\Delta P/w$ of a pipe is $(128/\pi g_c)(\bar{v}L/F^4)$. The equivalent resistance of series pipes is

$$\left(\frac{\Delta P}{w} \right)_s = \frac{128}{\pi g_c} \sum \left(\frac{\bar{v}L}{D^4} \right) \quad (45)$$

The equivalent resistance of parallel pipes is

$$\left(\frac{\Delta P}{w} \right)_p = \frac{128}{\pi g_c} \frac{1}{\sum \left(\frac{D^4}{\bar{v}L} \right)} \quad (46)$$

For turbulent flow a "turbulent resistance" $\Delta P/w^2$ is convenient. From Eq. (28) for pipes in series

$$\left(\frac{\Delta P}{w^2} \right)_s = \frac{32}{\pi^2 g_c} \sum \left(\frac{f_F L}{\rho D^5} \right) \quad (47)$$

For pipes in parallel

$$\left(\frac{\Delta P}{w^2} \right)_p = \left[\sum \left(\frac{w^2}{\Delta P} \right)^{1/2} \right]^{-2} = \frac{32}{\pi^2 g_c} \left[\sum \left(\frac{\rho D^5}{f_F L} \right)^{1/2} \right]^{-2} \quad (48)$$

Similar procedures can be used with other channels.

4.6 Liquid Flow with Thermal Buoyancy

Letting subscripts 1 and 2 refer to the inlet and the outlet, respectively, Eqs. (15) and (28) yield for a vertical channel with symmetrical heat generation

$$P_1 - P_2 - \frac{\rho_1 g(z_2 - z_1)}{g_c} = \frac{2f_F w^2 L}{\rho S^2 g_c D_e} - \frac{\rho_1 g \bar{\beta}_1 q(z_2 - z_1)}{2w c g_c} \quad (49)$$

This relation is useful for computing any one variable for a channel provided all others are known.

For parallel channels, the left-hand side is constant for all the tubes; therefore the right-hand side also is. The ratio of the buoyancy and the friction terms on the right side is

$$\frac{\rho^2 \beta g (t_2 - t_1) D_e}{4 f_F G^2} = \frac{Gr}{Ka} \quad (50)$$

where the Grashoff number Gr includes the temperature rise $t_2 - t_1$, not the usual wall-to-fluid Δt . If $Gr/Ka \ll 1$, buoyancy is minor and Eq. (20) or (28) yields the flow in any particular channel regardless of variations in heat generation among the tubes. If $Gr/Ka \gg 1$, friction is minor and the flow adjusts itself in each channel so that the outlet temperature t_2 is the same throughout, provided flow is upward.

Downward flow should be avoided, at least unless Gr/Ka always $\ll 1$. The reason for this is that instability may develop under certain conditions, so that a slight decrease in flow increases the buoyancy opposing the flow, thus decreasing the flow further until it stops and reverses. During the reversal burnout may occur. Differentiating Eq. (49) with respect to w and equating $d(P_1 - P_2)/dw$ to zero, the following critical flow w_c is obtained for downflow

$$w_c = \left[\frac{\rho^2 S^2 \beta g D_e q \Delta z}{8 f_{FC} L} \right]^{1/3} = \left[\frac{\bar{\beta}_1 g (t_2 - t_1) D_e \Delta z}{8 f_F L} \right]^{1/2} \rho S \quad (51)$$

Higher flow rates are stable, and lower flow rates unstable. One evident cause of instability is cutting back the flow in a reactor under low load or during shutdown to maintain the coolant temperatures constant and minimize thermal stresses. At low enough load w_c would be reached.¹

4.7 Unsteady-state Flow

The calculation of unsteady-state fluid flow is of importance in evaluating temperatures and stresses in rapid start-up, load change, or scram of a nuclear reactor. Initial maintenance of the flow by the momentum of the stream and by any flywheel effects, and subsequently by thermal buoyancy, is also important or necessary in the event of sudden power or pump failure in order to prevent fuel-element burnout by the delayed heat generation. This characteristic is the "flow coast-down" curve.

The calculation can be carried out by equating the pressure drops around the flow loop that oppose the flow to those which maintain the flow. Friction pressure drop during velocity changes is given adequately by Eq. (28). The momentum of a stream per unit length may be shown by Table 1 to equal w/g_c , as at uniform velocity. Thus the total forward pressure generated at any instant by acceleration or deceleration in a loop is $-(dw/g_c d\theta) \Sigma(L/S)$. Calling ΔP_P the pressure generated by the pump in the direction of flow, ΔP_B that of thermal buoyancy in the direction of flow [the last term of Eq. (49)], and ΣR_F the total of energy losses in the loop in the form $\Sigma(\Delta P_F/w^2)$, the time required to change from w_1 to w_2 is

$$\theta_2 - \theta_1 = \frac{1}{g_c} \left[\Sigma \left(\frac{L}{S} \right) \right] \int_{w_2}^{w_1} \frac{dw}{w^2 \Sigma R_F - \Delta P_B - \Delta P_P} \quad (52)$$

which may be integrated graphically. If most of the flow resistance is localized in one size of pipe (thus at the same Re) and $\Delta P_P = 0$, Eq. (52) can be generalized by replacing w by $(\mu S/D_e) Re$:

$$\frac{L_e \mu}{LD_e^2 \rho} \Delta \theta = \frac{1}{2} \int_{Re_2}^{Re_1} \frac{dRe}{f_F Re^2 - E/Re} \quad (53)$$

where $E = \rho^2 \beta g D_e^4 \Delta z q / 2CS\mu^3 L_e$. Equation (53) has been evaluated graphically for smooth pipes and is given in Fig. 3 from $Re_1 = 10^7$ to lower Re values for several values of E .

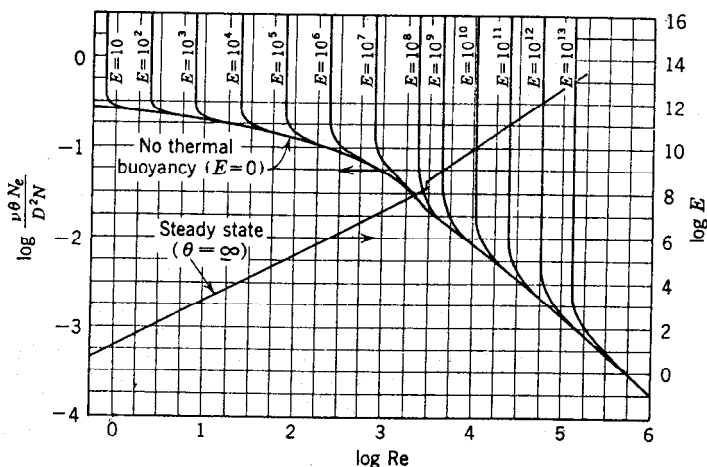


FIG. 3. Generalized solution for steady- and unsteady-state natural convection flow in a pipe loop with thermal buoyancy. (From C. F. Bonilla, Ref. 1.)

5 FLOW OF SLURRIES (BINGHAM BODIES)

Slurries may be useful in nuclear power on account of poor solubility of a fuel or fertile element in an otherwise desirable fluid medium, provided settling out does not occur or can be controlled. They may also offer processing advantages over a solution or a stationary solid.

Direct experimental determination of the flow-characteristic curve (Fig. 1) of a non-Newtonian fluid can in general be carried out only in a pipe and with streamline flow. A complete curve is obtainable from a series of tests at different flows. For each flow test, the volumetric flow Q , pressure gradient dP/dL , and radius R are known. The wall shear stress τ_w is $(R/2)(dP/dL)$. The wall velocity gradient can be computed from the slope of the curve of Q versus τ_w by the Rabinowitsch-Mooney equation:¹⁹

$$(du/dy)_w = [3Q + \tau_w(dQ/d\tau_w)]/\pi R^3 \quad (54)$$

Each pair of values of τ_w and $(du/dy)_w$ is a point on Fig. 1.

Most slurries when dilute are Newtonian (see Art. 1.3) and when concentrated are Bingham bodies (Fig. 1). For the former case Table 1 applies. For the latter, in streamline flow:¹

Pipes:

$$\bar{u} = \tau_w g_c \left\{ \frac{D}{8\eta} \left[1 - \frac{4}{3} \frac{\tau_y}{\tau_w} + \frac{1}{3} \left(\frac{\tau_y}{\tau_w} \right)^4 \right] + \frac{\delta'}{\mu} \right\} \quad \tau_w = \frac{D}{4} \frac{dP}{dL} \quad (55)$$

Flat ducts:

$$\bar{u} = \tau_w g_c \left\{ \frac{b}{6\eta} \left[1 - \frac{3}{2} \frac{\tau_y}{\tau_w} + \frac{1}{2} \left(\frac{\tau_y}{\tau_w} \right)^3 \right] + \frac{\delta'}{\mu} \right\} \quad \tau_w = \frac{b}{2} \frac{dP}{dL} \quad (56)$$

In the turbulent flow of suspensions Fig. 2 holds, using for μ the effective viscosity at infinite shear (i.e., the rigidity for Bingham bodies). For Newtonian suspensions ρ of the slurry and μ of the pure medium give the best agreement with Fig. 2.

6 FLOW OF VAPOR-LIQUID MIXTURES

6.1 Friction Pressure Gradient

Knowledge of the friction pressure gradient for vapor-liquid mixtures is useful in designing wet vapor-flow lines but is particularly valuable in predicting the effect of

intentional or unintentional boiling on flow distribution among parallel channels in a reactor.

In general, high gas- or vapor-flow rates tend to carry a coexistent liquid phase along as slugs in a small pipe or as a film on the wall of a large pipe, whereas high liquid rates tend to carry the gas or vapor as bubbles. When both rates are low, fluids in a horizontal pipe tend to stratify.

The friction pressure gradient near atmospheric pressure in such varied flows correlates with an average deviation of some 25 per cent²⁰ against the friction pressure gradients of the two phases flowing separately, each at its own flow rate. To find the two-phase friction pressure drop ΔP_{2P} , Re is first calculated for each fluid separately. For Re under 1,000 flow is assumed streamline and over 2,000 turbulent. ΔP is then computed from Fig. 2 for each fluid alone, and Table 5 entered with the ratio $\Delta P_L/\Delta P_G$ at the proper column. The corresponding $\Delta P_{2P}/\Delta P_L$ is read off or interpolated and multiplied by ΔP_L to give ΔP_{2P} . The fraction by volume of liquid and of gas also correlate reasonably well. That for the liquid R_L is listed in the table; that for the gas is $1 - R_L$. The columns headed P_c are for liquid and vapor at the critical pressure. For intermediate pressures $\log(\Delta P_{2P}/\Delta P_L)$ may be interpolated linearly with P . The column headed "down" is for downward flow of boiling water in a $\frac{1}{8}$ -in. annulus, and the columns headed "up" for upward flow in a 1-in. tube.

An alternative method of predicting the friction pressure drop employs Fig. 2 and considers the two-phase mixture as a single fluid. Specific volume and fluidity are assumed additive on a mass-flow rate basis. A straight-line plot of $1/\mu$ versus fraction vapor x does not change rapidly with pressure above the boiling point. The former method is more accurate, but the latter more convenient for repeated calculations.¹

In wall or "local" boiling of subcooled liquid coolant the pressure gradient exceeds that for nonboiling at the same heat and coolant flows. However, the expansion and therefore pressure gradient are less than for "bulk boiling" at the saturation temperature. In a $\frac{3}{8}$ -in.-ID pipe the local to nonboiling pressure gradient ratio for water at 30 to 85 psig²⁴ is

$$\cosh [(4.6 \times 10^{-6}q/A + 1.2)L/L_t] = \cosh (aL/L_t) \quad (57)$$

where q/A is in Btu per hour per square foot, L is the distance downstream from the incidence of local boiling, and L_t is the total length that would be required in local boiling before the liquid reaches the boiling point. Integrating over the local boiling length ΔP_{lb} , the total pressure drop at constant q/A is obtained as the nonboiling pressure gradient multiplied by $(L_t/a)(\sinh aL/L_t)$. The average density of local-boiling water has also been studied for evaluation as a moderator.²⁵ Local-boiling results cannot as yet be extrapolated safely beyond test conditions.

6.2 Pressure Drop in a Bulk-boiling Tube

Article 6.1 yielded the pressure gradient at any point in a boiling tube. The gradient must be integrated along the tube to obtain the total ΔP_F . Since many quantities vary irregularly a step-wise calculation is usually best. The "equivalent-fluid" method of Art. 6.1 will be outlined. The R_L values of Table 5 generally indicate a higher vapor than liquid velocity, or "slip flow." However, the equal velocity or "fog flow" assumption is simpler, and results agree well with experimental data.

Going downstream over an increment of length from m to n with $dW = 0$, Eq. (17) may be written

$$E_n = E_m + \Delta Q_{m/n} = \frac{z_n g}{g_c} + h_n + \frac{G^2 \alpha}{2g_c} V_n^2 = \frac{z_n g}{g_c} + h'_n + x_n h''_n + \frac{G^2 \alpha}{2g_c} (V'_n + x_n V''_n)^2 \quad (58)$$

where h' and V' are the enthalpy and specific volume of the saturated liquid and h'' and V'' are the increases on complete evaporation. It is desirable that $G^2 \alpha \Delta(V^2)/2g_c$

Table 5. Friction Pressure Gradient Correlation for Flow of Liquid-Gas Mixtures*†

log $\frac{\Delta P_L}{\Delta P_g}$	log $(\Delta P_{TP}/\Delta P_L)$							Volume fraction liquid R_L		
	Liquid and gas turbulent				Liquid viscous, gas turbulent	Liquid turbulent, gas viscous	Liquid and gas viscous	Up	P_a	P_c
	Up	Down	P_c	P_a						
-4.0			4.000	4.214	4.158	4.098	4.042			0.005
-3.5			3.505	3.762	3.705	3.624	3.556			0.010
-3.0			3.012	3.340	3.249	3.167	3.084	0.010		0.019
-2.5			2.526	2.930	2.800	2.732	2.630	0.019	0.03	0.036
-2.0			2.052	2.534	2.364	2.323	2.087	0.034	0.05	0.067
-1.5			1.598	2.172	1.978	1.954	1.774	0.06	0.08	0.12
-1.0		2.042	1.180	1.832	1.635	1.616	1.404	0.11	0.12	0.21
-0.5	1.790	1.727	0.817	1.519	1.328	1.321	1.086	0.17	0.17	0.34
0.0	1.389	1.473	0.527	1.246	1.083	1.083	0.833	0.30	0.23	0.50
0.5	1.050	1.267	0.317	1.027	0.879	0.879	0.663	0.45	0.30	0.66
1.0	0.771	1.088	0.181	0.831	0.696	0.723	0.537	0.60	0.37	0.79
1.5	0.567	0.925	0.099	0.651	0.534	0.580	0.440	0.81	0.45	0.88
2.0			0.0529	0.486	0.403	0.440	0.352	0.91	0.53	0.93
2.5			0.0279	0.366	0.311	0.338	0.281		0.63	0.96
3.0			0.0146	0.262	0.227	0.236	0.219		0.72	0.98
3.5			0.0076	0.169	0.159	0.159	0.159		0.81	0.99
4.0			0.0040	0.091	0.091	0.091	0.091		0.90	0.995

* R. W. Lockhart and R. C. Martinelli, *Chem. Eng. Progr.*, **45**: 39 (1949); R. C. Martinelli and D. B. Nelson, *Trans. ASME*, **70**: 695 (1948); R. P. Stein, et al., *Chem. Eng. Progr. Symposium Ser.*, **50**: 11 (1954); W. H. McAdams, "Heat Transmission," 3d ed., McGraw-Hill Book Company, Inc., New York, 1954.

† Values are for pressures near atmospheric and horizontal flow unless marked otherwise.

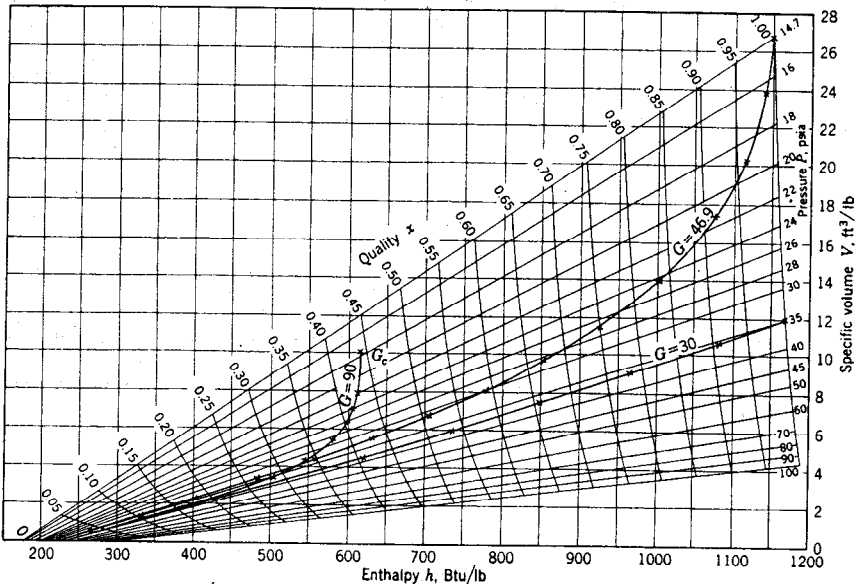


FIG. 4. Thermodynamic properties of wet steam. (From C. F. Bonilla, Ref. 1.)

be small compared with the total energy per unit mass E . Thus smaller length increments are preferable near the outlet. One increment may be adequate for the nonboiling portion.

A chart of h versus V for the two-phase region (Fig. 4) is drawn by joining the points for each saturated phase at a given P with straight lines. These isobars are then subdivided into equal fractions of their lengths, and curves of constant x drawn. The following procedure is used:

1. E_n is evaluated as $(E_m + \Delta Q_{m/n})$.
2. V_n is estimated (somewhat $> V_m$).
3. h_n is calculated by Eq. (58) and x_n read from the chart.
4. $\bar{R}c_{m/n}$ is computed as $D_c G \{ (1/\mu)' + \bar{x}_{m/n} (1/\mu)'' \}$, where ' and '' are defined as above and $\bar{x}_{m/n}$ is the average of x_n and x_m .
5. f_F is read from Fig. 2.
6. P_n is calculated by Eq. 29.
7. The chart is consulted to see if the estimated V_n and computed h_n and P_n agree. If not, a new V_n is estimated and steps 2 through 8 repeated.
8. The next increment is started.

It is evident that f_F will not change rapidly, so that Re and f_F will not ordinarily need to be determined for every increment. The three curved lines in Fig. 4 are condition curves for different flows through a given heated tube.¹ Integrated solutions not requiring the finite increment calculations are available for the special case of $\Delta P_F \ll P$ and Q linear in tube length.²¹

If Table 5 is employed to yield friction pressure gradient, the procedure is the same, except that use of this table replaces steps 4, 5, and 6.

6.3 Maximum Velocities of Compressible Fluids

A compressible fluid in a pipe can nowhere exceed the mass velocity G_c at which all the energy obtained from a differential pressure drop is used up in the corresponding increase in kinetic energy of the stream. At a point at which G_c is reached, the expansion is isentropic, as it will take place so rapidly that heat transfer and friction may be neglected. On further expansion the velocity would rise even more, which is not possible in a pipe of constant cross section; thus G_c is reached, if at all, at the outlet of the pipe.

The maximum mass velocity G_c for a boiling fluid can be shown¹ to be given by the relation

$$G_c = \rho g_c \left(\frac{dP}{d\rho} \right)_s^{1/2} = -g_c \left(\frac{dP}{dV} \right)_s^{1/2} \quad (59)$$

which is the same as for sonic velocity in a homogeneous compressible fluid. Table 6 is a skeleton table of G_c and E (kinetic energy plus enthalpy) as a function of exit quality and pressure, as computed by finite increments from steam tables. If in a downstream step-wise calculation at a given P_i , G_c and h_i with unknown P_o , as per Art. 6.2, G_c for the local values of P and x is reached before the pipe outlet, too low a P_i was employed.* The calculation should be repeated starting from the downstream end at the necessary P_o to yield $G_c =$ the desired G_c . If there is a constriction in the pipe upstream of the outlet, the local maximum velocity may be reached there as well as or instead of in the outlet.

Complete equilibrium between the two phases is usually not attained, particularly when x is small and the pipe size large. For instance, experience indicates that 221 lb/(ft²)(sec) (3.7 fps) of boiling water at atmospheric pressure with a trace of steam can be readily exceeded in a pipe. Preliminary results show that in $1/4$ - to 1-in. pipes²⁶ the ratio of observed to theoretical G_c for fog flow is roughly $2/(x + 1)$, though rising much higher for x under 2 per cent. For a $1/8$ -in. annulus the ratio is similar at low x but falls rapidly to about 1.1 at $x = 0.1$. Nevertheless, reasonable agreement between calculated and observed values of P_i is obtained by the above theoretical methods.

* The subscripts i and o indicate inlet and outlet respectively.

Table 6. Maximum Mass Velocity G_c in Feet per Second and Energy E in Btu per Pound above 32°F for Fog Flow of Saturated Steam-Water Mixtures

Quality, x , vapor fraction	Pressure, psia					
	14.7		50		200	
	G_c	E	G_c	E	G_c	E
0.995	53.8	1186.6	177.0	1214.4	680.9	1242.1
0.75	61.4	938.2	201.2	976.1	761.3	1021.8
0.50	73.7	684.7	240.7	733.2	918.2	799.1
0.25	98.9	431.4	317.5	490.3	1151.0	575.3
0.10	136.9	279.8	430.7	345.4	1522.6	442.6
0.005	221.0	184.9	609.1	254.7	2153.3	359.7

For all practical purposes, data for H₂O are valid also for D₂O pressure-drop calculations, except for the 10 per cent higher density.

7 FLOW-DISTRIBUTION CONTROL

7.1 Protection with Orifice against Burnout

A heated tube with a fixed outlet pressure and liquid coolant in its boiling range has a P_i versus w^2 characteristic as in Fig. 5. If the full inlet header pressure, say P_R , is available at the tube inlet, a flow of w_R would result. However, if there is an initial fixed orifice or nozzle, a flow-regulating valve, a length of pipe, a temporary accidental obstruction, or merely pressure loss at the inlet of the pipe, P_i will be less than P_R . In this case, P_i to the heated tube when computed from the inlet header will be given by a substantially straight line of negative slope, such as P_{RF} , which yields a flow of w_M . Operation at R or M will be stable, since if w should drop momentarily for external or statistical reasons, a net accelerating ΔP becomes available, and if it should rise, a net decelerating ΔP is produced, restricting the change in flow and returning the flow to the original value when the cause of the flow change disappears. However, S and S' are metastable (unstable) operating points. A positive value of $d(\Sigma\Delta P)/dw$ at the intersection indicates stability, and a negative value instability.

Permanent inlet resistances have a constant or almost constant ratio $\Delta P/w^2$, which may be called their turbulent resistance R :

$$\frac{\Delta P}{w^2} = R = \frac{1}{2g_c \rho_i C_D^2 S_0^2} = \frac{2f_R L_c}{g_c \rho_i D_e S^2} = \frac{K}{2g_c \rho_i S^2} \quad (60)$$

(orifices,
nozzles)
(pipes,
etc.)
(Table
4)

where S is the smaller area involved. The slope of any one of the inlet pressure lines, such as P_{RF} , is $-\Sigma R$ summed up for all the inlet resistances that are in series.

Figure 5 shows possible design situations:

1. If w_R is rated flow and no inlet resistance is employed ($P_i = P_R$), the tangent from P_R to the curve shows that an added inlet obstruction of resistance \overline{RG}/w_R^2 is possible before start of boiling.

2. If an inlet pressure P_Q is employed, a nozzle of resistance $(P_Q - P_R)/w_R^2$ is needed to cut the normal flow to w_R . Drawing the new tangent, an obstruction of up to \overline{RV}/w_R^2 can now be tolerated before instability appears.

3. In cases 1 and 2, if boiling starts, flow will drop to much less than w_R and will not recover to w_R if the obstruction disappears unless the power is decreased sufficiently to stop the boiling. To permit recovery to w_R without necessity of power decrease,

the tangent from *R* to *H* is drawn, yielding P_J as the necessary P_i ; and $(P_J - P_R)/w_R^2$ as the nozzle resistance.

4. If it is desired to be able to obtain stable flow at all possible flow rates by setting a valve at the channel inlet, as in an experimental setup, the inlet pressure must exceed P_E , the intercept given by the highest tangent to the curve.

In the design of protective nozzles, the accidental restriction R_i to be protected against should first be decided on, from the estimated probability, extent, and duration of the possible accidental restrictions; the fixed and pumping charges of the protective nozzles; required reliability and other characteristics of operation; hazards and

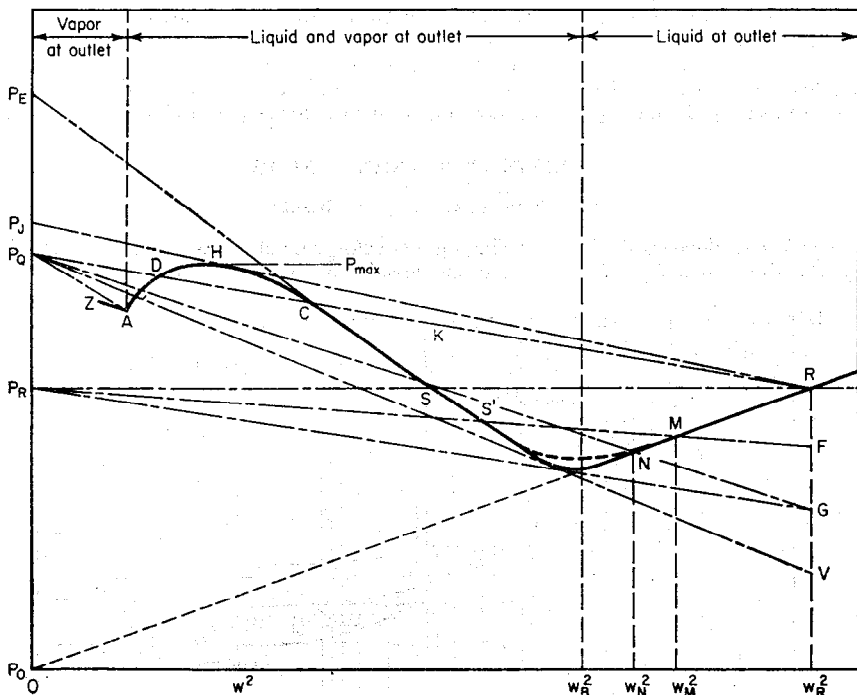


FIG. 5. Pressure drop in a tube with heat generation, and its protection with an inlet series nozzle. Outlet header constant at P_0 . (From C. F. Bonilla, Ref. 1.)

expenses of a burnout; etc. The lowest desired flow in the tube, say w_m , must also be selected. The corresponding inlet pressure is P_m . The necessary inlet manifold pressure may be shown to be

$$P_i = \left(R_i + \frac{P_m}{w_m^2} - \frac{P_R}{w_R^2} \right) / \left(\frac{1}{w_m^2} - \frac{1}{w_R^2} \right) \tag{61}$$

In actual practice, the inlet header pressure is commonly selected merely by adding an arbitrary reasonable excess above some minimum pressure, for instance 100 per cent of $(P_R - P_0)$ above P_R or 30 per cent of $(P_{max} - P_0)$ above P_{max} have been used, the inlet nozzle and piping dissipating the excess ΔP above P_R .

Upward flow in parallel tubes with boiling is inherently stable. However, in this case inlet nozzles are likely to decrease the stable range and would then be undesirable.¹ Protective nozzles and other resistances may also be located downstream of the heated channels, which considerably alters the flow curve after boiling has started. This arrangement must be calculated in detail but in general has the

advantage that boiling will not start until a lower flow is reached, due to the higher static pressure in the heated section. Once boiling has started, however, the pressure drop will rise faster. This arrangement may thus be preferable over a limited range. The use of a common nozzle for protection of several channels in parallel is impractical, since the necessary excess pressure for the same degree of protection increases rapidly with the number of channels.¹

7.2 Use of Nozzles for Flow-distribution Control

Optimum design in a reactor for power generation will normally require the coolant to issue at the same temperature from all channels or at otherwise related temperatures throughout the reactor. Thus the flow through the main lower power channels must be decreased by using smaller channels, separate pumps and inlet headers, or series nozzles. Whether or not protective nozzles are used in the high power channels, nozzles are usually the most practical flow control for the lower power channels.

8 LOSSES IN EXTERNAL FLOW

8.1 Flow Past Isolated Objects

The force F developed when a flowing fluid envelops an object is usually correlated by the drag coefficient C_d , the dimensionless ratio $2Fg_c/\rho Au^2$. u is the relative

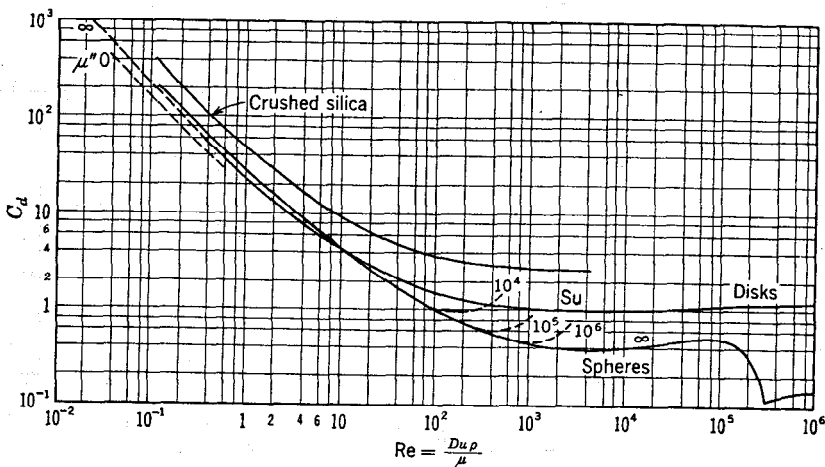


FIG. 6. Drag coefficients for steady motion in a fluid. Solid lines, solid particles; broken lines, bubbles and drops. (From C. F. Bonilla, Ref. 1.) The parameters are as follows:

$$\mu' = \mu_p - \mu_0 \quad Su = \frac{g_c \sigma_i D \rho_0}{\mu_0}$$

velocity of approach, ρ the fluid density, and A an arbitrarily defined area or (dimension)² of the object, generally the area projected in the direction of u . For any given geometry, C_d depends only on a Reynolds number up to a considerable fraction of sonic velocity. Figure 6 gives the relationship for shapes of interest in computing settling velocities of slurry particles and liquid droplets, pertinent to slurry fuels and breeding blankets, liquid-liquid fission-product extraction columns, etc.

Corrections are necessary because of molecular motion for particles under about 0.003 mm in diameter, because of the wall or other particles if they are not far away,²⁷ and because of acceleration.²⁸ In addition, suspended particles may flocculate by collision and adhesion and then settle out more rapidly.

For long fuel elements, the drag due to the flowing fluid is more readily obtained by a force balance, the total drag equaling the friction pressure drop by Arts. 3.11 through 4.22 multiplied by the total cross section of the stream.

8.2 Flow through Tube Banks

Flow parallel to the tubes in heat-exchanger shells can be handled by Arts. 3.12, 4.2, and 4.21. For flow perpendicular to tube banks the average velocity of the stream \bar{u}_{max} in passing between the tubes at their closest approach is employed. Each of five or more rows of tubes has a loss K of approximately 0.72 velocity heads or pressures for staggered tubes and 0.32 for tubes in line. Within 25 per cent accuracy, for 10 or more rows of staggered tubes on an equilateral triangular grid spaced up to $D/2$ between the tubes, the pressure drop per row is

$$\Delta P = 1.5\rho^{0.8}\bar{u}_{max}^{1.8}\mu^{0.2}/D_s^{0.2}g_c \tag{62}$$

where D_s is the open space between tubes.

If baffles are employed in the shell, two additional velocity heads may be lost at each. Actual pressure drops with baffles may be much lower at a given flow as a result of leakage around or through them, but for the same heat transfer, baffle leakage will require a larger flow and may actually thus increase the pressure drop.

8.3 Flow through Beds of Particles

Fixed packed beds of the normal 35 to 45 per cent voids follow the expressions below within ± 25 per cent, on the average:

$$\frac{D_p\bar{u}_{sp}}{\mu} < 40 \quad \frac{\bar{u}_s\mu L}{g_c\Delta P} = \frac{D_p^2}{1,700A_f} \tag{63}$$

$$\frac{D_p\bar{u}_{sp}}{\mu} > 40 \quad \frac{\bar{u}_s\mu L}{g_c\Delta P} = \frac{D_p^2}{76A_f} \left(\frac{D_p\bar{u}_{sp}}{\mu} \right)^{-0.35} \tag{64}$$

L is the bed depth, D_p is the particle diameter, \bar{u}_s is average velocity disregarding packing, and A_f is the wall leakage factor, varying linearly from 0.81 in streamline and 0.7 in turbulent flow at $D_p/D_{bed} = 0.1$ to 1 at $D_p/D_{bed} = 0$.

Five- to sixty-mesh-per-inch wire screens, as well as beds of spheres, fall²⁹ within some 20 per cent of the following correlation:

$\bar{u}_{sp}/\mu\alpha$	0.5	2.5	10	25	125
$\Delta P g_c \alpha^3 / \rho N \beta \bar{u}_s^2$	10	2.5	0.85	0.5	0.25

where α is the fractional volume of voids in the full screen thickness (usually twice the wire diameter) or bed thickness L and β is the total surface area per unit face area S and thickness L of the screen or bed.

8.4 Fluidization of Particulate Solids

If a particulate bed is not confined, at a fluid-flow rate such that the pressure drop across it (Art. 8.3) roughly equals its net weight per unit area but is below the transport velocity for the separate particles (Art. 8.1), the bed will become "fluidized." Good fluidization exhibits fast and thorough mixing of the bed and temperature uniformity throughout the bed and fluid and offers possibilities for nuclear fuel processing and reactor operation. Best fluidization is obtained with uniform particles fluidized by a liquid of low viscosity, and in the fluidized bed the particles occupy some 5 per cent of the total volume. Accurate predictions are difficult,³⁰ and tests are required on the specific system for quantitative design purposes.

9 MECHANICAL PUMPS AND BLOWERS

Centrifugal and axial-flow pumps and blowers are suitable for most fluid moving in nuclear power installations. They are available in a wide range of sizes, can stand reasonably high temperatures and pressures, and can be sealed well in case leakage is expensive or dangerous. Erosive fluids would damage them but would rule out other equipment also. These pumps are available with an inert-gas seal on the shaft or without emergent shaft thanks to a built-in motor or to a thin sealed nonmagnetic diaphragm through which magnetic drive occurs.

Variables in substantially constant-density operation of a pump or blower of a given geometrical design include rotational speed n in revolutions, a dimension such as the rotor diameter D , fluid pressure rise ΔP , density ρ , viscosity μ , and volumetric flow rate Q .

In common practice, the characteristics of a pump are plotted as constant-speed curves of ΔP (or of pressure head $\Delta P g_c / \rho g$), shaft horsepower P , and efficiency E versus Q for the desired fluid. If, instead, the appropriate dimensionless ratios are employed, operation for any fluid and conditions can be predicted, the size of a geometrically similar pump selected for a different Q , etc. The dimensionless ratios may be picked from the following: the rotational Reynolds number $D^2 n \rho / \mu$, the "capacity coefficient" $C_Q = Q / n D^3$, the "head coefficient" $C_H = \Delta P g_c / \rho n^2 D^2$, the "specific speed" $n_s = n Q^{1/2} (\rho / \Delta P g_c)^{3/4}$, and $\Delta P g_c D^4 / \rho Q^2$, a von Karman number.

When pump data are so handled, it is found that unless $D^2 n \rho / \mu$ is unusually small, it has no significant effect on the other ratios. Viscous friction losses are evidently relatively small. Thus, over its practical range, the characteristics of a centrifugal pump or blower can be expressed as any one of the other four above ratios plotted against any other one of them.

Cavitation occurs with a given liquid when the absolute pressure at any location in the pump falls to the vapor pressure at the same location. Noise, harmful hammering, and fall off in efficiency ensue. If the absolute static pressure at the inlet is P_1 and the absolute vapor pressure of the inlet fluid P_v , the "cavitation ratio" $(P_1 - P_v) / \Delta P$ below which cavitation develops has been found to be roughly constant for a given pump shape. For centrifugal pumps handling water it is recommended that $P_1 - P_v$ be at least some 7 or 8 psi (15 to 20 ft). Centrifugal pump and blower tip speeds are usually under 200 fps, and inlet opening velocities commonly below 10 fps for water and 100 fps for air.

The shaft power P can be expressed dimensionlessly as the "power coefficient" $C'_P = P g_c / \rho n^3 D^6$, which also plots as a function of any one of the four groups above, provided viscous and cavitation effects are absent.

Efficiency $(\Delta P g_c Q / P)$ is also a dimensionless ratio dependent on any one of the others. The maximum efficiency of a pump is obtained at some one point on the generalized efficiency curve, and thus at one value of each of the four other ratios above. The specific speed is particularly convenient in that D is absent and the other quantities in it are usually specified in a given pumping job (except for any possible

Table 7. Dimensionless Performance Coefficients for Commercial Single-stage Centrifugal Pumps and Fans

Coefficient	Pumps		Fans	
	At E_{max}	At $Q = 0$	At E_{max}	At $Q = 0$
C_H	3.5-5.8	4.4-6.5	3.5-11.	3.6-12
C_Q	0.01-0.4	0	0.2-1.3	0
n_s	0.03-0.3	0	0.1-0.3	0
E	0.4-0.9	0	0.4-0.9	0
C'_P	0.06-0.8	0.5-10

alternate values of n). Thus, for any given pumping operation the specific speed can be computed and a pump or blower of the desired type having the desired specific speed at its maximum efficiency selected from manufacturers' data or scaled up or down from data on a given shape. For commercial single-stage centrifugal pumps and fans of various designs the dimensionless coefficients usually fall in the ranges indicated in Table 7.

For single-stage axial flow pumps n_s at E_{max} usually ranges from 0.3 to 0.8. Actually, the optimum operating point is usually not exactly at maximum efficiency. Minimum pump size, investment, and total pumping cost are obtained by operation slightly beyond maximum efficiency (higher Q); high emergency reserve pumping capacity is obtained by normal operation below maximum efficiency (lower Q).

The combined characteristic ΔP versus Q curve of dissimilar pumps in series can be obtained by plotting the sum of the separate ΔP values at the same Q versus the value of Q . Similarly, for pumps in parallel ΣQ at each ΔP is plotted versus ΔP .

REFERENCES

1. Bonilla, C. F. (ed.): "Nuclear Engineering," McGraw-Hill Book Company, Inc., New York, 1957.
2. Bonilla, C. F., S. J. Wang, and H. Weiner: *Trans. ASME*, 1955.
3. Bonilla, C. F., R. D. Brooks, and P. L. Walker: "General Discussion of Heat Transfer," American Society of Mechanical Engineers, New York, 1953.
4. Bromley, L. A., and C. R. Wilke: *Ind. Eng. Chem.*, **43**: 1641 (1951).
5. Perry, J. H. (ed.): "Chemical Engineers' Handbook," 3d ed., McGraw-Hill Book Company, Inc., New York, 1950.
6. Goldstein, S.: "Modern Developments in Fluid Dynamics," Oxford University Press, New York, 1938.
7. Streeter, V. L.: "Fluid Dynamics," McGraw-Hill Book Company, Inc., New York, 1948.
8. Jakob, M.: "Heat Transfer," vol. 1, John Wiley & Sons, Inc., New York, 1949.
9. Deissler, R. G.: NACA TN-2410, 1951.
10. Moody, L. F.: *Trans. ASME*, **66**: 671 (1944).
11. Rothfus, R. R., et al.: *Ind. Eng. Chem.*, **31**: 618 (1939).
12. Deissler, R. G.: NACA TN-2138, 1950.
13. Deissler, R. G.: *ASME Paper* 53-S-41, 1953.
14. Keenan, J. H., and E. P. Neumann: *J. Appl. Mechanics*, **68**: A91-100 (June, 1946).
15. Poppendiek, H. F., and L. D. Palmer: ORNL-1395.
16. Rubesin, M. W., and H. A. Johnson: *Trans. ASME*, **71**: 383 (1949).
17. Rothfus, R. R., and R. S. Prengle: *Ind. Eng. Chem.*, **44**: 1686 (1952).
18. Kays, W. M.: *Trans. ASME*, **72**: 1067-1074 (1950).
19. Alves, G. E., D. F. Boucher, and R. L. Pigford: *Chem. Eng. Progr.*, **48**: 385 (1952).
20. Lockhart, R. W., and R. C. Martinelli: *Chem. Eng. Progr.*, **45**: 39 (1949).
21. Martinelli, R. C., and D. B. Nelson: *Trans. ASME*, **70**: 695 (1948).
22. Stein, R. P., et al.: *Chem. Eng. Progr. Symposium Ser.*, **50**: 11 (1954).
23. McAdams, W. H.: "Heat Transmission," 3d ed., McGraw-Hill Book Company, Inc., New York, 1954.
24. Reynolds, J.: ANL-5178, 1954.
25. Jens, W. H., and P. A. Lottes: ANL-4627, 1951.
26. Isbin, H. S.: Personal communication, 1953.
27. Lapple, C. E., et al.: "Fluid and Particle Mechanics," University of Delaware Press, Newark, Del., 1951.
28. Hughes, R. R., and E. R. Gilliland: *Chem. Eng. Progr.*, **48**: 497 (1952).
29. Coppage, J. E.: Ph.D. thesis in mechanical engineering, Stanford University, Stanford, Calif., 1952.
30. Weintraub, M., and M. Leva: *Ind. Eng. Chem.*, **45**: 76-7 (1953).

9-3 HEAT REMOVAL FROM NUCLEAR REACTORS

BY

Charles F. Bonilla

PRINCIPAL NOMENCLATURE

- A = surface area
 c = specific heat; also concentration
 C = electrical capacity
 c_p = specific heat at constant pressure
 c_v = specific heat at constant volume
 D = diameter
 D' = diameter, in.
 D_e = equivalent diameter = $4 \frac{\text{cross section}}{\text{wetted perimeter}}$
 D_v = diffusivity
 E = electrical potential
 F' = mass-transfer coefficient
 f_F = Fanning friction factor
 G = mass velocity
 g = gravitational acceleration
 g_c = ratio between units of force and of mass \times acceleration
 H = rate of heat generation per unit volume. H_i = rate at inner face
 h = local film heat-transfer coefficient
 I, i = electrical current
 I_0, J_0, K_0 = zero-order Bessel functions
 J = radiation intensity; also mechanical equivalent of heat
 k = thermal conductivity
 L = length; also dimension in general
 L = diffusion length
 M = molecular weight
 m = mass
 N = number of atoms per unit volume
 P = pressure
 P = pump shaft power
 p = per cent gas by volume; partial pressure
 Q = quantity of heat
 q = rate of heat flow
 q/A = heat flux. $(q/A)_c$ = critical heat flux
 R = fraction by volume; also thickness; also resistance in general; R_v = vapor fraction by volume
 r = radius
 r_e = electrical resistivity
 S = cross-sectional area
 s = surface tension
 T = absolute temperature

- t = thermometric temperature. \bar{t} , t_f , t_w = bulk, film, wall temperatures, respectively
 u = velocity. u_L , u_s = liquid, slip velocity, respectively
 V = volume; specific volume
 w = mass rate of flow
 x = fraction by weight; also vapor quality; also distance along a channel
 x' = fraction by volume
 y = distance transverse to a flow, or away from a channel wall
 z , Z = height above a horizontal datum
 α = thermal diffusivity = $\frac{k}{c\rho}$
 β = volumetric coefficient of thermal expansion
 Γ = mass flow rate per unit of width
 ϵ = eddy diffusivity
 θ = time
 λ = latent heat of vaporization
 μ = molecular viscosity, γ -ray attenuation coefficient
 ν = kinematic viscosity
 ρ = density. ρ_f , ρ_L , ρ_v = film, liquid, vapor densities, respectively
 σ = microscopic cross section; also standard deviation
 ψ = wetting angle

Gr, Gz, j , Nu, Pe, Pr, Ra, Re, Sc, Sh, St

= dimensionless ratios (see Table 3 of Sec. 9-2 or context)

Removal of the generated heat is an absolute requirement for continuous operation of a nuclear reactor, since otherwise the temperature will rise indefinitely until failure of the fuel elements or container and dissemination of the fuel and the fission products occur. In any commercially valuable power reactor the rate of heat generation per unit volume and of heat removal per unit surface area will be high in order to optimize the fixed charges, i.e., minimize the total cost. Temperatures will tend to be high to favor efficient conversion to electrical power. Thus, thermal design of fuel elements and coolant systems is very exacting. For a number of research reactors the cost of the coolant system has been about 18 per cent of the total cost. For power reactors some 25 per cent may be closer to the optimum allocation of funds.*¹

1 THE SPATIAL DISTRIBUTION OF HEAT GENERATION IN REACTORS

The distribution of the total energy generated by an average fission is shown in Table 1. The prompt energy includes 168 ± 5 Mev of fission-fragment kinetic energy, expended within 0.001 in. in metals, 5 ± 0.5 Mev of neutron kinetic energy, and 4.6 ± 1 Mev of γ rays. Radioactive decay of fission products and of unstable nuclei produced by reactions of stable nuclei with neutrons yields about 8 Mev of short-range β rays and 12.5 Mev of γ rays. The prompt fission-fragment and β energy appears in the fuel. The γ energy is dissipated roughly according to the mass through which it is passing, so that in a small reactor most of it appears in the shield. However, in a large reactor it may distribute itself roughly equally among the shield, fuel, and moderator. Typical distributions are given in Table 1. If the heat in the reflector and/or thermal shield is not gainfully recovered, the percentage of the useful power in the fuel is, of course, greater. The prompt energy is more significant in power surges, and a higher fraction is dissipated in the fuel. This difference is usually neglected, however.

Detailed calculations of the fissioning (generally, thermal) neutron flux n_v throughout the reactor are described in Sec. 6-2. If this information is available, the heating density H_f per unit volume of the fuel due to fission is obtained for any location by

* Superscript numbers refer to References at end of subsection.

$$H_f = Q'nv \sum \sigma_f N_f = 6.02 \times 10^{23} Q'nv \rho \sum \frac{\sigma_f x_f}{M_f} \quad (1)$$

where Q' = heat generated within the fuel per fission, any heat unit

σ_f = fission cross section of fuel, cm^2

N_f = number of atoms of fuel per cubic centimeter of fuel element, cm^{-3}

ρ = density of fuel element, g/cm^3

x_f = weight fraction of fuel in fuel element

M_f = atomic weight of fissionable nuclide or nuclides (i.e., U^{235} and Pu^{239}), g

A simpler method of computing the distribution of γ heat rate per unit volume H is frequently employed when the fuel is uniformly distributed, as in a homogeneous reactor or in a heterogeneous uniform lattice. The fraction of the total reactor heat q_t appearing in the moderator and in the fuel elements is first determined or estimated (e.g., by Table 1). Then q_t is accordingly divided, and the over-all average values \bar{H} per unit volume of fuel and of moderator are computed by dividing by the corresponding volumes. The value of H in any location is then obtained by multiplying the corresponding \bar{H} by the appropriate ratio of neutron flux to over-all average neutron flux (see Sec. 6-2).

Table 1. Approximate Distribution of Steady-state Heat Dissipation in Representative Reactor Types

	Approx core size, ft	Fuel element	Moderator	Reflector	Thermal shield
Large thermal reactor (natural U):					
Total Mev per fission...	..	175	12	2	5
% of total	90	6	1	3
% of heat generated in fuel and moderator...	..	93	7	Unrecovered	
Small thermal reactor (U^{235}):					
Total Mev per fission...	..	168	7	2	17
% of total	86	4	1	9
% of heat generated in fuel and moderator...	..	96	4	Unrecovered	
Specific reactors:					
Fast breeder (EBR-I)...	1	72% (core)		28% (blankets)	Unrecovered
Thermal water-cooled, water- and beryllium-moderated (MTR)....	3	94.3% (including water)	3.9% (Be)	1.6% (graphite)	0.16% (steel)
Intermediate, sodium-cooled, beryllium-moderated (SIR).....	4		95% (including 4% Be)		1% (steel) (biological 0.1%)
Thermal, graphite-moderated, air-cooled, natural U (BNL).....	25	92%	6%	>1%	<1%
Sodium-cooled, enriched U (SRE).....	6	91.5%		7%	1.5%
Sodium-cooled, enriched U (SGR).....	7	92.3%		7%	0.7%
Thermal, diphenyl-moderated and -cooled (OMRE).....	3	91%		5.5%	3.5%

2 HEAT CONDUCTION

2.1 Heat-conduction Relations

Fourier's law gives the time rate of heat conduction $dQ/d\theta$ or q through a plane area A as

$$q = dQ/d\theta = -kA dt/dx \quad (2)$$

where t is temperature and distance x is measured normally to A and in the direction of the heat flow. Equation (2) also serves as the defining equation for the thermal conductivity k .

Usually k is a known function of t , and for many cases A and q are theoretically known or experimentally measured functions of x . Thus, to integrate Eq. (2) for steady-state heat conduction between isothermal surfaces at x and x_1 , it is usually rewritten

$$\int_x^{x_1} \frac{q}{A} dx = \int_{t_1}^t k dt \quad (3)$$

Since k may usually be assumed constant or at most a linear function of t , Eq. (3) equals $\bar{k}(t - t_1)$, where \bar{k} is the arithmetic mean of k at t and t_1 . If q is not constant along the heat-flow path under consideration, for steady-state heat flow it can be obtained by integration of H :

$$q = q_0 + \int_0^x HA dx \quad (4)$$

then substituted into Eq. (3). q_0 is any heat entering at $x = 0$. Results of this double integration are given in Arts. 2.3 to 2.5 for the one-dimensional geometries and the simple distributions of H .

Including motion of the conduction field (i.e., a flowing fluid), unsteady-state heat conduction, and two- and three-dimensional shapes, the appropriate differential equation is

$$\frac{\partial t}{\partial \theta} = \alpha \nabla^2 t + \frac{H}{c_p} - \left(u_x \frac{\partial t}{\partial x} + u_y \frac{\partial t}{\partial y} + u_z \frac{\partial t}{\partial z} \right) \quad (5)$$

where c is the specific heat, u is the velocity, and the thermal diffusivity α is k/c_p . The Laplacian ∇^2 is defined in Art. 4.4 of Sec. 3-2.

2.2 Thermal Conductivity

2.21 Gases and Liquids. Thermal conductivity for most reactor fluids is tabulated in Sec. 9-1. The NBS-NACA Thermal Tables² also provide the thermal conductivity, specific heat, enthalpy, and many other properties of gases over fairly wide temperature and pressure ranges. For interpolation of k or extrapolation to higher temperatures, the Sutherland equation [Eqs. 2 to 10 of Sec. 9-2] is satisfactory; \sqrt{T}/k plots reasonably straight against $1/T$. For monatomic gases k can also be computed³ as $\mu c_v(2.4 + 0.016 \sqrt{M})$, and for the common linear molecules except H_2 as $\mu(1.45c_p - 0.13c_v)$. The thermal conductivity for a mixture of gases can be higher or lower than the molar interpolation from the pure components but can be predicted⁴ within several per cent. The thermal conductivity of gases increases exponentially with the ratio P/T . For coolants and conditions so far considered, however, the effect is not significant. CO_2 shows the greatest increase, 3½ per cent at 10 atm and 200°F.

The thermal conductivity of nonmetallic liquids is not readily predicted or extrapolated theoretically, and empirical values are desirable (see Sec. 9-1).

2.22 Metals. The thermal conductivity of solid materials used in reactors is given in Sec. 10-2. Among solid pure metals k varies twentyfold, and empirical values should be used when available. It usually decreases slightly as temperature rises, then on melting falls abruptly to one-third the solid value. Cold-worked metal has k somewhat lower than annealed, and cast metal even lower. Impurities in solid metal, including fission products, decrease k considerably. Alloys generally have a conductivity of 50 to 100 per cent of the linearly interpolated value.

Practically all the heat conducted in metals is transported by the free electrons. The Lorenz relation between thermal and electrical conduction

$$k = \frac{23T}{r_e} \quad \text{watts/(cm)(}^\circ\text{C)} \quad (6)$$

is useful for predicting k if the electrical resistivity r_e is known or can be measured. In Eq. (6) T is in degrees Kelvin and r_e in ohm-centimeters. The constant is 23 ± 1 for most solid and liquid metals and ranges from two-thirds to twice this for alloys.⁵

2.23 Two-phase Mixtures. The thermal conductivity k_m of two-phase mixtures in which the discontinuous-phase particles seldom touch each other or have their conductivity k_d lower than k_c of the continuous phase can be approximately predicted⁶ by Maxwell's formula

$$k_m = k_c \frac{2k_c + k_d - 2x_d(k_c - k_d)}{2k_c + k_d + x_d(k_c - k_d)} \quad (7)$$

where x_d is the volume fraction of discontinuous phase.

For packed beds of solid particles of conductivity k_s permeated with a stagnant fluid of lower conductivity k_f , k_m can be conservatively estimated⁷ within some 20 per cent by Table 2. If the fluid is flowing through the bed, the effective conductivity normal to the flow is given⁸ by $k_m = 3.7(\bar{\mu}_p/x_f)(G \sqrt{a/\bar{\mu}})^{1/3}$, where G is the over-all or superficial mass velocity, a is the surface area per particle, and $\bar{\mu}$ is the average viscosity.

Table 2. Thermal-conductivity Ratio k_m/k_f for Packed Beds Filled with a Stagnant Fluid

k_s/k_f	0	Fractional void volume						
		0.2	0.3	0.4	0.5	0.6	0.8	1
1	1	1	1	1	1	1	1	1
3	3	2.4	2.1	1.9	1.7	1.5	1.2	1
10	10	5.4	4.3	3.4	2.8	2.2	1.5	1
30	30	10.7	7.5	5.4	4.0	3.0	1.7	1
100	100	22	13	8.3	5.5	3.7	1.9	1
300	300	42	20	11	7.0	4.5	2.0	1
1,000	1,000	83	32	15	8.5	5.3	2.2	1

2.3 Steady-state Conduction in an Infinite Slab

In nuclear reactors, the surface temperature of the fuel elements, moderator, and shielding is controlled by the coolant. Thus, internal temperatures are computed with respect to surface temperature. For Eqs. (8) and (9) one surface is at $x = 0$, and the cooled surface at x_1 is at temperature t_1 .

2.31 Constant Heat Flow. For constant heat flow $q = \text{constant}$ and $H = 0$, as in fuel-element cladding that generates relatively little heat:

$$t - t_1 = \frac{x_1 - x}{k} \frac{q}{A} \quad t_0 - t_1 = \frac{x_1 q}{kA} \quad (8)$$

2.32 Uniform Heating Density. For $q_0 = 0$ and constant heating density ($H = \text{constant}$), as in homogeneous fuel elements, slabs of moderator, cladding, shields, etc., with appreciable heat generation but thin enough so H is uniform:

$$t - t_1 = \frac{x_1^2 - x^2}{2k} H \quad t_0 - t_1 = \frac{x_1^2 H}{2k} = \frac{x_1 q_1}{2kA} \quad (9)$$

If there are simultaneously q_0 entering at $x = 0$ and heating density H from 0 to x_1 , the total $t - t_1$ or $t_0 - t_1$ is obtained by adding Eqs. (8) and (9).

2.33 Thermal-neutron Heating. In a bare reflector or shield of inner surface at x_2 and outer surface at x_3 from the reactor midplane, for cooling at the inner surface:

$$\frac{q}{A} = H_i L \frac{\cosh [(x_3/L) - (x/L)] - 1}{\sinh [(x_3/L) - (x_2/L)]} \quad (10)$$

$$t_3 - t_2 = \frac{H_i L^2}{\bar{k}} \left\{ 1 - \frac{(x_3/L) - (x_2/L)}{\sinh [(x_3/L) - (x_2/L)]} \right\} \quad (11)$$

where H_i is the inner surface (maximum) heating density and L is the average neutron diffusion length.

Similarly, for cooling at the outer surface:

$$t_2 - t_3 = \frac{H_i L^2}{\bar{k}} \left[\left(\frac{x_3}{L} - \frac{x_2}{L} \right) \coth \left(\frac{x_3}{L} - \frac{x_2}{L} \right) - 1 \right] \quad (12)$$

If \bar{H} is available instead of H_i , the latter can be eliminated from the above expressions by

$$\frac{\bar{H}}{H_i} = \frac{\cosh [(x_3/L) - (x_2/L)] - 1}{[(x_3/L) - (x_2/L)] \sinh [(x_3/L) - (x_2/L)]} \quad (13)$$

2.34 Gamma-ray Heating. As in a reflector, blanket, or thermal shield, the thickness Δr of separately cooled thermal shields and other special γ -ray absorbers is small compared with r . In this case H_γ can be represented approximately by $H_\gamma = be^{-\mu r}$, where μ is a linear energy attenuation coefficient. H_2 and H_3 are calculated as described in Sec. 7-3, and

$$\mu = \frac{1}{r_3 - r_2} \ln \frac{H_2}{H_3} \quad \bar{H} = \frac{H_2 - H_3}{\mu(x_3 - x_2)} \quad (14)$$

For cooling at r_2 , the inner surface:

$$t_3 - t_2 = \frac{H_2 - H_3}{\bar{k}\mu^2} - \frac{H_3(r_3 - r_2)}{\bar{k}\mu} \quad (15)$$

For cooling at r_3 , the outer surface:

$$t_2 - t_3 = \frac{H_2(r_3 - r_2)}{\bar{k}\mu} - \frac{H_2 - H_3}{\bar{k}\mu^2} \quad (16)$$

2.35 Actual Reflectors and Shields. These usually have heat generation by several simultaneous methods, and the heat is removed to various extents and at different temperatures through the two faces. Assuming that the coolant temperature is known on both sides at the desired level, the distribution of the heat generated between the two sides is assumed, the two surface temperatures are computed from estimated heat-transfer coefficients, and the intermediate plane located at which the temperature is the same when computed from either side with the known distribution of H . Then the assumed distribution on both sides of the heat dissipation must be checked, and the calculation repeated with the new distribution if agreement is poor. The dissipation on each side can also be calculated as if the temperatures on both sides were equal, then adding to the cold side and subtracting from the hot side the heat that would be conducted through the plate as a result of the given surface temperatures alone.

In best design, however, all coolant streams are usually so apportioned that their temperature rise is about the same, and the simpler case of equal wall temperatures is adequate. In this case, even with a ratio H_2/H_3 as high as 10, the hottest plane is located within 10 per cent of the midplane, at least one-third of the heat leaves

through the outer surface, and the maximum temperature rise is within several per cent of the value it would be with uniform H^{98} :

$$t_{\max} - t_w = \frac{\bar{H}(\Delta x)^2}{8\bar{k}} \quad (17)$$

Thermal shields and other slabs with high heat generation are generally subdivided into thinner parallel layers with intermediate coolant streams as necessary to keep t_{\max} or the thermal stress below their permissible maximum values. The layers are made thicker the farther away they are from the axis of the reactor.

2.4 Steady-state Conduction in an Infinite Cylinder

Cylindrical fuel elements are useful because they are easy to fabricate and replace and because tubes are desirable as fuel-element jackets and coolant channels. The cylindrical shape is also desirable for reactors in which through-flow cooling channels are necessary, as is the usual case.

2.41 Constant Heat Flow Through a Hollow Cylinder. Here $q = \text{constant}$ and $H = 0$, as in cylindrical fuel-element cladding. The temperature drop in either direction of heat flow between radii r_2 and r_3 is, by Eq. (3),

$$|t_2 - t_3| = \frac{1}{2\pi\bar{k}} \frac{q}{L} \ln \frac{r_3}{r_2} = 0.367 \frac{q}{\bar{k}L} \log \frac{r_3}{r_2} \quad (18)$$

where q/L is the rate of heat flow per unit length.

2.42 Fission Heating in a Homogeneous Cylindrical Fuel Element. In such elements, with $I_0(r/L)$ neutron flux distribution:

$$t_0 - t_1 = \frac{H_0 r_1^2}{4\bar{k}} \left(1 + \frac{r_1^2}{4^2 L^2} + \frac{r_1^4}{4^2 6^2 L^4} + \dots \right) \quad (19)$$

2.43 Constant Heating Density in a Solid Cylinder. This holds for the case of homogeneous cylindrical fuel elements of radius less than about half of the neutron diffusion length:

$$t - t_1 = \frac{H}{4\bar{k}} (r_1^2 - r^2) \quad t_0 - t_1 = \frac{H}{4\bar{k}} r_1^2 = 0.0795 \frac{q}{\bar{k}L} \quad (20)$$

In the frequent case that the axial temperature t_0 and surface temperature t_1 are both specified, the total required length L of fuel elements can be directly computed from the power q .

2.44 Constant Heating Density in a Hollow Cylinder. With external cooling at r_3 :

$$t_2 - t_3 = \frac{H}{4\bar{k}} r_3^2 [1 - (r_2/r_3)^2 (1 + 2 \ln r_3/r_2)] \quad (21)$$

With internal cooling at r_2 Eq. (21) holds on interchanging the subscripts 2 and 3. With cooling to the same temperature at both r_2 and r_3 , equating the internal temperatures yields the maximum temperature t_m at

$$r_m = \sqrt{\frac{r_3^2 - r_2^2}{2 \ln (r_3/r_2)}} \quad (22)$$

t_m is obtained from Eq. (21) by replacing subscript 2 or 3 by m .

2.45 Homogeneous Cylindrical Reactor. Though cooling at the outer surface alone is entirely impractical for power production, it might be useful for removing

fission-product heat in small reactors in the event of coolant-system failure, particularly on complete loss of the coolant in the core. \bar{k} must be an appropriate average for radial conduction through the core. Based on a J_0 radial distribution of H :

$$t_0 - t_1 = \frac{H_0 r_1^2}{4\bar{k}} \left[1 - \left(\frac{r'_1}{4}\right)^2 + \left(\frac{r'_1}{4.6}\right)^4 - \left(\frac{r'_1}{4.6.8}\right)^6 \dots \right] \quad (23)$$

where $r'_1 = 2.4048r_1/R_0$, R_0 being the extrapolated radius to zero neutron flux.

2.5 Steady-state Conduction in a Sphere

Although spherical fuel elements are not normally practical in power reactors for mechanical reasons, their resonance escape probability can be higher, and suitable designs may evolve. This case also approaches that of fuel suspensions.

2.51 Constant Heat Flow Through a Hollow Sphere. This, as for fission heat passing through cladding on a spherical fuel element, is equal to

$$t_2 - t_3 = \frac{q}{4\pi\bar{k}} \left(\frac{1}{r_2} - \frac{1}{r_3} \right) \quad (24)$$

2.52 Constant Heating Density in a Solid Sphere. As in homogeneous spherical fuel elements of radius less than about three-fourths of the neutron diffusion length, this equals

$$t - t_1 = \frac{H}{6\bar{k}} (r_1^2 - r^2) \quad t_0 - t_1 = \frac{H}{6\bar{k}} r_1^2 \quad (25)$$

For an externally cooled spherical shell

$$t_2 - t_3 = \frac{H}{6\bar{k}} \left(2 \frac{r_2^3}{r_3} + r_3^2 - 3r_2^2 \right) \quad (26)$$

2.53 Fission Heating in a Homogeneous Spherical Fuel Element. With $(\sinh r/L)/(r/L)$ neutron flux distribution, the result is

$$t_0 - t_1 = \frac{H_0 r_1^2}{\bar{k}} \left(\frac{1}{3!} + \frac{r_1^2}{5!L^2} + \frac{r_1^4}{7!L^4} + \dots \right) \quad (27)$$

2.54 Homogeneous Spherical Reactor. With $(\sin \pi r/R_0)/(\pi r/R_0)$ neutron flux distribution, the result is

$$t_0 - t_1 = \frac{H_0 r_1^2}{\bar{k}} \left[\frac{1}{3!} - \frac{(\pi r_1)^2}{5!R_0^2} + \frac{(\pi r_1)^4}{7!R_0^4} - \dots \right] \quad (28)$$

3 CONVECTION

3.1 Heat-transfer Coefficients

Heat generated in nuclear reactors is usually removed by fluids flowing past solid walls. In general, the heat gained or given up by a fluid determines or is determined by its average, bulk, or "mixing-cup" temperature \bar{t} . The temperature t_w of the solid wall must exceed \bar{t} in order to transfer heat to the fluid, or vice versa. This temperature difference is designated Δt . The ratio between the heat velocity q/A and Δt at any point is known as the *local film heat-transfer coefficient* h . Thus:

$$\frac{q}{A} = |h(t_w - \bar{t})| = h \Delta t \quad (29)$$

A principal phase of thermal design is the prediction of the magnitude of h and thus Δt for the desired coolant-flow conditions. For pure streamline flow this can be done mathematically by solving simultaneously the appropriate heat and fluid-flow relations, particularly Eq. (1) of Sec. 9-2 and Eq. (5), etc. For turbulent flow, certain cases have been solved semitheoretically by also using Eqs. (31) through (36) of Sec. 9-2. The bulk of available heat-transfer-coefficient information, however, consists of generalized dimensionless correlations of actual test values of h for standard simple shapes and flow directions in terms of the significant dimensions, physical properties, and flows.

According to the Buckingham "pi theorem" the number of dimensionless ratios needed is the least number of necessary variables (including h) minus the number of independent physical dimensions. The principal dimensionless ratios in heat transfer are listed in Table 3 of Sec. 9-2.

In most cases the variation of a physical property throughout Δt has a negligible to moderate effect on h . The property is then generally taken at the arithmetic mean or "film" temperature t_f , namely, $(t_w + \bar{t})/2$. In all heat-transfer correlations in this article all physical properties are taken at t_f unless stated to be at t_w or at \bar{t} by the subscripts w or b (for bulk), respectively, or at some specially defined temperature. In most nuclear thermal problems q is given and t_w or \bar{t} , thus also t_f , is unknown. Accordingly trial-and-error solution for the unknown temperature is frequently necessary. However, usually a rough preliminary estimate of t_f yields an accurate enough h and thence Δt , so that there is no need to calculate t_f , then h and Δt again.

3.2 Forced Convection in Uniform Channels

Fuel elements are generally thin compared with their length, so that heat leaves the fuel element at or very near the section at which it was generated. Thus the distribution of superficial q/A for Eq. (29) is closely obtainable from Art. 1. The same information also yields the local average coolant temperature \bar{t} (see Art. 6.1).

3.2.1 Turbulent Flow. Figure 1 shows graphically the principal cases for nonmetals. Table 3 gives in algebraic form the pertinent correlations for nonmetals.

From Table 3, case b , it is seen that there is an appreciable decrease in h for a short distance downstream from the entrance to a channel. Since this "thermal entry length" is short, it is neglected in most experimental studies and correlations, which

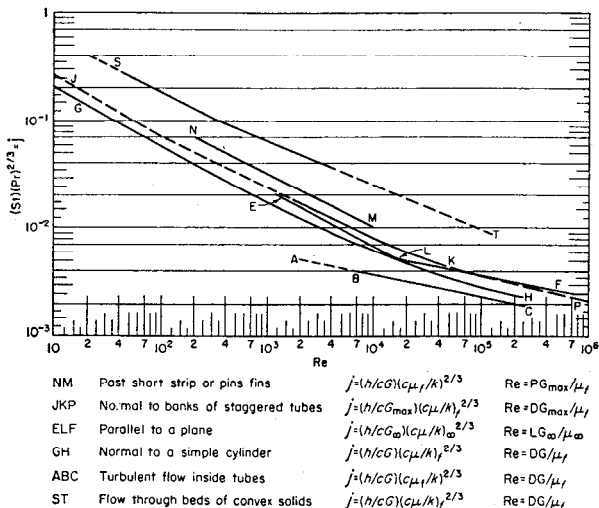


FIG. 1. Mean heat-transfer coefficients for nonmetallic fluids in forced convection. (From C. F. Bonilla, Ref. 98.)

Table 3. Turbulent-flow Heat Transfer for Nonmetallic Fluids

Designation	Case	Limitations, etc.	Relation	Reference
a	Flow in long channels	$2,000 < Re < 300,000$	$Nu = 0.023 Re^{0.8} Pr^{1/4} = Nu^0$	9
b	Local h in short channels: downstream distance L	$2,000 < Re < 60,000$	$Nu_L = \left[\frac{2.8}{Re^{0.98}} \left(\frac{L}{D} \right)^{-2.25/Re^{0.3}} \right] Nu^0$	10
c	Local h in short channels	$60,000 < Re$	$Nu_L = 1.5 Nu^0$ at $L/D_s = 1$ $Nu_L = 1.1 Nu^0$ at $L/D_s = 5$	
d	Flow in coils		$Nu = (1 + 3.5D/D_{coil}) Nu^0$	9
e	Flow in wide concentric annuli	Heat transfer at outer surface	$Nu = Nu^0$ (using D_s)	11
f	Flow in wide concentric annuli	Heat transfer at inner surface	$Nu = 0.87 \sqrt{D_1/D_2} Nu^0$	12
g	Liquid in tubes with p' % of gas by volume	Upflow with $25 < G < 100$ lb/(ft ²)(sec)	$Nu = (1 + 6.1G^{-0.33} \log_{10} p') Nu^0$	13
h	Gases in long tubes at high Δt	$t_{e,s} = 0.4t_w + 0.6\bar{t}$	$Nu_{0.4} = 0.236[D\bar{u}(\rho/\mu)_{e,s}]^{0.78}$	14
i	Gases at high \bar{u}	Case a holds with $\Delta t = t_w - \bar{t} - \frac{\bar{u}^2}{2g_0 c_p} Pr^{1/2}$		9
j	Flow parallel to tube bundles	Axial spacing/diameter < 1.3	$Nu = Nu^0$ (using D_s)	15
k	Flow parallel to tube bundles	Axial spacing/diameter = 1.46	$Nu = 1.4 Nu^0$ (using D_s)	16

Table 4. Turbulent-flow Heat Transfer for Molten Metals

Designation	Case	Limitations, etc.	Relation	Reference
a	Flow in a long tube	Constant q/A	$Nu = 7 + 0.025 Pe^{0.8} = Nu^0$	17
a'	Flow in a long tube	Constant q/A	$Nu = 6.3 + 0.016 Pe^{0.91} Pr^{0.3}$	21
b	Flow in a long tube	Constant t_w	$Nu = 4.8 + 0.025 Pe^{0.8}$	17
b'	Flow in a long tube	Constant t_w	$Nu = 4.8 + 0.015 Pe^{0.91} Pr^{0.3}$	21
c	Flow in a long tube	$50 < Pe < 20,000$	$Nu = 0.625 Pe^{0.4}$	18
d	Local h in a short tube	Constant t_w	$Nu_L = 1.31(Pe D/L)^{0.455}$	19
e	Flow in a flat channel	One wall $q/A = 0$, other q/A constant	$Nu = 5.8 + 0.02 Pe^{0.8}$ (using D_s)	17
f	Flow in a flat channel	Both walls with q/A constant	$Nu = 10.5 + 0.036 Pe^{0.8}$ (using D_s)	17
g	Flow in a flat channel	Each wall with different constant q/A	17
h	Flow in a concentric annulus	$D_1/D_2 < 1.4$	Relation e, f, or g, as applicable	
i	Flow in a concentric annulus	$D_1/D_2 > 1.4$	$Nu_2 = 0.75(D_1/D_2)^{0.3} Nu^0$	
j	Flow in a concentric annulus	Constant q/A at D_2	$Nu_2 = (5.25 + 0.0175 Pe)(D_1/D_2)^{0.33}$	20
k	Flow along an un-baffled bundle	$D =$ tube or rod outer diam	$Nu_D = 11.6(Pe_D)^{0.6}(D_s/L)^{1.2}$	20

thus give, in effect, the "long tube" h . Since the downstream h is lower and also the \bar{t} is higher, long-tube h values are correct for calculating fuel-element hot spots. For a more accurate profile of the temperature along a fuel element, however, local h values are used.

Figure 2 shows the principal data for liquid metals, recalculated on a consistent basis.¹⁸ The large discrepancies seem to be due mainly to errors in temperature readings or to the presence of entrained gas from incorrectly designed gas-pressurizing

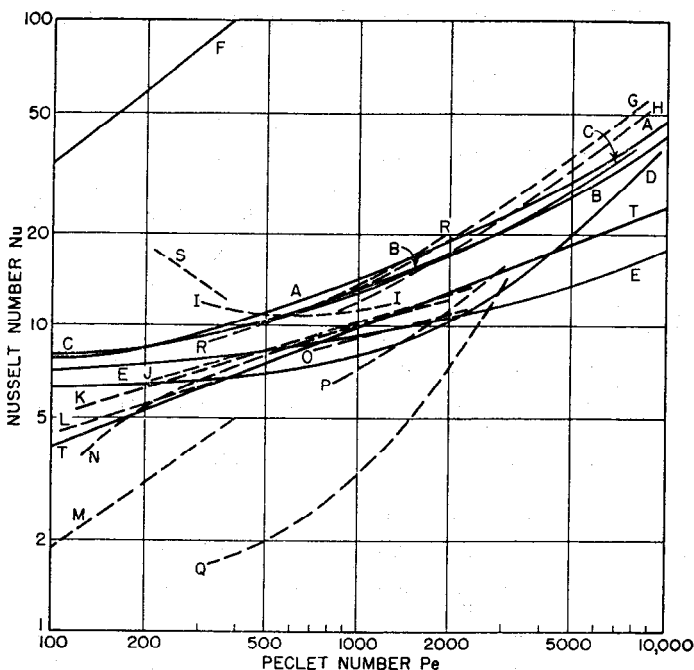


FIG. 2. Heating of liquid metals in turbulent pipe flow. Solid lines A to F, theoretical relations; dashed lines G to T, experimental results. U, unwetted; W, wetted. (From C. F. Bonilla, Ref. 98.)

- | | |
|---|------------------------------------|
| A. Martinelli ($Pr = 10^{-2}$) | K. Trefethan (W and U) |
| B. Martinelli ($Pr = 10^{-3}$) | L. Doody and Younger (W) |
| C. Lyon (Table 4a) | M. Doody and Younger (U) |
| D. Deissler | N. English and Barrett (U) |
| E. Kennison | O. Johnson et al. (1950) |
| F. Colburn ($Pr = 0.027$) | P. Lubarsky (U) |
| G. Isakoff and Drew ($x/d = 58$) (U) | Q. Untermeyer (U) |
| H. Isakoff and Drew ($x/d = 138$) (U) | R. Werner, King, and Tidball (W) |
| I. Untermeyer (W) | S. Keen |
| J. Johnson et al. (1951) | T. Lubarsky and Kaufman (Table 4c) |

liquid expansion tanks.²⁷ Gas impairs heat transfer more if the liquid metal does not wet the walls, as has been shown for flow of mercury through a tube bank.²⁶

The principal relations that have been obtained are listed in Table 4. The constant term represents the strong conduction contribution, and the Pe term the turbulent convection contribution. The lowest h computed among all appropriate relations, further decreased by a moderate safety factor, should be used for conservative designs.

3.22 Laminar Flow. In laminar flow h is smaller than in turbulent flow under conditions that are otherwise the same, since radial heat convection by eddies is absent. However, laminar flow may be entirely adequate for full-power operation when Δt is low in any case, such as with low heat velocities, liquid-metal coolants, and/or small channels. In addition, laminar flow may be employed at low circulation rates or at low-power operation or obtained unintentionally during coast-down and during steady-state natural circulation following pump failure.

The principal laminar-flow relations for "short" channels are listed in Table 5. In laminar flow the effect of the thermal entry length is greater than in turbulent flow (i.e., see case *f*). However, even in laminar flow the long-channel relations are suitable for hot-spot calculations, since they are almost correct, simpler, and somewhat

conservative. \overline{Nu}_{AM} (cases *d* and *e*) employs $h_{AM} = q/[A(\Delta t)_{AM}]$, where Δt_{AM} is the arithmetic mean of the inlet and local Δt .

Tables 6 and 7 give long-channel values of local h for the principal channel shapes. The Δt_{max} values are useful in computing from the usual $\Delta t_{flow\ mean}$ [Δt in Eq. (29)] the maximum temperature variation in the stream, for thermal shock estimating, etc. The $\Delta t_{space\ mean}$ values yield the volumetric average temperature of the coolant, useful for calculating the mass of coolant in the tube, its buoyancy, etc.

Table 5. Laminar-flow Heat Transfer in "Short" Tubes

Designation	Case	Limitations	Relations	Reference																
<i>a</i>	Local h in a short tube—parabolic flow	Constant t_w ; $Gz = cGD^2/kL > 12$	$Nu = 1.15Gz^{1/3}$	23																
<i>b</i>	Local h in a short flat duct—parabolic flow	Constant t_w ; $Gz' = cGD_e^2/kL > 70$	$Nu = 1.3(Gz')^{1/3}$	23																
<i>c</i>	Local h in a tube—plug flow	Constant t_w ; $Gz = 1$, $Gz = 10$	$Nu = 1.3 \pm$ $Nu = 3.7 \pm$	24																
<i>d</i>	Average h in a tube—actual flow	Constant t_w ; $Re > 10$	$\overline{Nu}_{AM} = 1.76 Gz^{1/3} \left(\frac{\mu_b}{\mu_w} \right)^{0.14}$ $\frac{2.25(1 + 0.01 Gr^{1/2})}{\log Re}$	9																
<i>e</i>	Average h in a flat duct—actual flow	Constant t_w ; $Re > 10$ $D = D_e$	$\overline{Nu}_{AM} = 15\%$ above relation <i>d</i> at same Gz																	
<i>f</i>	Local h in a tube—parabolic flow	Constant q/A	<table border="1"> <thead> <tr> <th>Nu</th> <th>Gz</th> </tr> </thead> <tbody> <tr> <td>4.36</td> <td>0-10</td> </tr> <tr> <td>5</td> <td>34.4</td> </tr> <tr> <td>6</td> <td>73.7</td> </tr> <tr> <td>8</td> <td>191</td> </tr> <tr> <td>10</td> <td>378</td> </tr> <tr> <td>14</td> <td>632</td> </tr> <tr> <td>19</td> <td>2000</td> </tr> </tbody> </table>	Nu	Gz	4.36	0-10	5	34.4	6	73.7	8	191	10	378	14	632	19	2000	
Nu	Gz																			
4.36	0-10																			
5	34.4																			
6	73.7																			
8	191																			
10	378																			
14	632																			
19	2000																			

Because of viscosity change with temperature, h for a liquid being heated or a gas being cooled will fall between the parabolic and uniform velocity cases. The same method applies, in either cooling or heating, for estimating h for slurries that have Bingham body or pseudoplastic properties.

3.3 Forced Convection Normal to Cylinders, Tube Banks, Screens, and Beds

The principal correlating equations for these cases are given in Table 8. In all these cases the local h or Nu varies considerably around the perimeter of the body. The values correlated herein are all experimental surface-average results. Theoretically, average coefficients are slightly higher at constant q/A than at constant t_w . Most experimental results and most nuclear applications involve small, solid elements and are close to constant t_w . Table 8 thus is reasonably accurate or else slightly conservative under all practical conditions and may be safely employed for design purposes regardless of the precise thermal conditions.

3.4 Free Convection

Free convection is the circulation by gravity of a fluid having density variations due to thermal expansion caused by heat transfer. If the circulation is inside an open channel that is at least several diameters long or a closed loop, it is *internal convection*, or *natural circulation*. In this case the rate of circulation can be predicted approxi-

Table 6. Local Nusselt Number and Temperature Differentials in Streamline Flow in Long Channels
(Axial conduction neglected)

Channel shape	Constant heating conditions	Velocity	Nu based on flow mean temperature ^a	$\frac{\Delta t_{\max}}{\Delta t_{\text{flow mean}}}$	$\frac{\Delta t_{\text{space mean}}}{\Delta t_{\text{flow mean}}}$
Round pipe.....	q/A	Parabolic	4.36 ^b	1.636	0.727
	q/A	Uniform	8	2.013	1.000
	t_w	Parabolic	3.66		
Flat channel (infinite width)....	t_w	Uniform	5.80		1.000
	q/A	Parabolic:			
		Heated 1 side	5.384	1.346	0.942
		Heated 2 sides	8.240	1.288	0.824
	q/A	Uniform:			
		Heated 1 side	6	1.500	1.000
		Heated 2 sides	12	1.500	1.000
	t_w	Parabolic:			
		Heated 2 sides	7.60		
		Uniform:			
	Heated 1 side	4.94 ^c	1.571	1.000 ^e	
	Heated 2 sides	9.88 ^c	1.571	1.000 ^e	
Square.....	q/A	Uniform [†]	6 ^c	2.00 ^f	
	q/A	Parabolic	3.68 ^e		
Triangular: ^d					
	$60^\circ \times 60^\circ \times 60^\circ$	q/A	Uniform	4 ^c	3.00 ^f
	$45^\circ \times 45^\circ \times 90^\circ$	q/A	Uniform	2 ^c	4.10 ^f
$30^\circ \times 60^\circ \times 90^\circ$	q/A	Uniform	2 ^c		
Rectangular:					
	$a/b = 2$	q/A	Parabolic	4.16 ^e	
	$a/b = 3$	q/A	Parabolic	4.78 ^e	
	$a/b = 5$	q/A	Parabolic	5.55 ^e	
	$a/b = 10$	q/A	Parabolic	6.77 ^e	

NOTE: The length in Nu is D_e for all channels.

^a R. H. Norris and D. D. Streid, *Trans. ASME*, **62**: 525 (1940).

^b For gases with large Δt take k at $1.27t - 0.27t_w$. Similarly, for liquid metals multiply 4.36 by $(\mu_b/\mu_w)^{0.14}$. See Ref. 25.

^c To include axial conduction divide by $\{1 + [1 + (\alpha/bu)^2]^{1/2}\}/2$.

^d "Liquid Metals Handbook" (2d ed., R. N. Lyon, editor; 3d ed., C. B. Jackson, editor), Government Printing Office, Washington, D.C., 1956.

^e Based on mean wall temperature t_w . Conservative, since circulating currents are neglected.

^f $[(t_w)_{\max} - t]/(t_w - t)$.

Table 7. Local Nusselt Number for Streamline Flow in Long Concentric Cylindrical Annuli Heated at Constant q/A on One Side*

(Nu based on D_e ; $D_e = D_1 - D_2$)

$\frac{D_{\text{insulated}}}{D_{\text{heated}}}$	Uniform velocity, Nu	"Parabolic" velocity (μ constant)	
		Nu	$\frac{\Delta t_{\max}}{\Delta t_{\text{flow mean}}}$
54.60	32.96	34.78	1.1
7.389	9.71	10.18	1.16
2.718	6.748	6.758	1.23
1.649	6.168	5.898	1.29
1.284	6.040	5.606	1.31
†	6	5.384	1.35
0.7788	6.036	5.222	1.37
0.6065	6.132	5.104	1.40
0.3679	6.442	4.962	1.46
0.1353	7.144	4.854	1.55
0‡	8	4.364	1.64

* L. M. Trefethen, NP-1788, 1950.

† Flat duct.

‡ Round pipe.

mately by analysis (see Art. 6.21) and h obtained by the usual forced-convection correlations (Tables 3 through 7).

The product $Gr \times Pr = L^3 \rho^2 g \beta \Delta t c / \mu k$, which applies to laminar free convection, is abbreviated Ra , the Rayleigh number. As in forced convection, the physical properties should be evaluated at t_f for either heating or cooling. The thermal and velocity boundary layers are rather thin ($2.7 Z/Nu$ for case e , Table 9), so that free-convection h values are generally the same for the unsteady-state heating or cooling of a fluid and for the steady-state process with another sink or source of heat, respectively.

Table 8. Surface Average Nusselt Number in Forced Convection Normal to Tubes, Screens, and Beds

Designation	Case	Limitations	Relation	Reference
a } b } c }	Nonmetals normal to a circular or streamline section cylinder	$0.1 < Re < 1000$	$\bar{Nu} = (0.35 + 0.47Re^{0.52})Pr^{0.3}$	28
	Gases normal to a cylinder	$1000 < Re < 50,000$	$\bar{Nu} = 0.26 Re^{0.6} Pr^{0.3}$	
		High Δt ; $Re'' = D\bar{u}_p/\nu_f > 100$	$\bar{Nu} = 0.46(Re'')^{1/2} + 0.00128 Re''$	
d	Metals normal to a cylinder Nonmetals through a staggered bank of tubes:	"Turbulent"	$\bar{Nu} = 0.80 Pe^{1/2}$	20
e	5th and later banks	$500 < Re < 75,000$	$\bar{Nu} = 0.36(Re)_{max}^{0.6} Pr^{1/2}$	29
f	5th and later banks	$75,000 < Re$	$\bar{Nu} = 0.38(Re)_{max}^{0.6} Pr^{1/2}$	30
g	1st, 2d, 3d, and 4th banks		60, 75, 94, and 97% of e , above	
h	Nonmetals through tubes in line:		60% of e , above	
i	1st and 2d banks		70% of e , above	31
j	3d and 4th banks		80% of e , above	
k	5th and later banks			
l } m }	Mercury (100°F) through a staggered bank of 1/2-in. tubes 3/8 in. apart (all but 1st, 3d, and last banks)	$10^4 < Re_{max} < 10^5$	$\bar{h} = 11.6 Re^{0.52}$	26
		nonwetting	$\bar{h} = 3.45 Re^{0.66}$	
		wetting	$\bar{Nu} = 4 + 0.23 Pe_{max}^{3/5}$	
n	NaK through a staggered tube bank		$\bar{Nu} = 1.17(Pe_{max})^{0.8} Pr^{1/2}$	31
o	Any liquid on the shell side of a heat exchanger with segmental baffles	$D =$ tube OD, $D' = D$, between tubes, in.	$\bar{Nu}_D = 0.19(D')^{0.6} Re_D^{0.6} Pr^{1/2}$	32, 37
p	Nonmetal flowing past normal pins or small parallel strips	$200 < Re_p = \frac{pG_{max}}{\mu} < 20,000$ where $p =$ perimeter	$\bar{Nu}_p = 1.0 Re_p^{1/2} Pr^{1/2}$	33, 34
q	Heat transfer between packed bed and nonmetal flowing through $D =$ diameter of sphere of same surface	$Re_D < 350$	$\bar{Nu}_D = 1.96 Re_D^{0.59} Pr^{1/2}$	35
		$Re_D > 350$	$\bar{Nu}_D = 1.06 Re_D^{0.48} Pr^{1/2}$	35
r	Heat transfer between cylindrical wall of packed bed of diameter D_w and nonmetal flowing through		$\bar{Nu}_D = 0.813 e^{-0.2D/D_w} Re_D$	36

If there are no other walls near the heat-transfer surface or surfaces, "external" or "local" free circulation is obtained. Table 9 and Fig. 3 give available empirical correlations. These have generally been determined for uniform t_w or for cases intermediate between uniform t_w and uniform q/A . The former case gives somewhat lower \bar{h} values. Thus Table 9 is reasonably accurate for cases of constant t_w and slightly conservative for constant q/A . More detailed summaries are available³⁹ of natural convection under various conditions, including with heat generation within the fluid.

When conditions are such that free convection and forced convection exist simultaneously, the values of h expected by each separate mode should be calculated. If one is considerably larger, it controls the heat transfer. Approximate rules for intermediate cases are given in Table 10; for rough estimates they can be extended to other geometries.

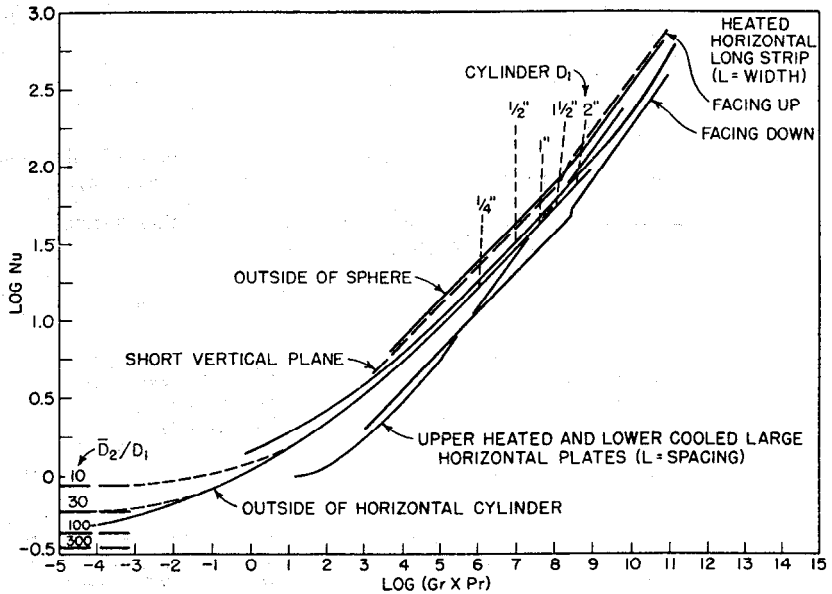


FIG. 3. Heat transfer by free gravity convection between solid surfaces and nonmetallic liquids. (From C. F. Bonilla, Ref. 98.)

Table 9. Local Free- or Gravity-convection Heat Transfer without Fluid-phase Heat Generation

Designation	Case	Limitations	Relation	Reference
a	Nonmetals at a vertical wall or large tube ($L = \text{height}$)	$10^{-2} < Ra < 10^3$	$Nu = 1.12 Ra^{0.16}$	5
b		$10^3 < Ra < 10^4$	$Nu = 0.555 Ra^{1/4}$	5
c		$10^4 < Ra < 3 \times 10^{10}$	$Nu = 0.73 Ra^{1/4}$	5
d		$3 \times 10^{10} < Ra < 10^{12}$	$Nu = 0.13 Ra^{1/5}$	5
e	Any fluid at a vertical wall	$Ra < 10^8$	$Nu = 0.667 [Pr^2 Gr / (Pr + 0.952)]^{1/4}$	38
f	Nonmetals at a vertical wire ($L = \text{diameter}, Z = \text{height}$)	$10^{-11} < Ra \frac{D}{Z} < 3 \times 10^{-5}$	$\frac{1}{Nu} = 1.15 \log \left[1 + 4.47 \left(Ra \frac{D}{Z} \right)^{-0.26} \right]$	40
g	Nonmetals with heat flow between enclosed parallel flat vertical walls ($L = \text{spacing}, H = \text{height}, 3 < H/L < 42$)	$Ra < 10^3$	$Nu = 1$	5
h		$10^4 < Ra < 10^5$	$Nu = 0.20 Ra^{1/4} \left(\frac{L}{H} \right)^{1/6}$	5
i		$10^5 < Ra < 10^7$	$Nu = 0.072 Ra^{1/3} \left(\frac{L}{H} \right)^{1/6}$	5
j	Any fluid at a horizontal cylinder or bank of cylinders ($L = \text{cylinder diameter}; \text{add twice the mean free path if appreciable}$)	$Ra < 5,400L \text{ ft}$	$\frac{1}{Nu} = 1.15 \log \left[1 + 3.77 \left(\frac{Pr + 0.952}{Pr^2 Gr} \right)^{1/4} \right]$	42
k		$D > 0.01 \text{ ft}$	$Nu = 0.53 \left(\frac{Pr^2 Gr}{Pr + 0.952} \right)^{1/4}$	42
l	Nonmetals between concentric horizontal or vertical cylinders ($L = D_2 - D_1$)	$Ra < 10^4$	$Nu = 1$	5
m		$5 \times 10^4 < Ra < 10^7$	$Nu = 0.060 Ra^{0.29}$	5
n		$10^7 < Ra < 10^9$	$Nu = 0.26 Ra^{0.20}$	5
o	Nonmetals at a horizontal strip facing upward ($L = \text{width}$)	$10^3 < Ra < 10^9$	$Nu = 0.71 Ra^{1/4}$	5
p		$10^9 < Ra$	$Nu = 0.162 Ra^{1/5}$	5

Table 10. Combined Free and Forced Convection

Designation	Case	Limitations	Relation	Reference
a	Nonmetals flowing normal to a horizontal cylinder (turbulent)	$3 < Nu_{forced}/Nu_{free} < 1/3$ $2 > Nu_{forced}/Nu_{free} > 1/2$	$Nu = \text{the larger } Nu$	43
b	Nonmetals flowing normal to a horizontal cylinder (turbulent)	Counterflow	$Nu = 0.9 \times \text{the larger } Nu$	43
c	Nonmetals flowing normal to a horizontal cylinder (turbulent)	Crossflow	$Nu = 1.1 \times \text{the larger } Nu$	43
d	Nonmetals flowing normal to a horizontal cylinder (turbulent)	Parallel flow	$Nu = 1.2 \times \text{the larger } Nu$	43
e	Nonmetals flowing upward in a short, heated, vertical tube (turbulent)	$Re/Ra^{0.4} < 8.25$	$Nu = Nu_{free}$	44
f		$8.25 < Re/Ra^{0.4} < 15$	$Nu > 0.75 Nu_{forced}$	44
g		$Re/Ra^{0.4} > 15$	$Nu = Nu_{forced}$	44
h	Nonmetals flowing downward in a short, heated, vertical tube (turbulent)	$Re/Ra^{1/3} > 18$	$Nu > Nu_{free}$	44
i	Nonmetals flowing in vertical pipes at constant q/A (laminar)	Theory		45
j		$500 < Gz < 2500; 10^4 < Ra \frac{D}{L} < 10^7$	$h_{down} = 2h_{up} \pm$	46

4 CONDENSING VAPORS

The theoretical formulas assume that the $(\Delta t)_f$ across the condensate film is uniform. At substantially all reasonable condensation rates⁵ the outer condensate layer temperature may be assumed equal to the saturation temperature of the vapor, though "temperature jump" occurs at the vapor-condensate interface at high q/A and low pressure.⁴⁷

Streamline film-wise condensation on vertical surfaces:

$$\bar{h} = 0.943 \left(\frac{\lambda g \rho^2 k^3}{\mu L \Delta t} \right)^{1/4} = 0.925 \left(\frac{k^3 g \rho^2}{\mu \Gamma} \right)^{1/3} \quad (30)$$

where λ is the latent heat of vaporization and Γ the condensate mass flow rate per unit width at distance L down. The local h at L is three-fourths of \bar{h} down to L . For a plane ϕ off the vertical, multiply h by $\cos \phi$.

Turbulent film-wise condensation on vertical surfaces (actual for nonmetals):

$$\bar{h} = 0.0134 \left(\frac{k^3 \rho^2 g}{\mu^2} \right)^{1/3} \left(\frac{\Gamma}{\mu} \right)^{0.4} \quad (31)$$

Streamline film-wise condensation on n horizontal tubes in a vertical bank:

$$\bar{h} = 0.724 \left(\frac{\lambda g \rho^2 k^3}{\mu n D \Delta t} \right)^{1/4} = 0.76 \left(\frac{k^3 g \rho^2}{\mu \Gamma} \right)^{1/3} \quad (32)$$

\bar{h}_n for the n th tube = $\bar{h}_1 [n^{3/4} - (n-1)^{3/4}]$. Valid for a single tube with $n = 1$.

Theory for metals:⁴⁹ Use Eq. (30) for $0 < 4\Gamma/\mu < 10^4+$. Actual h may be much lower at high Δt ;⁴⁷ that is, q/A in Btu per hour per square foot for Hg vapor up to 15 psia = $400,000 + 1000\Delta t$ for Δt in degrees Fahrenheit and = $22,000\Delta t - 36,000$ for Na vapor whenever these Δt values $> \Delta t$ by Eq. (30) or (32).

High downward vapor velocity can increase h 10-fold.^{48,50}

Ripples start in vertical film-wise condensation when $(s^3 \rho / \mu^4 g) < 0.3 Re^{0.8}$, increasing h appreciably (s = surface tension).

Drop-wise condensation on vertical surfaces occurs on smooth surfaces when the vapor-phase wetting angle is appreciably less than 180° . It may be maintained by adding an unwetted nonvolatile compound that will adhere to the surface. With

nonmetals h is usually increased 5 to 10 times over Eq. (30). With metals h may be lower than in film condensation; i.e., for Hg vapor at 15 psia.⁴⁷

$$\frac{q}{A} = 500,000 \text{ Btu}/(\text{hr})(\text{ft}^2) \text{ at } \Delta t = 300^\circ\text{F}$$

Presence of noncondensable gas even in traces³⁸ will greatly decrease h if it is not swept away effectively parallel to the surface, and somewhat even if it is. Small diameters decrease h on horizontal tubes below Eq. (32), as the pendant drops cover appreciable fractions of the condensing surface. Yet smaller diameters increase h above Eq. (32) because surface tension keeps the condensate film thin by squeezing it over to preferred spots, from which it drops off.

5 BOILING LIQUIDS

5.1 Boiling in Nuclear Reactors

Originally it was generally assumed that saturated boiling could not be permitted in nuclear reactors.⁵¹ This assumption was due primarily to fear of the flow instability obtainable in parallel coolant channels, which might immediately decrease the flow rate until boiling dry and burnout occurred in any channel in which boiling might commence. Other adverse possibilities were burnout due to film boiling even without flow instability (see Fig. 4) and burnout due to scale formation, as occurs in fuel-fired boilers. It was also anticipated that jumps in reactivity and thus power level might take place, and possibly nuclear runaway, if the bubbles collapsed as a result of a pressure or cold-liquid surge. Scramming might also occur with increased turbine load owing to reactor-pressure falloff and coolant flashing just when more power is needed. Thermal fatigue of the fuel elements might also occur as a result of local oscillation of coolant density and thus of cooling power and surface temperature. Local thermal-neutron flux and therefore heating density fluctuations would also occur because of the boiling, particularly with H₂O on account of its short neutron-diffusion length, and might also cause thermal fatigue. While subcooled boiling is much less unstable than saturated boiling, in that the increase in pressure drop and in volume are much smaller, some fluctuation would occur, and it was considered too close to saturated boiling for safety.

However, tests with the Borax reactors and with EBWR have shown that boiling reactors can operate smoothly and protect themselves against reasonable sudden reactivity jumps. Borax 1 was not damaged until a reactivity of nearly 4 per cent, corresponding to a period of 0.0026 sec, was suddenly applied to the cold core. In the hot or boiling conditions the protection would be better, as further bubble formation would occur sooner. EBWR in normal operation bypasses straight to the condenser, through an automatically controlled valve, some 5 per cent of the steam generated. This corrects for any sudden reactivity changes, control rods taking care of slower load changes. When the reactor was running at 600 psi and full load, for instance, a sudden closing of the turbine inlet valve was accomplished without the reactor pressure rising even to 630 psi, the scram setting. It is evident that boiling reactors, with their considerable saving in operating pressure, will have importance in commercial power. In addition, the study of boiling is necessary in predicting the course of power surges and in design to prevent accidents.

Boiling can occur at a heated surface in two ways according to the temperature of the liquid, three according to the temperature of the surface, and three according to the method of circulation of the liquid and vapor. If the liquid is at the boiling point, "saturated," "bulk," or "net" boiling is said to occur. If the liquid is below the boiling point, "subcooled," "local," or "surface" boiling is obtained. If the temperature of the surface is not much above the boiling point, "nucleate" boiling occurs; if it is well above, "film" or "stable-film" boiling; and if it is intermediate, "partial-film," "mixed," "unstable-film," or "metastable-film" boiling. If the circulation is by natural convection in a large vessel, "pool" boiling is occurring; if it

is in a restricted pipe or loop, "thermal-siphon" or "thermal-circulation" boiling. If a pump maintains the flow regardless of buoyancy, "forced-convection" boiling is present. The 18 possible combinations of these characteristics have almost all been studied, and almost all have actual or potential interest in nuclear power. All these, plus homogeneous boiling, are listed in Table 11.

Table 11. Types of Boiling

Method of fluid circulation past heated surface	Liquid temperature	Method of vaporization	Type
Free or external natural convection (in a large volume or pool of liquid)	Subcooled	Nucleate	1
		Mixed	2
		Film	3
	Saturated*	Nucleate	4
		Mixed	5
		Film	6
Confined or internal natural convection (by "thermal siphon" in a closed loop or conduit)	Subcooled	Nucleate	7
		Mixed†	8
		Film	9
	Saturated*	Nucleate	10
		Mixed†	11
		Film	12
Forced convection (past open surfaces or inside of conduits)	Subcooled	Nucleate	13
		Mixed	14
		Film	15
	Saturated*	Nucleate	16
		Mixed†	17
		Film	18
No heated surface—homogeneous heat generation and boiling.	Saturated*	Nucleate	19

* Actually slightly superheated at the lower pressures. (M. Jakob, "Heat Transfer," John Wiley & Sons, Inc., New York, 1949.)

† These cases have not been studied experimentally so far.

The stages of saturated pool boiling, shown in Fig. 4, will be discussed qualitatively to illustrate certain general characteristics.

In most equipment low heat velocities can be dissipated without boiling, usually by natural convection of the liquid to a cooled wall or to the free surface, vaporization occurring there because of the lower boiling point. When natural convection cannot maintain the heating surface below the boiling point (point *A*), bubbles begin to form at favored nuclei in the surface, which constitutes nucleate boiling. Natural convection of the liquid is still the principal cause of circulation at low boiling rates (i.e., zone *A-A'*).

If the liquid has not yet heated up to its boiling point or is kept below it by simultaneous cooling, type 1 boiling occurs, or even type 2 or 3 at high enough Δt . If and when the liquid rises to its boiling point, type 4 boiling commences. Beyond *A'* the bubbles increase the natural convection circulation, so that beyond *A'* in strong nucleate boiling the whole mass of liquid is usually circulating rapidly at a very uniform temperature, except for a small amount of superheat near the heating surface. As t_w and thus Δt are increased, the number of nuclei for which Δt is sufficient superheat to initiate ebullition goes up rapidly, as well as the agitation by the bubbles formed. The line *A'DC* usually has a slope from 3.4 to 3.6 and is fairly straight.

Once the heating surface and immediately adjacent liquid film have reached the necessary superheats, vapor formation starts immediately, several milliseconds being adequate with a large power burst for expulsion of a small volume of liquid.⁵¹

At some point *B* a maximum is reached in the rate at which the vapor bubbles can leave the boiling surface and the liquid can yet reach it by simultaneous counterflow. When liquid cannot reach the surface at the same rate at which it is boiling away, depletion of liquid at the surface occurs immediately, the surface temperature rises further (at least locally), and the increasing molecular velocity of the vapor finally forms a vapor "film" that holds the liquid away from the surface. This vapor binding

or "film boiling," which causes the "spheroidal state" of water drops on a hot stove, irregularly but increasingly replaces nucleate boiling over the region *BEG* of film boiling (type 5). Beyond *G*, film boiling (type 6), and radiation to an increasing amount, are the methods of heat transfer.

If the heated surface is maintained at a definite temperature t_w by a condensing vapor or a rapidly circulating fluid stream and the boiling liquid temperature l is fixed by pressure control, Δt is constant and the corresponding q/A by Fig. 4 will be obtained. No over-all instability will be observed at any operating condition, except the local instantaneous fluctuations due to bubbling, or to alternate nucleate and film boiling in region *BEGF*. Most design is in the region *ADC*, to obtain the smallest necessary Δt . Film boiling, however, is useful if it is desired to "waste temperature," as in cooling a high-temperature loop by boiling water at atmospheric pressure. It may also be employed at low q/A for more accurate control.

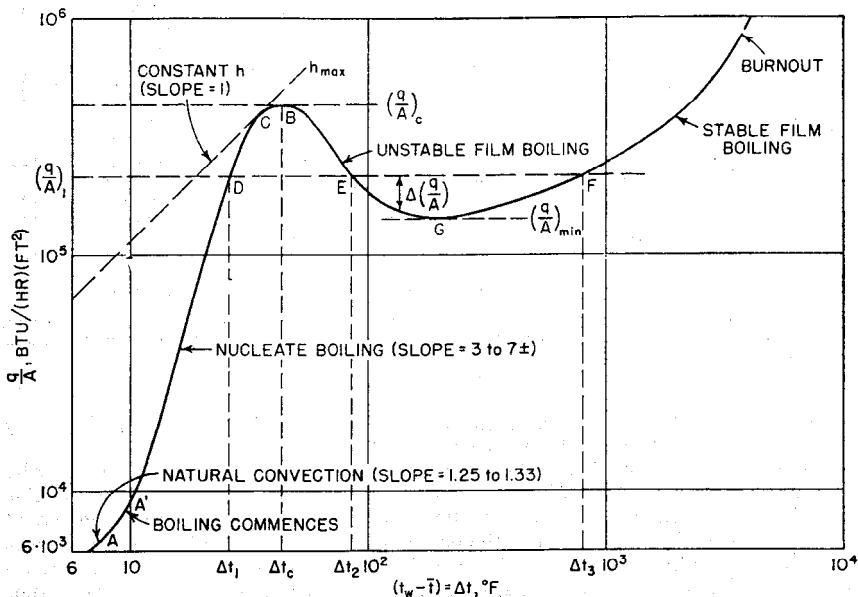


FIG. 4. Saturated pool boiling at a submerged horizontal plate or tube. (From C. F. Bonilla, Ref. 98.)

However, if q/A to the boiling surface is set at $(q/A)_1$ in Fig. 4, as in a nuclear-reactor fuel element, there are evidently three possible values of Δt . *E* is shown as follows to be unstable. If an instantaneous increase occurs in heat velocity to the boiling surface, its temperature will rise. But by the curve this means that q/A removed by boiling will drop. Thus an even larger net q/A remains to heat the surface further. This rate of heating of the surface is proportional to $\Delta(q/A)$ in Fig. 4 and accelerates to a maximum at *G*, then decelerates and again yields steady operation at *F* if the surface or the heat-generating element behind it have not melted or otherwise "burned out" in the process. By the same analysis, an instantaneous decrease in q/A carries Δt down to Δt_1 at *D*. A similar consideration shows that *D* and *F* are stable operating points. If operation at high film-boiling temperatures is to be avoided, the "critical" heat velocity $(q/A)_c$ must, of course, not be reached.

Available information on the 19 types of boiling is summarized in Arts. 5.2 to 5.5. Equations are in consistent units when dimensionless. Other quantities are in units of feet, pounds, hours, degrees Fahrenheit, and Btu, particularly if primed, unless otherwise stated.

5.2 Free Natural-convection Boiling

5.21 Subcooled Liquid.* Subcooled free- or gravity-convection boiling could be significant in nuclear reactors cooled by internal natural convection or slow forced convection. However, very little information on it is available. The following can be used as a guide in design work, but tests under actual conditions are called for in most cases.

1. *General.* This type of boiling has been studied over a wide range of Δt by quenching the desired shapes in cold water and following their temperature. The results are probably also reasonably valid for steady-state operation. A general correlation has been proposed⁵² for the quenching of steel rods of radius R :

$$\text{Nu} = 407,000 \left(\frac{s}{\rho_L R^2} \right)^{1.275} - \text{Pr}^{-1/3} \left(\frac{\Delta t_{\text{sub}}}{\Delta t_{\text{sat}}} \right)^{2.466} \quad (33)$$

where s is the surface tension of the liquid. However, other experience⁵³ shows very irregular effects of small changes in subcooling and gas content. Considerable noise and vibration usually develop in subcooled boiling. The average life of a bubble is of the order of 0.001 sec and correlates with bubble size $(q/A)_c$ and the physical properties.⁵⁴

2. *Effect of Diameter on $(q/A)_c$.* Steady data for wires are also available. Platinum wire of 0.0039-in. diameter burns out⁵ at a $(q/A)_c$ of 1,200,000 Btu/(hr)(ft²), 55 per cent of that for the 2-in. cylinder,[†] and 0.0079-in. nickel wire⁶⁶ at about 1,320,000. Values of $(q/A)_c$ for other diameters in water at 14.7 psia and 144°F subcooling could be approximated by a log-log interpolation of $(q/A)_c$ versus D . A tight horizontal coil with turns as little as $D/2$ apart still agrees with straight wire.⁵⁵

3. *Effect of Liquid, Subcooling, and Pressure on $(q/A)_c$.* For other liquids, subcoolings, and/or pressures, $(q/A)_c$ may be obtained within some 20 per cent by the correlation⁵⁷

$$\left(\frac{q}{A} \right)_{c,\text{sub}} = \left(\frac{q}{A} \right)_{c,\text{sat}} \left[1 + \frac{c_p \Delta t_{\text{sub}}}{25\lambda} \left(\frac{\rho_L}{\rho_V} \right)^{0.923} \right] \quad (34)$$

Δt_{sub} is $t_{\text{sat}} - \bar{t}$; at t_{sat} pressure of the liquid plus any dissolved gas equals that on the system.⁵⁵ $(q/A)_{c,\text{sat}}$ is obtained from Fig. 7 and seems to vary little with diameter. $(q/A)_{c,\text{sub}}$ by Eq. (34) is for small wires; thus it should be conservative for most fuel elements (according to 2, above). Values of $(q/A)_{c,\text{sub}}$ for type 1 boiling could also be approximated from reliable correlations for type 11 boiling by substituting zero velocity.

4. *Effect of Subcooling on Δt_c .* Available data⁵ show t_c for a wire constant as subcooling is changed all the way to zero. Thus Δt_c for any subcooling can be computed if it is known at one subcooling or for saturated boiling (i.e., Fig. 6).

5. *Type 1 Boiling on Wires.* If $(q/A)_c$ and $(\Delta t)_c$ are known or can be estimated, Δt can be approximated for lower values of q/A because q/A falls off about as $(\Delta t_{\text{sat}})^{3.1}$. For 0.0079- and 0.01-in. wires in water at 0 psig⁵⁵ $q/A = 0.54(\Delta t_{\text{sat}})^{3.1}$ Btu/(hr)(ft²)(°F) for $\Delta t > 30^\circ\text{F}$. No large effect of diameter on this curve would be expected, the same as in type 4 boiling, since the circulation is similar to that in liquid-phase natural convection, in which h is independent of L or almost so (Table 9, items d , k , and p).

6. *Effect of Dissolved Gas.* Dissolved gas is of interest because of the dissociation of H_2O and D_2O , etc., in reactors. Increasing the dissolved-gas content decreases t_{sat} at a given pressure. Since Δt_{sat} is primarily a function of q/A for each liquid, t_{sat} , Δt and t_w decrease about equally.⁵⁵ Accordingly, a given q/A can be dissipated with a

* Table 11, types 1, 2, and 3.

† This lower $(q/A)_c$ must in part be due to the small heat capacity per unit surface for wires and thus high susceptibility at constant heat-generation rates to overheating from local instantaneous fluctuations in heat-removal rate caused by bubbles. It must also in part be due to nonuniformities in wires, which cause hot spots, and to the (usual) increase of electrical resistance with temperature, which causes an overheated spot to generate yet more heat. Direct-current heated wires thus yield conservative values of $(q/A)_c$ compared with nuclear heating and larger shapes, and a-c even more so.

considerably lower t_w in the presence of gas. On the other hand, vapor phase would start to form at a lower q/A than with degassed water, which would be undesirable for smooth operation because of the change in moderation or neutron economy, though it might be desirable as a safety feature. Gas also decreases $(q/A)_c$ significantly,⁵⁵ as is shown in Fig. 5.

5.22 Saturated Liquid, Nucleate Boiling.* Saturated nucleate pool-boiling data for useful reactor coolants are shown in Fig. 6. D₂O may be assumed to follow the H₂O curves.

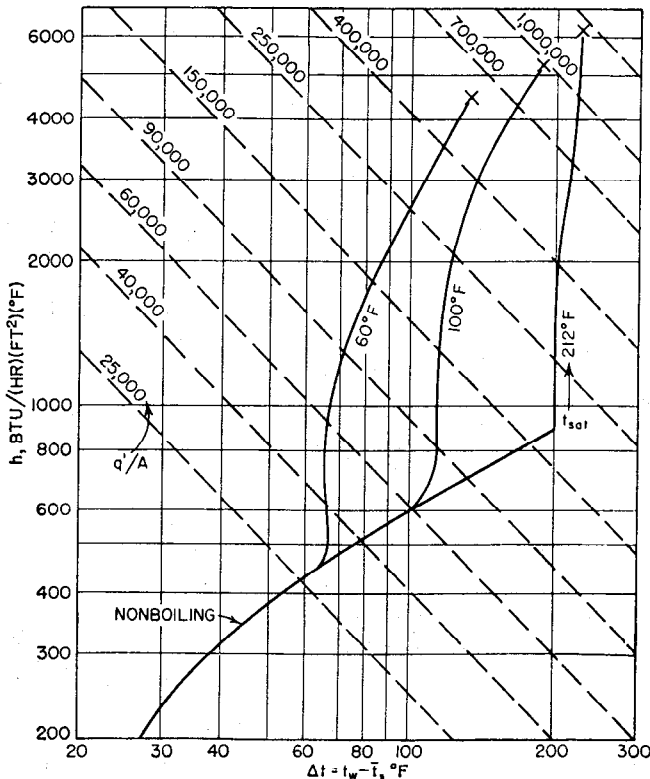


Fig. 5. Effect of dissolved gas on natural convection subcooled boiling water at atmospheric pressure from wires. X = burnout (nickel wire). (From C. F. Bonilla, Ref. 98.)

1. *Effect of Shape.* Cylinders and plates and even 10 vertical banks of tubes²⁹ yield the same coefficients at the same P and q/A . Addition of shallow fins decreases Δt for a given heat dissipation, as would be predicted with the fin area and efficiency. Wires⁶² give up to about one-fourth higher $(q/A)_c$ and h , because of the greater accessibility to surrounding liquid. At low q/A , h at wires also falls less because of more effective natural convection and because of surface tension squeezing the vapor to fewer locations before release.⁶³

2. *Effect of Pressure.* Increase of pressure and temperature always decreases Δt ⁶⁴ or increases h in nucleate boiling. A correlation⁶² for any one liquid is

$$\frac{c \Delta t}{\lambda} = K \left[\frac{q/A}{\mu \lambda} \left(\frac{g c s}{g \Delta \rho} \right)^{1/2} \right]^{0.33} \text{Pr}^{1.7} \quad (35)$$

* Table 11, type 4.

$K = 0.013$ for water on clean platinum and 0.0060 on clean brass. Other surfaces and liquids require other values of K . Uncertainty is about ± 30 per cent. λ is the latent heat of vaporization, and s is the surface tension in force per unit length. Increase of pressure narrows down the range in which boiling can occur by bringing together the natural-convection limit below and the threshold of film boiling above.⁵⁸ Moderate increases in P at normal pressures⁵⁶ roughly increase h proportionally to $P^{0.25}$ to $P^{0.4}$. The highest h values are near the critical pressure and are about $18P_c$ Btu/(hr)(ft²)(°F) for P_c in pounds per square inch absolute.

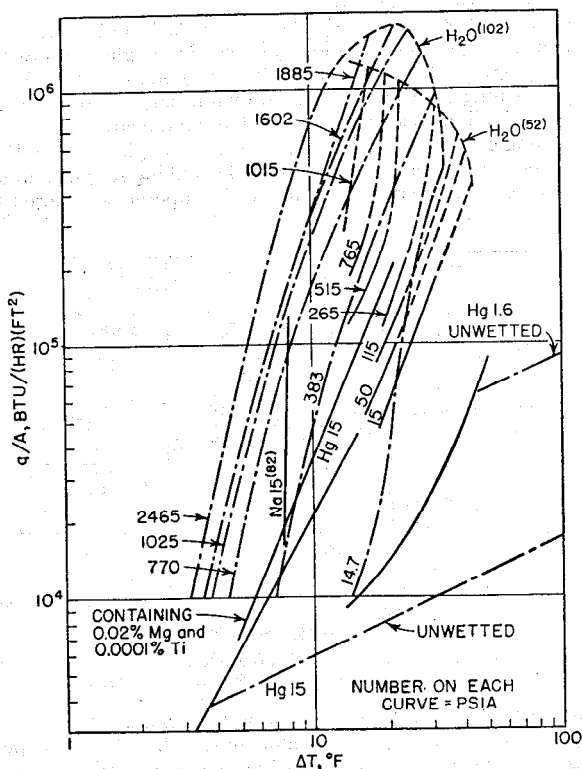


FIG. 6. Heat transfer to liquids in pool boiling at plates and tubes under pressure. (From C. F. Bonilla, Ref. 98.)

3. *Effect of Agitation.* At low q/A additional agitation by forced convection or by bubbles or particularly vapor jets may increase h several fold.⁵⁹ A liquid velocity \bar{u} past a boiling surface multiplies the nonboiling h by $\left(1 + \frac{\bar{u}\lambda\rho_L}{q/A}\right)^{0.18}$ approximately.⁶⁰

At high q/A there is no appreciable increase in h , nor in $(q/A)_c$ or $(\Delta t)_c$. Vapor flow past the top of a vertical plate, tube, or deep bundle may even decrease the local h .

4. *Effect of Surface Roughness.* Long operation can cause h to decrease as much as 70 per cent without apparent soiling. Cleaning or aeration restores it. Coarse scratches increase h more than fine ones, and separated deep scratches even more so; 0.25 in. apart is best for water at atmospheric pressure.⁶¹

5. *General Correlations.* A rough general correlation of type 4 boiling is Lukomskii's plot²⁹ of $(q/A)/(q/A)_c$ versus $\Delta t/(\Delta t)_c$. Averaging many data, he suggests a straight line on rectangular coordinates going upward from $q/q_c = 0.15$ and $\Delta t/\Delta t_c = 0.3$ to $(0.9, 0.9)$, then curving over to a slope of 0 at $(1, 1)$.

6. *Liquid Mixtures.* Both miscible and immiscible mixtures require a Δt up to several times that interpolated or estimated, respectively, from the pure components.

7. *Effect of Metal Surface.* There is a definite effect of the metal, due probably to wetting angle, centers for nucleation, and thermal diffusivity. For instance, in boiling ethanol, freshly polished Cu, Au, and Cr and aged Cr show successive 20 per cent increases in Δt at a given q/A .⁵⁶

8. *Low Boiling Rates.* If Δt is so small that $(Ra) < 10^{10}$, liquid natural convection predominates and Table 9, item b, or equivalent applies for vertical surfaces and Table 9, item o, for horizontal surfaces.⁵

9. *Bubble Volume and Frequency.*^{5,56} The theoretical bubble volume V on release as a function of surface tension for liquid-phase wetting angles ψ up to 140° in degrees is $0.000048(\psi^2 s g_c / g \Delta \rho)^{3/2}$. If ψ is unknown, 50° is a good average. Above the boiling surface V in rapid boiling grows to an ultimate value some 50 per cent larger (several times larger in slow boiling) because of the liquid superheat. Bubble frequency per second from a boiling nucleus at moderate pressures is roughly $64V^{-0.215}$ for breakup V in cubic millimeters. A bubble is stable in superheated liquid if its diameter = $4s/\Delta p$, where Δp is the increase in vapor tension due to the superheat. Larger bubbles grow, and smaller ones condense.

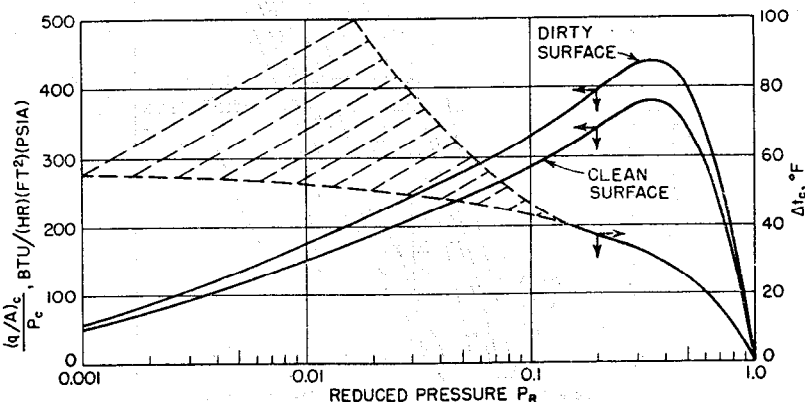


FIG. 7. Correlation of Δt_c and $(q/A)_c$ at peak of nucleate boiling for nonmetallic liquids under pressure at plates and tubes. (From C. F. Bonilla, Ref. 98.)

Vapor volume holdup is important in predicting the change in moderation it causes and in selecting the volume of expansion tanks required. General experience is that up to 50 per cent of the total volume between closely spaced tubes or flat vertical plates can safely be, and will be, vapor at high heat-transfer rates when there is negligible restriction of the recirculating liquid.

The relative or "slip" velocity u_s of the vapor bubbles with respect to the liquid can be estimated by Fig. 6, Sec. 9-2. For low q/A boiling, a conservatively high value of per cent vapor volume could be estimated by neglecting the liquid velocity. For higher q/A a liquid velocity \bar{u}_L up from the heat source can be assumed, the vapor volume V_V at vapor velocity $u_s + \bar{u}_L$ computed, and then a check made as to whether the liquid velocity head $\bar{u}_L^2/2g_c$ equals the buoyant head $V_V(\rho_L - \rho_V)/A_H \rho_L$, where A_H is the horizontally projected area of the heat source. This method is rough, partly because higher u_s is observed than given by Fig. 6 of Sec. 9-2 (i.e., Fig. 8), vapor momentum is neglected, and stream cross section is uncertain. For reliable design, tests should be carried out for the specific conditions of interest.

Although high t_w is required for rapid initiation of boiling, it is of importance in providing safety for boiling reactors that no additional time delay has been found to occur prior to steam formation.⁵¹

10. *Maximum Boiling Rate $(q/A)_c$.* The critical $(q/A)_c$ at which film boiling initiates is obtainable from Fig. 7 for liquids normally boiling above room tempera-

ture.⁵⁸ $(q/A)_c$ is increased slightly by stirring.⁶⁴ The following correlations also yield accuracy of about ± 20 per cent but require physical properties:

Addoms⁵⁹ for $P_r < 0.7 \pm$:

$$\left(\frac{q}{A}\right)_c = 2.2\lambda\rho_V \left(\frac{gk}{c_p\rho}\right)_L^{1/3} \left(\frac{\rho_L}{\rho_V} - 1\right)^{1/2} \quad (36)$$

Rohsenow,⁶⁵ using feet and hours:

$$\left(\frac{q}{A}\right)_c = 14.3\lambda\rho_V \left(\frac{\rho_L}{\rho_V} - 1\right)^{0.6} \quad (37)$$

Kutateladze:⁶⁷

$$\left(\frac{q}{A}\right)_c = 0.16\lambda[sgc_p\rho_V^2(\rho_L - \rho_V)]^{1/4} \quad (38)$$

Soiled surfaces average 25 per cent higher $(q/A)_c$. Though these relations include no effect of the metal, other data on wires show over 2-to-1 variation in $(q/A)_c$ under identical conditions with different metals.⁵

11. Δt_c . The temperature difference Δt_c at or causing the termination of saturated pool nucleate boiling (see Fig. 7) is increased slightly by stirring.⁶⁴ It increases with viscosity,⁴¹ going, for instance, from 58 to 220°F on changing from pure water to pure glycerin boiling at atmospheric pressure from a platinum wire. It also varies with the metal; for water at 1 atm Pt black gave 55°; shiny Pt, 58°; Fe, 59°; Ag, 72°; Ni, 83°; Cu, 87°; and Pb, 104°F (this series is the same as for hydrogen overvoltage). Of these metals, only Pt did not melt on going into film boiling at $(q/A)_c$.

12. *Surface-active Additives.* h for boiling water at moderate pressures can be increased some 20 per cent by adding soluble wetting agents.²⁹ h for mercury is also improved by Na or Mg, but more important is the increase in $(q/A)_c$. Effect of additives on $(q/A)_c$ for H₂O has not been reported. Soluble salts generally decrease h .

13. *Liquid Metals.* As per Fig. 6, liquid metals give h values comparable to water when they wet the boiling surface. However, Hg and Cd tend not to wet stainless steel even with traces of Na and Mg, respectively, as dissolved wetting agents.⁷³ Pure Hg on stainless steel and on plain steel tends to shift on use and deaeration from type 6 to 4 boiling if $q/A > 10,000 \pm \text{Btu}/(\text{hr})(\text{ft}^2)$. On wetted steel or other surfaces it tends to superheat and bump because of the high surface tension and bubble-formation superheat of liquid metals.⁷⁴

5.23 Saturated Liquid, Mixed Boiling.* On log scales the region *BE* (Fig. 4) is roughly a mirror image of *BD*. *BEG* may thus be approximated by drawing a mirror image of *DB* from $(q/A)_c$ and Δt_c , then curving it to tangentially intersect *FG* (see Art. 5.24 discussion). Alternatively, a Lukomskii plot (see paragraph 5 under Art. 5.22) can be extended on linear coordinates by a curve from $q/q_c = 1$ and $\Delta t/\Delta t_c = 1$ roughly to (0.9,1.1), then straight to (0.2,1.8). Strong stirring can raise the curve 100 per cent.⁶⁴

5.24 Saturated Liquid Film Boiling.† Saturated natural-convection "stable-film" pool boiling at atmospheric pressure yields h values of only some 15 to 80 Btu/(hr)(ft²)(°F), about 1 per cent of those in nucleate boiling. The blanketing vapor film rises because of its buoyancy in the same way that a condensate film falls by gravity in condensation, and similar relations apply. There is no appreciable effect of surface metal or roughness except on the radiation contribution.

1. *Minimum q/A .* The minimum q/A (at *G*, Fig. 4) ranges from about 10 to 30 per cent of $(q/A)_c$, regardless of pressure or liquid, averaging about 20 per cent of $(q/A)_c$.⁵⁷ At pressures at least up to $P_r = 1/4$, $(q/A)_{\min}$ on tubes⁶⁶ is roughly directly proportional to P .

If a fuel element has gone over into film boiling (and not burned out), q/A must decrease to $(q/A)_{\min}$ to leave the film-boiling region. This takes place by a jump along the curve *GEBCD* and down on the nucleate-boiling branch to the existing q/A .

* Table 11, type 5.

† Table 11, type 6.

2. *h without Radiation.* Bromley has shown,⁸⁷ for the boiling film on horizontal cylinders 0.19 to 0.47 in. in OD at atmospheric pressure, that \bar{h}_{con} for conduction is given within ± 15 per cent by

$$\bar{h}_{con} = 0.62 \left[\frac{k_V^3 \rho_V (\rho_L - \rho_V) g \lambda}{D_{\mu V} \Delta t} \right]^{1/4} = 0.53 k_V \left[\frac{\rho_V (\rho_L - \rho_V) g \lambda}{D_{\mu V} q/A} \right]^{1/4} \quad (39)$$

where subscripts *V* and *L* represent vapor (at its average temperature) and liquid, respectively. The coefficient 0.62 is halfway between 0.724, theoretically derivable for no resistance to vapor flow by the liquid [see Eq. (32)] and 0.512 if the liquid is stationary.

By the same method, for a vertical wall,

$$\bar{h}_{con} = 0.80 \left[\frac{k_V^3 \rho_V (\rho_L - \rho_V) g \lambda}{L_{\mu V} \Delta t} \right]^{1/4} = 0.74 k_V \left[\frac{\rho_V (\rho_L - \rho_V) g \lambda}{L_{\mu V} q/A} \right]^{1/4} \quad (40)$$

where 0.80 is halfway between 0.943 [Eq. (30)] and 0.666 for stationary liquid.

3. *Effect of Superheat.* The sensible heat of the vapor stream is usually significant. Correction can be made²⁹ by multiplying λ by $(1 + 0.4 \Delta t c_p / \lambda)^2$.

4. *Effect of Diameter.* On small wires h is 30 to 100 per cent higher than predicted.²⁹ To fit wires as well as larger cylinders, Banchero et al.⁶⁸ replace $0.62 D^{-1/4}$ in Eq. (39) by $a_1/D + a_2$. From boiling O_2 and N_2 , $a_1 = 0.00375 \text{ ft}^{3/4}$ and $a_2 = 1.64 \text{ ft}^{-1/4}$ for D from 0.025 to 0.75 in.

5. *Effect of Radiation.* Radiation transfers additional heat but in so doing increases the film thickness, decreasing \bar{h}_{con} . The approximate effect is to add $\frac{3}{4} h_r$. If the other quantities are given, the wall temperature T_w can be most accurately computed⁶⁷ by trial and error from

$$\frac{q'}{A} = \left\{ 0.53 k_V \left[\frac{\rho_V (\rho_L - \rho_V) g \lambda}{D_{\mu V}} \right]^{1/4} \right\}^{4/3} \frac{(T_w - T_L)^{4/3}}{(q/A)^{2/3}} + \frac{1.73 \times 10^{-9} (T_w^4 - T_L^4)}{1/\epsilon_w + 1/\epsilon_L - 1} \quad (41)$$

ϵ_w is the wall emissivity, ϵ_L the effective liquid absorptivity (1 may be used for H_2O and D_2O and 0.1 for clean metals), and 1.73×10^{-9} is the Stefan-Boltzmann constant in $\text{Btu}/(\text{hr})(\text{ft}^2)(^\circ\text{R}^4)$.

5.3 Confined Natural-convection Boiling*

Thermal-siphon boiling has characteristics intermediate between the local-natural-convection and the forced-convection types. It differs from local natural convection in that the rest of the loop affects the circulating flow and h . It differs from forced convection in that the flow is directly dependent on the heat transferred. It occurs in water-tube boilers, evaporators, and free-boiling nuclear reactors with vertical tubes. Boiling between vertical parallel plates and in tube bundles in closed vessels also falls in this type, particularly if the circulation is reinforced by a vertical mixed-flow tube or chimney.

There are practically no data on subcooled or on film natural-convection boiling in tubes (types 7, 9, and 12). However, subcooled natural-convection boiling usually cannot be very effective by itself because of the small vapor volume, and film boiling probably also cannot promote strong circulation because of the film location of much of the vapor. Thus the relations for types 1, 3, and 6 boiling should apply, respectively, to types 7, 9, and 12.

Natural-convection nucleate boiling in tubes (type 10) has been studied frequently,²⁹ but again no useful general correlations are available to give h or w directly from given dimensions and conditions. Accordingly, one of the following three methods must be used to obtain rough design information:

1. Rough interpolation between values estimated for free natural convection and for slow forced convection by the methods of this chapter.

* Table 11, types 7 to 12.

2. Use of actual operating data for type 10 boiling in commercial boilers, etc. Large, 1,200- to 1,400-psi natural-circulation boilers⁷² generally employ 2.5- to 3-in.-ID tubes and yield inlet water velocities of 1.5 to 2 fps. Outlet qualities are 3 to 10 per cent, rising to 15 to 20 per cent at 2,400 psi. As with commercial type 16 boiling, their average q/A and other operating conditions are too low for optimum boiling nuclear-reactor design. The highest q/A is about 250,000 Btu/(hr)(ft²) of internal projected area but is seldom reached. The actual local maximum is lower because of conduction around the tube wall. However, these conditions are useful as conservative lower limits. If the circulating flow is regulated to a desired value, the methods for type 16 boiling may be used to estimate h . Some direct data on h are also available³⁸ for unregulated flow.

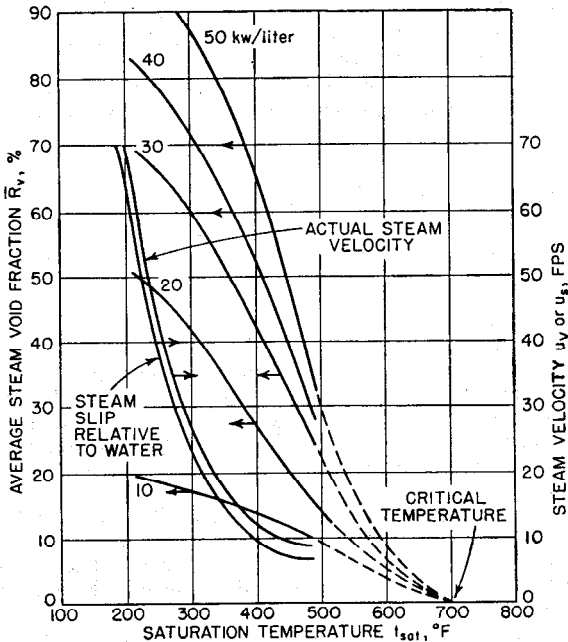


FIG. 8. Typical exit-steam velocity and exit-steam "slip" velocity at 50 kw/liter, and over-all average steam volume, in natural convection boiling of saturated water between vertical plates 5 ft high and $\frac{1}{2}$ in. apart. (From C. F. Bonilla, Ref. 98.)

Some experimental results are also available for possible boiling reactor geometries. Untermyer⁵¹ reports a definite slip velocity u_s , decreasing with pressure but independent of liquid velocity. u_s and R_V for upflow between parallel plates $\frac{1}{2}$ in. apart are given in Fig. 8. Bailey⁷⁰ also found u_s independent of u_L ; for water at room temperature and pressure, u_s equaled $1/R_L$ fps. Cook,⁷¹ for $\frac{1}{4}$ -in. spacing at 600 psi, found instead that \bar{u}_V/\bar{u}_L remains roughly constant at 2.5 ± 0.5 . R_V was substantially proportional to boiling length at constant q/A , which facilitates prediction of buoyancy pressure ΔP_B from an assumed outlet R_V . However, with $\frac{1}{2}$ -in. spacing Lottes⁶⁹ reports \bar{u}_V/\bar{u}_L about 1.5 at 250 psia, 2 at 100 psia, and 8 at 25 psia.

3. Estimating the flow rate by a trial-and-error calculation. A flow rate w is first assumed. The over-all average "voids" or fractional volume \bar{R}_V of vapor held up is next estimated. For the lower pressures $R_V = 1 - R_L$, from the upflow column of Table 5, Sec. 9-2. For higher pressures R_V is obtainable by interpolation between the low pressure and the P_c columns of Table 5, Sec. 9-2, or from the slip u_s , or from the relative velocity of vapor and liquid (see Art. 6.2 of Sec. 9-2). The buoyant pressure

$$\Delta P_B = (\rho_L - \rho_V) \frac{g}{g_c} \bar{R}_V \Delta z = (\rho_L - \rho_V) \frac{g}{g_c} \int R_V dz \quad (42)$$

is computed. Then the sum of the frictional and acceleration pressure drops ΔP_{FA} around the loop is evaluated as per Art. 6.2 of Sec. 9-2. If L/D_c is low, friction is negligible, and ΔP_{FA} approximately equals 1 to 2 times the velocity pressure of the stream leaving the boiling channel. If $\Delta P_B < \Delta P_{FA}$, the trial w or G was too high, and vice versa.* After circulation has been determined, Eq. (62) can be used to predict h , or the h by Table 3, item a , and Eq. (35) added.⁷⁵

Between closely spaced parallel cylinders or vertical plates, \bar{R}_V increases approximately as the square root of q/S , the heat dissipation per unit horizontal cross section. † Vertical plates 5 ft high and $\frac{1}{4}$ in. apart in a tank, as an illustration, can safely reach over 90 per cent voids at the top and an average \bar{R}_V of about 0.8 and can dissipate a q/S of about 20 million Btu/(hr)(ft²) [see also Eq. (64)]. Figure 8 gives data for a $\frac{1}{2}$ -in. spacing.⁵¹ Burnout occurs when R_V reaches 1 at the top, but it is not readily predictable; tests at the desired conditions are necessary. For conservative design (EBWR, etc.) an exit quality of 20 per cent is not generally exceeded.

5.4 Forced-convection Boiling

When a liquid is pumped through a pipe and heated at constant q/A , the flow-mean temperature \bar{t} of the subcooled liquid has a substantially constant axial gradient $d\bar{t}/dx = (q/A)\pi D/wC$. Wall temperature t_w rises at almost the same rate:

$$t_w - \bar{t} = \frac{q}{Ah}$$

t_w rises until it is somewhat above the boiling point before type 11 boiling, commonly designated "local boiling," initiates. In this phenomenon small flattened bubbles form at nuclei on the wall, grow very rapidly to a small thickness, then are condensed by the subcooled liquid flowing past and collapse noisily. The total vapor volume is very small, so that no important loss in moderation (reactivity) would occur. The pressure gradient increases somewhat [Eq. (57), Sec. 9-2]. After the necessary length of channel in local boiling, the liquid has reached its boiling point and type 16 forced-convection "bulk" boiling starts. If q/A is high enough, type 18 film boiling occurs and the tube generally burns out. Forced convection sweeps the bubbles away strongly, so the necessary q/A to initiate type 18 boiling exceeds that for type 6 for the same liquid and pressure.

Though not so far reported, short L/D may exert some effect, since the radial distribution of subcooling (or of vapor content) will differ from low to high L/D . Strong mechanical vibrations or "singing" of small tubes with internal cooling water flow operating at high pressure and subcooling near burnout have been reported.⁷⁶ For such reasons it is necessary to conduct tests under the exact desired operating conditions to obtain reliable design data. Dissolved gas has some effect; unless otherwise stated, t_{sat} refers to gas-free liquid.

5.41 Subcooled Liquid, Nucleate Boiling. † Forced-convection subcooled boiling has been studied under many conditions, but no fundamental correlation has as yet been proved. Results are usually given in dimensional equations in terms of liquid subcooling $\Delta t_{sub} = t_{BP} - \bar{t}$, and average linear velocity of the liquid before boiling \bar{u}_L

* Employing u_s from Fig. 8 and setting the buoyant head up to any level equal to two liquid-phase velocity heads at that level yield a close check on the observed \bar{R}_V in Fig. 8.

† $G_L = u_L \rho_L (1 - R_V)$ and $G_V = (u_L + u_s) \rho_V R_V$ for upward flow. Eliminating u_L :

$$G_V = \left[u_s + \frac{G_L}{\rho_L (1 - R_V)} \right] \rho_V R_V$$

Since $G_V = q_V/\lambda S$ and $G_L = G_{total} - G_V$, R_V at any elevation z can be computed from the vaporizing heat q_V for trial values of G_{total} .

‡ Table 11, type 13.

t' is in degrees Fahrenheit, q'/A in Btu per hour per square foot, and u'_L in feet per second. There are a number of relations available; the most applicable should be used in each case, with an appropriate safety factor.

1. q'/A versus Δt . McAdams et al.⁷⁸ give, for water in an annulus 0.09 to 0.26 in. thick heated at its ID of 0.25 in., clean 304 stainless steel 3.75 to 11.5 in. long, 20 to 150°F subcooling, 30 to 90 psia, 1 to 36 fps upward flow,

$$\Delta t'_{sat} = t'_w - t'_{sat} = a_1 \left(\frac{q'}{A} \right)_t^{0.26} \quad (43)$$

where $a_1 = 1.97$ for degassed water and 1.54 when saturated with air. $\Delta t'_{sat}$ increased slightly with pressure. $(q'/A)_t$ is the total heat velocity.

Clark and Rohsenow⁷⁹ subtract the computed nonboiling $(q'/A)_{nb}$ (by Table 3, 5, or 6) from $(q'/A)_t$ to obtain the boiling $(q'/A)_b$. For water heated in a tube at 0 to 2,000 psig, 0 to 30 fps upward flow and 0 to 300°F subcooling,

$$\Delta t'_{sat} = a_2 \frac{\lambda^{3/4}}{c_L} \left[\frac{(q'/A)_b}{\mu_L} \sqrt{\frac{gcs}{g(\rho_L - \rho_V)}} \right]^{0.33} \text{Pr}_L^{1.7} \quad (44)$$

within ± 50 per cent, where $a_2 = 0.006$ in a 0.18-in.-ID nickel tube and 0.014 in a 0.54-in.-ID 304 stainless tube. Given $(q'/A)_t$, \bar{t} , and t'_{sat} at a given location in a tube, t'_w can be found by trial-and-error or other solution of the equation

$$\left(\frac{q}{A} \right)_t = \left(\frac{c_L}{a_2} \right)^3 \frac{\mu_L}{\lambda_2 \text{Pr}_L^{5.1}} \left[\frac{g(\rho_L - \rho_V)}{gcs} \right]^{1/2} (t_w - t'_{sat})^3 + h_L(t_w - \bar{t}) \quad (45)$$

Jens and Lottes⁸⁰ conclude, for water at $P' = 85$ to 2,500 psia and $\bar{u}_L = 3$ to 40 fps,

$$\Delta t'_{sat} = 1.9 \left(\frac{q'}{A} \right)^{1/4} e^{-P'/900} \quad (46)$$

Dissolved gas and nature of the surface have little effect.

Other approximate simple relations for water:

With 0.226-in.-ID 347 stainless tube, 0 to 900 cm³ N₂ per liter, 5 to 40 fps, (q'/A) to 3,800,000, and $(\Delta t)_{sub}$ to 236°F:⁸¹

$$\Delta t'_{sat} = 123 - 35 \log P' \quad (47)$$

for 1,000 < $P' < 2,500$ psia, also with reasonable accuracy down to $P' = 15$ psia.

With 0.18-in.-ID *L*-nickel tube, 10 to 30 fps, $P' = 1,000$ to 2,000 psia:

$$\Delta t'_{sat} = 28 - 0.012P' \quad (48)$$

2. *Incidence of Local Boiling.* Forced-convection subcooled boiling commences at a subcooling $(\Delta t_{sub})_0$ equal to that for nonboiling heat transfer. From Table 32 and Eq. (43), in units of degrees Fahrenheit, Btu, feet, and hours,

$$(\Delta t_{sub})_0 = \frac{43.5 D e^{0.2} \mu^{0.8}}{k G^{0.8} \text{Pr}^{1/3}} \frac{q}{A} - a_1 \left(\frac{q}{A} \right)^{0.26} \quad (49)$$

For q/A low and G high, Eq. (49) will be negative, indicating that nonboiling heating passes directly into saturated boiling without the appearance of local boiling. This can occur at moderate pressures but has not been observed at high pressures.⁷⁹

Dissolved gas decreases by up to 20 per cent the q/A at which local boiling initiates at 2,000 psi if $\Delta t_{sat} < 36^\circ\text{F}$, and at 500 psi if $\Delta t_{sat} = 100^\circ\text{F}$.⁸¹

In any study of reactor cooling in which subcooled or saturated boiling is anticipated, complete plots of the nonboiling and boiling regimes should be made for all anticipated conditions. The feasible regime giving the lowest t_w for any particular value of \bar{t} will be the one obtained.

3. *Maximum Heat Velocity* (q/A)_c.* McAdams⁷⁸ gives, for water in an annulus 0.26 in. thick, 0.25 in. ID, and 3.75 in. long ($L/D_e = 7.2$), $\Delta t'_{sub} = 20-100^\circ\text{F}$, $\bar{u}'_L = 1$ to 12 fps upward flow, and 30 to 90 psia,

$$\left(\frac{q'}{A}\right)_c = (400,000 + 4,800\Delta t'_{sub})(\bar{u}'_L)^{1/2} \quad (50)$$

Gunther⁸² gives, for water heated on one side of a $1/8$ -in.-square channel at $\bar{u}'_L = 5$ to 40 fps, $P = 14$ to 160 psia, and $\Delta t'_{sub}$ 20 to 280°F ,

$$\left(\frac{q'}{A}\right)_c = 7000(\bar{u}'_L)^{1/2} \Delta t'_{sub} \quad (51)$$

Buchberg⁸¹ gives, for water in a 0.226-in.-ID tube at $\bar{u}'_L = 5$ to 30 fps, $L/D = 110$, $P = 250$ to 3,000 psia, and $\Delta t'_{sub} = 3$ to 160°F , for G' in pounds per hour per square foot,

$$\left(\frac{q'}{A}\right)_c = 520(G')^{1/2}(\Delta t'_{sub})^{0.20} \quad (52)$$

McGill and Sibbitt's results⁸⁰ under similar conditions for ID = 0.143 in. and $L/D = 21$ are represented by replacing 520 by 530 and 0.20 by 0.28.

Jens and Lottes⁸⁰ give, for Buchberg's data,

$$\left(\frac{q'}{A}\right)_c = 10^6 a_3 \left(\frac{G'}{10^6}\right)^m (\Delta t'_{sub})^{0.22} \quad (53)$$

where a_3 is 0.817, 0.626, 0.445, and 0.250 and m is 0.16, 0.28, 0.50, and 0.73, respectively, at 500, 1,000, 2,000, and 3,000 psia.

For published data on water in round, square, and annular ducts from 14 to 3,000 psia, \bar{u}'_L from 1 to 54 fps, $\Delta t'_{sub}$ from 65 to 380°F , and $(q'/A)_c$ from 360,000 to 1,130,000 Btu/(hr)(ft²), Bernath obtained⁸³

$$\left(\frac{q'}{A}\right)_c = \left[5710 \left(\frac{D'_e}{D'_h}\right)^{0.6} + 48 \frac{\bar{u}'_L}{(D'_e)^{0.6}} \right] \left[102.6 \ln P' - 97.1 \frac{P'}{P' + 15} - \frac{\bar{u}'_L}{2.22} \left(\frac{D'_h}{D'_e}\right)^{0.6} + 32 - \bar{v}_b \right] \quad (54)$$

The equivalent diameter D'_e of the stream and the heated diameter D'_h (= heated perimeter/ π) are in feet and P' is in pounds per square inch absolute. The second bracket is the over-all Δt_c , and thus the first is h_c . This method correlates the data mentioned previously within ± 15 per cent on the average, and ± 30 per cent at worst.

These equations do not agree particularly well among themselves. Thus a design with q/A at all locations and times less than some two-thirds of the lowest pertinent correlation and no flow instability seems necessary for safety. For any desired higher q/A , burnout and stability tests at the identical conditions and dimensions are called for.

For flow normal to tubes, $(q'/A)_c$ about double Eq. (50) has been reached at comparable conditions. For upward flow of atmospheric-pressure water subcooled 50 to 125°F past $1/16$ -in. wires, at 3 to 10 fps, $(q'/A)_c = 27,500\Delta t_{sub}(u)^{1/2}$ within an average of 10 per cent.⁸⁴

It is evident from the previous relations that a heated tube with uniform q/A and a given G , on increasing q/A will burn out at the outlet, where Δt_{sub} has its lowest value. Although the formulas do not correlate burnout at varying conditions very accurately, tests in a single tube show high stability; safe operation is usually obtain-

* In general, and certainly at the higher velocities, no effect of direction of flow on $(q/A)_c$ is observed. $(q/A)_c$ is also the same for substantially steady state or for rapidly changing conditions. These equations are for degassed water; presumably dissolved gas decreases $(q/A)_c$ somewhat in subcooled boiling.

able indefinitely at constant q and G within several per cent of $(q/A)_c$. However, a small increase in q/A or decrease in G also decreases Δt_{sub} and will thus cause burnout to approach faster than otherwise. Furthermore, an increase in q/A will decrease G more or less, depending on orificing and other system characteristics.

Thus a careful calculation of coolant pressure and temperature throughout the reactor under all possible conditions is desirable in order to estimate the safety of the operation and the power at which boiling and/or burnout will occur. If bulk boiling occurs, calculation by finite increments is desirable (Art. 6.2 of Sec. 9-2). A convenient procedure is to plot for each desired channel the q/A versus position, then the P , \bar{l} , and t_{sat} from given inlet or outlet conditions. Next t_w is computed by the possible methods of heat transfer, the lowest t_w fixing the method and $(q/A)_c$ by that method.

If $(q/A)_2$ is comparable to $(q/A)_{av}$ or larger, as in fast or intermediate reactors with a neutron-thermalizing reflector or thermal reactors having higher neutron losses in the core than in the reflector, on burnout the (q/A) and $(q/A)_c$ curves will intersect at the outlet. If $(q/A)_2$ falls to a small fraction of $(q/A)_{av}$, as in thermal reactors with low neutron losses in the core, the two curves will meet by tangency at some earlier position A_c .

In some cases it is possible to predict directly the burnout power of a reactor. In the first case, $(q/A)_2$, which from the neutron-flux distribution is in known proportion to total power q_t , is equated to $(q/A)_c$ at the outlet. If \bar{l}_2 is given, any one of Eqs. (50) to (53) can be directly solved for w , P_2 [Eq. (53) requires trial and error] or $(q/A)_2$ and q_t . If \bar{l}_1 is given or desired instead of \bar{l}_2 , $(\Delta t_{sub})_2 = (\Delta t_{sub})_{1-c} - (q_t/w\bar{c})$ is substituted for Δt_{sub} and the unknown quantity obtained directly or by trial and error, as required. Equations (50) and (51) can also be solved directly for q_t , yielding, respectively,*

$$q'_{t,c} = \frac{400,000 + 4,800(\Delta t_{sub})_{1-c}}{\frac{(q/A)_2}{q_t} \left(\frac{\rho_2 S}{w}\right)^{1/2} + \frac{1.33}{w\bar{c}}} \quad (55)$$

$$q'_{t,c} = \frac{7,000(\Delta t_{sub})_{1-c}}{\frac{(q/A)_2}{q_t} \left(\frac{\rho_2 S}{w}\right)^{1/2} + \frac{1.95}{w\bar{c}}} \quad (56)$$

In the second case [$(q/A)_2 < (q/A)_c$], the two simultaneous equations† $q/A = (q/A)_c$ and $d(q/A)/dA = d(q/A)_c/dA$ must be solved‡ to find the burnout conditions analytically. This is generally impractical, and in any case the full temperature profiles for a number of operating conditions are usually desirable for stress and other purposes. Thus a graphical solution is best.

4. *Density and Vapor Volume.* The vapor quality x in the bubble boundary layer at $(q/A)_c$ has been estimated⁷⁹ to be near 0.8. However, this corresponds to a very small volume of vapor in any reasonable channel. The decrease in mass of water per unit of heated surface⁸⁰ is, within a ratio of about 2:1,

$$\frac{\Delta m}{A} = \frac{15,600\rho_L}{\bar{u}'_L(\Delta t'_{sub})^4} \left[\frac{q/A}{(q/A)_{nb}} \right]^{1.5} \quad (57)$$

* ρ_2 is for the liquid phase only. $(\Delta t_{sub})_{1-c}$ is $\bar{l}_{sat,c} - t_1$. w in Eqs. (55) and (56) is in lb/sec.

† For brevity, q/A has been used for the local heat velocity dq/dA , in which q is the total time rate of heat gain by the stream up to the given position. Similarly, $d(q/A)/dA$ is more properly d^2q/dA^2 .

‡ For the simple case of a bare reactor with cosine distribution of q/A along the channel and substantially constant t_{sat} , Gunther's equation yields

$$\frac{\pi N_o - X}{2} \frac{X}{X} = \tan^{-1} \frac{0.619 A_t}{\bar{c}(w\rho S)^{1/2}} = \tan^{-1} B$$

$$\frac{(\Delta t_{sub})_{1-c}}{q_t} = \frac{1 + \sin B}{7200w\bar{c}_{1-c}} + \frac{\cos B}{4460A_t} \left(\frac{\rho LS}{w}\right)^{1/2} \quad (58)$$

Units are the same as for Eq. (55).

in units of pounds, feet, seconds, and degrees Fahrenheit, $(q/A)_{nb}$ being at incipient local boiling.

Visual observation of subcooled boiling near atmospheric pressure⁷⁸ seems to show a significant and fluctuating volume of vapor. However, quantitative methods yield volumes low enough and fluctuations rapid enough so as probably to cause no difficulty in reactors if the subcooling is at least 20°F at high pressures⁸⁰ or somewhat more at low pressures for q/A of the usual magnitude desired in nuclear power reactors. For instance, water at 100 psia, 80°F subcooling, and 1 fps showed less than 0.0001 in. of vapor at $q'/A = 400,000$.⁸⁵ Also⁸² water at 23.5 psia subcooled 155°F, flowing at 10 fps with $q'/A = 2,330,000$ [60 per cent of $(q'/A)_c$], had only 4 per cent of the surface covered with bubbles, which had maximum radii of 0.01 in. and lifetimes of 0.0002 sec. Water at 2,000 psia⁸¹ in a 1/4-in.-ID tube showed less than 1 per cent $\Delta\rho$ with local boiling if $\Delta t_{sub} > 35^\circ\text{F}$. A decrease of 3 per cent was observed at $\Delta t_{sub} = 4^\circ\text{F}$. $\Delta\rho$ and its fluctuations increased the lower the pressure; at 100 psia the standard deviation of ρ was about 10 per cent.

5.42 Subcooled Liquid, Mixed Boiling.* This case has been studied⁵⁴ for water at 16 to 60 psia, subcooled 50 to 100°F, flowing at 1 to 5 fps along the outside of a 1/4-in. tube. $\Delta t'_{sat} = 600^\circ\text{F}$ and agreed well with

$$\frac{q'}{A} = 880,000(\Delta t'_{sat})^{-2.4} \quad (59)$$

5.43 Subcooled Liquid, Film Boiling.† Forced-convection subcooled film boiling in tubes has not yet been studied, except for the conditions required for its initiation, summarized earlier (Art. 5.42, paragraph 2). However, nonaqueous liquids subcooled 20 to 80°F have been flowed upward at 3 to 13 fps⁸⁶ past film-boiling horizontal 3/8- to 5/8-in.-OD cylinders. The subcooling raised the values of h almost to those for nucleate boiling. The results are approximately correlated by the dimensionless relation (see Art. 5.24, paragraphs 2 and 5):

$h_{con} \left(\frac{D \Delta t_{sat}}{u \bar{k}_{\nu} \bar{\rho} \bar{\nu} \lambda} \right)^{1/2} - \frac{7.29}{h_{con}} \left(\frac{u \bar{k}_{\nu} \bar{\rho} \bar{\nu} \lambda}{D \Delta t_{sat}} \right)^{1/2}$	-2*	0.5*	3*	5*	7*	9*
$\Delta t_{sub} c_L \rho_L^{0.95} \left[\frac{(u_0 D_0)^{0.90} \mu_L^{0.1}}{\Delta t_{sat} \bar{k}_{\nu} \bar{\rho} \bar{\nu} \lambda} \right]^{1/2}$	0	100	200	300	500	800

* Average deviation = ± 1 ; maximum deviation = ± 2 .

where u is the velocity past the cylinder, u_0 and D_0 are for the duct creating the turbulence in the stream, and λ is the enthalpy decrease from t_{ν} to saturated liquid. For ethanol, benzene, and hexane h_{con} was roughly $10u'$ Btu/(hr)(°F)(ft²) at $\Delta t_{sub} = 0$ and varied linearly with Δt_{sub} to $30u'$ at $\Delta t_{sub} = 80^\circ\text{F}$. The total $h = h_{con} + 1/8 h_r$.

5.44 Saturated Liquid, Nucleate Boiling.‡ Forced-convection saturated nucleate boiling in channels yields rather low values of Δt , which are fairly independent of dissolved gas content⁸¹ and of velocity and channel dimensions. Because of the considerable pressure drop and its high negative slope vs. flow rate at constant q , type 16 boiling in parallel channels in nuclear reactors may be dangerously unstable unless the channels are roughly equiaxed in cross section and heavily orificed individually at the inlet (Art. 7.1, Sec. 9-2) or have individual pumps or flow is upward§ and the channels are large so that the buoyant pressure of the vapor is significant compared with the friction.

The negative pressure coefficient is even important in burnout tests on individual tubes. In a system in which the flow drops appreciably if ΔP across the heated tube

* Table 11, type 14.

† Table 11, type 15.

‡ Table 11, type 16.

§ Carter⁸⁷ predicts that boiling downflow is more stable than upflow, but his tests show that in parallel downflow channels q cannot safely exceed about one-half that for a single channel.

risers (as with a low-pressure centrifugal pump and no inlet orifice), the values of $(q/A)_c$ observed may be considerably lower than for constant flow and may be misleading. Nonuniformity of q/A or of velocity distribution, as in a square duct⁸⁷, also lowers $(q/A)_c$.

1. q/A versus Δt . In general, h near the inlet of a tube containing boiling water is not very different from that in type 4 pool boiling if the velocity is low or from non-boiling flow if the velocity is high, and correlations for these cases may be accepted as conservative. It is generally observed at low pressures that h approximately doubles²⁹ as the quality (and thus velocity) increases downstream to about 50 per cent. Thereafter wetting is poorer and h starts to drop, particularly after 80 per cent vaporization. Turbulence promoters are not advantageous.

For light petroleum oils at 3 to 30 fps in an annulus of 0.225-in. heated ID and 0.012-in. width and $\Delta t'_{sat} = 50$ to 250°F ,⁸⁸

$$\left(\frac{q'}{A}\right) = 0.000097(\Delta t'_{sat})^2 \quad (60)$$

For a number of liquids heated near 15 psia at constant q/A in slow vertical upflow, entering at 0 per cent quality and leaving at under 5 per cent, the average h in pipes is correlated within several per cent by⁷⁵

$$\text{Nu} = 0.0086(\text{Re}_m)^{0.8} \text{Pr}^{0.6} \left(\frac{s_{H_2O}}{s}\right)^{1/3} \quad (61)$$

where Re_m employs the log mean of the average inlet and exit velocities, neglecting vapor slip. s is surface tension, and all physical properties are for the liquid.

For water entering 0.465-in.-ID 347 stainless-steel tubes at 1.5 to 6 fps and boiling at 45 to 200 psia and $q/A = 50,000$ to $250,000$ Btu/(hr)(ft²), the local Nu_L , in terms of the quality x and total flow G , is⁸⁹

$$\text{Nu}_L = \left[4.3 + 0.0005 \left(\frac{V_V - V_L}{V_L} \right)^{1.64} x \right] \left(\frac{q}{AG\lambda} \right)^{0.464} \text{Re}_L^{0.308} \quad (62)$$

Equation (62) held within 10 per cent on the average and was independent of L/D , from $x = 0$ to 0.4. Above $x = 0.5$, h decreased toward the value for steam at $x =$ about 0.7. Above $x = 0.6$, temperatures fluctuated widely. In Nu_L and Re_L , k_L and μ_L are used.

2. *Maximum Heat Velocity* $(q/A)_c$. The highest values of $(q/A)_c$ are obtained⁸⁸ near or somewhat below a reduced pressure of one-third, as in saturated pool boiling (Fig. 7).

$(q/A)_c$ compared with nonboiling $(q/A)_{NB}$ by Table 3, item *a*, calculated for the same fluid and wall temperatures is given for JP-3 (gasoline) and JP-4 (80 per cent gasoline, 20 per cent kerosene) hydrocarbon jet fuels⁸⁸ of critical pressure P_c approximately = 550 psia, in tubes at $\bar{u}_L = 3$ to 80 fps, $P' = 30$ to 500 psia, $D_c = 0.15$ to 0.6 in. and G' in pounds per hour per square foot by

$$\frac{(q/A)_c}{(q/A)_{NB}} = 2,000(P'G')^{-1/3} = \frac{h_c}{h_{NB}} \quad (63)$$

In soiled tubes burnout may ensue⁹⁰ below $(q/A)_c$ for clean tubes. In square or other angular sections at constant q/A , $(q/A)_c$ may be only a fraction of that in tubes.

For $q'/A > 100,000$ burnout with water in general occurs when x reaches about 0.7⁸⁹ to 0.8.⁷⁹ Burnout x seems to increase slowly with pressure and with decrease in q/A .

Deissler has correlated all the available data for $(q/A)_c$ for water in tubes in saturated and slightly subcooled boiling, within ± 25 per cent on the average, by the ratios $G_V/G_L = (q/A)_c/\lambda G_L$ and $G_L D/\mu_V = \text{Re}_b$. If $\text{Re}_b < 20,000$, $G_V/G_L = 0.006$; and if $\text{Re}_b > 20,000$,

$$\frac{G_V}{G_L} = 1.25(Re_b)^{-0.54}$$

G_L is for liquid in the pipe and G_V for vapor generation at the wall (based on wall area).

A rough general correlation⁹¹ of effect of velocity on the safe q/A for water [a lower limit of $(q/A)_V$ for saturated boiling in tubes], for quality x from 0.05 to 0.6, is

$$\bar{u}'_L x_2 = 0.8 \quad (64)$$

This yields the following value of safe production rate of saturated vapor G'_V and heat of vaporization q'_V/S per second per square foot of boiling channel cross section S :

P' , psia.....	14.7	100	500	1,000	1,500	2,000
G'_V	47.8	45.0	40.6	37.0	34.0	31.1
q'_V/S	46,400	40,000	30,700	24,000	18,900	14,400

In general, these values of burnout quality do not hold below $L/D = 25$. At lower L/D the burnout x_2 can (conservatively) be considered to decrease proportionally to L/D .

3. *Commercial Boiler Operation.* Some commercial high-pressure boilers operate with forced convection.⁹² The main purpose of the pumps is to maintain the desired distribution of the water among the tubes and thus decrease the danger of burnout by boiling dry or scaling; make up for low buoyancy at low heads or high pressures; permit smaller, lighter, and thinner-walled tubes; and obtain higher exit quality. It is also possible to force the inlet water along any desired path, such as first past the region of highest q/A , rather than being limited to substantially vertical upward flow. Each tube usually has a flow-distribution orifice (Art. 7.2 of Sec. 9-2) with ΔP_o approximately equal to the friction and acceleration ΔP_{FA} in the highest flow tubes and greater in the others.

Recirculation is used commercially above about 1,500 psi with 1- to 1½-in.-ID tubes and 2.5 to 5 fps inlet liquid water velocities.* The maximum local q/A_i ranges up to about 200,000 Btu/(hr)(ft²). At the exit, quality is usually 10 to 30 per cent (95 or 100 per cent in the Sulzer and Benson boilers †), but q/A is much lower. Because of the presence of some scale-forming salts in the usual boiler water and the limited q/A values obtainable in fuel-fired furnaces, these operating conditions may be considered conservative lower limits for nuclear reactors.

4. *Location of Bubbles.* Free bubbles tend to accumulate in the center of the stream because of shear stress distribution and Bernoulli forces. This decreases R_V and the effect of the bubbles on moderation. Whirling of the coolant as it passes through the tubes has the same effect, owing to centrifugal acceleration, and should considerably increase boiling reactor stability and permissible heating density. Vapor volume or the total coolant mass in boiling coolant channels can be computed subject to any desired assumptions. For instance, for a slip velocity u_s and heat pickup distribution $q(x)$, the liquid velocity u_L can be computed as a function of x , the distance from start of boiling, by trial and error from

$$S = \frac{w}{\rho_L u_L} + \frac{q(x)}{\lambda} \left[\frac{1}{\rho_V (u_L + u_s)} - \frac{1}{\rho_L u_L} \right] \quad (65)$$

The total vapor volume in the channel is then the graphical integral

$$\int_0^X S_V dx = \frac{1}{\rho_V \lambda} \int_0^X \frac{q(x) dx}{u_L + u_s} \quad (66)$$

* It is found permissible to operate for an hour or more at about 75 per cent of these normal inlet velocities (half the pumps shut down).

† Superheater tubes are used at 2,500 psi and 1050°F.

If $u_s = 0$ and q/A and pressure are substantially constant, the correct mean specific volume \bar{V} over the boiling length is the log mean of the liquid and outlet specific volumes. For a bare reactor with cosine distribution of heating and saturated inlet coolant \bar{V} is the geometric mean. For this case and weighting the density by the flux distribution, as would be appropriate in computing coolant irradiation, the geometric mean is again correct, in conjunction with the mean neutron flux and the total residence time.

5. *Liquid Metals.* In a well-wetted tube, obtainable by Na or K additions or strong turbulence, h for mercury is reported⁹³ to be substantially the same function of dP/dx whether the mercury is below the boiling point, boiling, or superheated vapor. It could thus be approximated from relations for liquid metals or gases in tubes; also⁹³ by $h = 6100(\Delta P/\Delta x)^{0.445}(D)^{1/2}$ Btu/(hr)(ft²)(°F) for D in., x ft, and P psi. Poorly wetted tubes fluctuate unpredictably in temperature between wetted and unwetted (hotter) operation.

5.45 Saturated Liquid, Film Boiling.* Forced-convection saturated film boiling, as for type 15 boiling, has been studied for upward flow of nonaqueous liquids past horizontal cylinders of $\frac{3}{8}$ - to $\frac{5}{8}$ -in. diameter.⁹⁴ It was found that at low liquid velocity [$u/(gD)^{1/2} < 1$], the same relation for h_{con} [Eq. (39)] as for natural convection is valid, and $\bar{h} = \bar{h}_{con} + \frac{3}{4}h_r$. For $u/(gD)^{1/2} > 1$,

$$\bar{h}_{con} = 2.7 \frac{\sqrt{uk\nu\rho r\lambda}(1 + 0.4 \Delta t c/\lambda)}{\sqrt{D \Delta t}} \quad (67)$$

and $\bar{h} = \bar{h}_{con} + \frac{7}{8}h_r$. The local h_{con} and q/A are considerably larger along the leading edge than farther around.

In natural-convection nucleate boiling at a given q/A , burnout of the heating surface generally occurs when $(q/A)_c$ is reached and film boiling starts. Only high-melting surfaces like platinum and graphite, which can stand the temperature necessary to radiate a large part of the $(q/A)_c$, generally avoid burnout. In forced convection, however, the vapor film is thinner and can conduct more heat, particularly at high pressures. Thus burnout in film boiling is more readily avoided. For instance, for hydrocarbon jet fuels⁸⁸ above 25 fps and 300 psia, stable-film boiling can be obtained above $(q/A)_c$ in 347 stainless tubes. At $(q/A)_c$, Δt_{sat} jumps some 200 to 300°F but then stabilizes there. For further increases in the film-boiling region, $\log q/A$ increases about three times as fast as $\log \Delta t_{sat}$, until the burnout wall temperature is reached.

In another case, the film-boiling plot of $\log q/A$ versus Δt for hydrocarbon mixtures has, after a nucleate boiling jump in q/A , fallen back on the extension of the non-boiling curve. This has been attributed⁹⁰ to the presence of higher boiling constituents. If so, addition of such a substance to a reactor coolant may provide a method of protecting or warning against overheating.

5.5 Homogeneous Boiling†

Saturated homogeneous boiling would be expected in a homogeneous reactor or in a heterogeneous reactor using a liquid-fuel solution if the fuel solution reached the boiling point plus the necessary small superheat to nucleate bubbles. Actually, because gaseous fission and decomposition products increase the vapor pressure and because fission fragment recoil forms nuclei, boiling would no doubt occur sooner, probably with negligible superheat. It does not seem likely that local *subcooled* boiling with bubble collapse could be obtained in a homogeneous fuel solution or even in aqueous suspensions of fuel-element compounds.

Boiling of an aqueous fuel solution may eventually become a desirable or feasible normal operating condition in power reactors. In any case, however, it offers a valuable safety feature for homogeneous reactors—a negative coefficient of sub-

* Table 11, type 18.

† Table 11, type 19.

stantially infinity. Accordingly it has been studied primarily from the standpoint of speed of response to a sudden heat pulse.

5.51 Superheat to Initiate Boiling. Available theories predict higher superheat than is actually observed⁹⁵ before bubbling of pure liquid occurs in a container. For water at 100, 400, and 1,000 psia the maximum superheat required was, respectively, 85, 35, and 10°F, the average superheat required being 25 per cent lower. Theory yields 275, 175, and 80°F, respectively, for pure liquid. In another study⁹⁶ 40°F superheat was sufficient at 15 psia with an exponential power rise period of 0.017 sec, corresponding to a time delay of only 0.005 sec.

5.52 Steady-state Boiling. The higher the heating density H , the higher the necessary superheat, since more new nuclei need to develop into vapor bubbles per unit of time, and the lower the density of the vapor liquid mixture. Circulation rate and mixture density along each assumed vertical streamline can be roughly estimated by trial and error from a reasonable slip velocity and a method similar to that outlined under type 10 boiling. In pool homogeneous boiling the friction is negligible and the buoyancy pressure ΔP_B would all go to acceleration of the fluids. The "slip" velocity in feet per second for water up to moderate pressures⁷⁰ roughly equals R_V , the fraction of vapor by volume.

5.53 Rate of Bubble Growth.⁹⁵ Bubble growth is steady for any one bubble at about 0.02 to 0.09 fps radially, which checks available theory. Rate of collapse of bubbles of substable size has also been studied.

5.54 Rate of Density Change. The decrease in density with time due to an increase in the heating density H follows available theory⁷⁷ for bubble initiation and growth. A sudden jump from low power to about 4 to 30 kw/liter for water boiling at atmospheric pressure requires a further superheat of about 1°C before the volume starts to increase, or about 0.3°C if gas is present. At 135 psia some 2°C is required either way, gas having little effect. The volume then increases at about 50 per cent/sec.⁷⁷ This delay of 0.1 to 0.3 sec decreases in higher power pulses but does not disappear.

6 STEADY-STATE THERMAL DESIGN OF REACTORS

6.1 Temperature Rise of the Coolant

Although power reactors will have high q/A and thus high transverse temperature gradients in the coolant streams, the coolant channels will generally be thin. Thus for heat balances it will usually be adequate to consider the coolant temperature uniform at l at any given cross section of a stream. If the axial heat flow in the solid metal and coolant due to the coolant temperature rise is computed, it will generally be found negligible compared with the total power. Usually also the heat transferred from one channel to another in a direction normal to coolant flow is found to be negligible. Thus all the heat q generated per unit time in the "cell" of fuel, coolant, and moderator nearest to each coolant channel, from coolant inlet at x_1 to position x , is assumed to have gone into the coolant stream by position x .

The total heat dq/dx transferred to the coolant per unit length in any channel can be obtained by integrating Eq. (1) over the appropriate cross section of fuel cooled by the channel and multiplying by a factor to include the additional heating by γ absorption, moderation, and radioactive disintegration after neutron capture. The total heat q transferred from x_1 to x is then the integral $\int_{x_1}^x (dq/dx) dx$.

It is usually more convenient to work with the total desired reactor heat rate q_L and the ratios \bar{H}/H_i and H/H_i of average and local H to the maximum, H_i . The total heat rate q_L for a given channel is

$$q_L = \frac{q_i}{N_c} \left(\frac{H}{\bar{H}} \right)_n \quad (68)$$

where N_c is the total number of channels and $(H/\bar{H})_n$ is the local to average ratio for the position of the channel in the plane of the reactor normal to the coolant flow. The

local dq/dx at position x along the channel, for $x = 0$ at the midplane so that $x_1 = -x_2$, is

$$\frac{dq}{dx} = \frac{q_L}{2x_2} \left(\frac{H}{\bar{H}} \right)_x \quad (69)$$

The total q at x for the channel is thus

$$q = \frac{q_L}{2x_2 N_c} \left(\frac{H}{\bar{H}} \right)_n \int_{x_1}^x \left(\frac{H}{\bar{H}} \right)_x dx = \frac{q_L}{2x_2} \int_{x_1}^x \left(\frac{H}{\bar{H}} \right)_x dx \quad (70)$$

The only practically important orientation for coolant channels is normal flow between parallel inlet and outlet planes, or through a "slab." For homogeneous fuel loading, the cosine distribution obtained can be integrated analytically. For "roof-topped" or other irregular distributions a numerical or graphical integration is necessary for Eq. (70).

If the coolant undergoes a significant change in density and velocity while traversing the reactor, such as in boiling at low pressures, the method of Art. 6.2 of Sec. 9-2 is used to obtain the relation between \bar{t} and x from that between q and x .

If the pressure is high and the coolant expands significantly, as with supercritical or subcooled water at high temperatures, but velocities remain low, Eq. (17) is used in the form

$$h' = h'_1 + \frac{q}{w} \quad (71)$$

If the pressure is substantially constant, \bar{t} is obtainable directly from the calculated enthalpy h' and a table of h' versus t at the given pressure. If the pressure decreases with x , P is calculated by Eq. (28) and t obtained from the table at the corresponding values of h and P .

For small expansions and moderate temperature rises the specific heat c as well as velocity remain substantially constant. This is usually the case with liquid metals, with subcooled water under about 500°F, etc. In this case \bar{t} is directly obtainable as a function of q :

$$\bar{t} = \bar{t}_1 + \frac{q}{wc} = \bar{t}_1 + (\bar{t}_2 - \bar{t}_1) \frac{q}{q_L} \quad (72)$$

For the cosine distribution with reflector,

$$\frac{H}{\bar{H}} = \frac{x'_1 \cos x'}{\sin x'_1} \quad (73)$$

and Eqs. (70) and (72) yield

$$\bar{t} = \bar{t}_1 + \frac{\bar{t}_2 - \bar{t}_1}{2} \left(1 + \frac{\sin x'}{\sin x'_2} \right) = \bar{t}_1 + \frac{qN}{2wc} \left(1 + \frac{\sin x'}{\sin x'_2} \right) \quad (74)$$

where $x' = \pi x/2X_e$. Without reflector, $X_e = x_2$.

6.2 Fuel-element Temperature

6.21 Control of Fuel-element Temperatures by the Coolant. The normal or local average wall temperature t_w at any position x is obtained by adding to \bar{t} the Δt from the wall to the fluid at that position. If q/A and the coolant velocity are uniform over the heated perimeter P' at each position along a given channel or stream, as is usually substantially true, t_w will also be uniform and will be given by

$$t_w = \bar{t} + \frac{q}{A} \frac{1}{h} = \bar{t} + \frac{q_L}{2x_2 h P'} \left(\frac{H}{\bar{H}} \right)_x \quad (75)$$

The normal maximum temperature t_0 of the fuel element at x , which is at its axis or midplane, is obtained by adding to Eq. (75) the temperature drop Δt_e across the fuel element from Eqs. (9), (20), etc. Expressing $t_0 - t_w$ as equal to q/A times the ratio $\Delta t_e/(q/A)_1$, from the above equations

$$t_0 = \bar{t} + \frac{q}{A} \left[\frac{1}{h} + \frac{\Delta t_e}{(q/A)_1} \right] = \bar{t} + \frac{qL}{2x_2 P'} \left(\frac{H}{\bar{H}} \right)_x \left[\frac{1}{h} + \frac{\Delta t_e}{(q/A)_1} \right] \quad (76)$$

A plot of t_x or t_0 against x for a symmetrical bare reactor will always show a maximum t_x between $x = 0$ and $x = x_2$ and a maximum t_0 between $x = 0$ and x at $(t_x)_{\max}$. A reactor with reflector may show the maximum t_x either at x_2 , or before x_2 .

For a cosine distribution by reflector, substituting for \bar{t} by Eq. (74) and for H/\bar{H} , by Eq. (73)

$$t_0 = \bar{t}_1 + \frac{qL}{2} \left\{ \frac{1}{wc} \left(1 + \frac{\sin x'}{\sin x'_2} \right) + \frac{\pi}{2X_e P'} \left[\frac{1}{h} + \frac{\Delta t_e}{(q/A)_1} \right] \frac{\cos x'}{\sin x'_2} \right\} \quad (77)$$

The position x_{\max} of maximum temperature is obtained by setting $dt_0/dx' = 0$, which yields

$$\frac{\pi x_{\max}}{2X_e} = x'_{\max} = \tan^{-1} \frac{2X_e P'}{\pi wc \left[\frac{1}{h} + \frac{\Delta t_e}{(q/A)_1} \right]} \quad (78)$$

Substituting x'_{\max} from Eq. (78) for x' in Eq. (77) and simplifying yield

$$\begin{aligned} qL &= \frac{2wc(t_{0,\max} - \bar{t}_1)}{1 + 1/(\sin x'_2 \sin x'_{\max})} \\ &= \frac{2wc(t_{0,\max} - \bar{t}_1)}{1 + \frac{1}{\sin x'_2} \left\{ 1 + \left(\frac{\pi wc}{2X_e P'} \right)^2 \left[\frac{1}{h} + \frac{\Delta t_e}{(q/A)_1} \right]^2 \right\}^{1/2}} \end{aligned} \quad (79)$$

For t_w instead of t_0 the same equations (77), (78), and (79) may be employed by deleting the term $\Delta t_e/(q/A)_1$.

It is evident from Eq. (79) that if \bar{t}_1 and w have been fixed and the maximum satisfactory $t_{0,\max}$ is set by the uranium phase change, strength, or other reasons, the maximum permissible power qL of the channel is fixed. Similarly, if the maximum permissible t_w is set by corrosion, incidence of boiling, or other factors, the permissible qL is fixed.* Again, if qL , \bar{t}_1 , and maximum t_w or t_0 are fixed,† the necessary w can be computed. However, w appears twice in Eq. (79) and also affects h . It must thus be found by repeated trials.

It is seen that all the temperatures in a nuclear reactor depend directly on the coolant inlet temperature and flow rate and the power. In a nuclear power plant the reactor coolant inlet temperature \bar{t}_1 may, of course, be kept constant by suitable instrumentation and controls, or it might be allowed to drop as low as possible or to swing between limits, with changes in the power generated, main-condenser-coolant temperature, and other variables. In the latter case the temperature would have to be traced from the condenser-coolant inlet to the outlet, through the condenser, and through any intermediate boilers and heat exchangers before \bar{t}_1 could be estimated.

6.22 Hot-channel Factors. By Secs. 6.1 and 6.21 theoretical or "average" values of \bar{t} , t_w , $t_{0,\max}$, and qL at a given w , q , and t_1 can be computed, based on known average values of the local dimensions, physical properties, fuel concentration, neutron-flux density, etc. These average values are important in the design and operation of a reactor. However, when a reactor is being designed for maximum performance, as will in general be true for power reactors, it is even more important not to exceed the permitted temperatures *anywhere*. For instance, the several coolant channels nearest

* Maximum t_0 is generally limiting in liquid-metal-cooled reactors, and maximum t_w in water-cooled reactors.

† As in computing coolant distribution among the channels of a reactor to obtain constant t_w or t_0 instead of h .

the axis of a reactor will all have identical values of $t_{0,\max}$ by Eq. (79) if all other factors in the equation are (substantially) equal. In actual fact, however, there are bound to be appreciable differences among them in q_L , in w and thus in $t_{0,\max}$ and $t_{w,\max}$. It is evidently necessary to estimate safety factors that will allow for these differences if it must be assured that nowhere does t_w or t_0 exceed the set maximum. For nuclear reactors, safety factors are known as *hot-channel* or *hot-spot* factors.

Table 12. Typical Hot-channel Factors

Uncertainty in	Coolant temperature rise, $\bar{t} - \bar{t}_1$	Film temperature difference, Δt_f	Fuel temperature difference, Δt_e
Neutron flux.....	1.20	1.20	1.20
Fuel channel concentration.....	1.10	1.20	1.20
Eccentricity and diameter.....	1.40	1.25	1.10
Flow distribution.....	1.02	1.02	
Fuel-element warpage.....	1.04	1.03	
Total product*	1.95	1.90	1.60
Film coefficient, h		1.20	
Fuel-element thermal conductivity, k			1.05
Fuel-element thickness.....			1.05
Total product.....	$1.95 = F_c$	$2.28 = F_f$	$1.76 = F_e$

Maximum possible coolant temperature = $\bar{t}_1 + 1.95(\bar{t} - \bar{t}_1)_{\text{calc}}$

Maximum possible surface hot spot = $\bar{t}_1 + 1.95(\bar{t} - \bar{t}_1)_{\text{calc}} + 2.28(\Delta t_f)_{\text{calc}}$

Maximum possible metal hot spot = $\bar{t}_1 + 1.95(\bar{t} - \bar{t}_1)_{\text{calc}} + 2.28(\Delta t_f)_{\text{calc}} + 1.76(\Delta t_e)_{\text{calc}}$

* S. McLain, ANL-5424, 1955.

The hot-channel factor for a given source of inaccuracy is a multiplier applied to the normal design value of a temperature differential to yield the maximum possible value of that differential. Such factors must be determined by careful analysis of manufacturing and inspection procedures and tolerances, the reliability of the physical properties and design relations used, methods of reactor control* and fuel-element routing in the reactor, tests on models, critical assemblies or "mock-up" reactors, etc. LeTourneau and Grimble⁹⁷ outline details of estimating hot-channel factors from dimensional tolerance data, etc. Some can also be measured from model tests.⁹⁸

Table 12 lists possible values of these factors for the three significant temperature differentials in computing the hottest spot. These or similar factors apply at all positions in the reactor, but the values of most importance are usually those at the positions of maximum t_w and t_0 , found in Art. 6.21. It is seen that the maximum possible t_0 in this case is about twice as much above the coolant inlet temperature \bar{t}_1 as the normal design hot spot. †

To design with hot-channel factors, in Eqs. (74) through (79) w should be replaced by w/F_c , h by h/F_f , and Δt_e by $F_e \Delta t_e$. Equations (78) and (79) become, respectively,

$$\frac{\pi x_{\max}}{2X_e} = x'''_{\max} = \tan^{-1} \frac{2X_e P' F_c}{\pi w c \left[\frac{F_f}{h} + \frac{F_e \Delta t_e}{(q/A)_1} \right]} \quad (80)$$

$$q_L = \frac{2wc(t_{0,\max} - \bar{t}_1)}{F_c + \frac{F_e}{\sin x'_2 \sin x'''_{\max}}} \quad (81)$$

Evidently, q_L is decreased by the ratio $1/F_c$, and if F_c , F_f , and F_e are equal, x_{\max} is not changed. As before, $t_{0,\max}$ can be replaced by t_w by setting $\Delta t_e = 0$.

* For instance, the neutron-flux density varies much more with poison-control rods than with reflector or fuel solution level control.

† In later power reactors, considerably smaller F values are perforce being employed in order to obtain reasonable designs. These are justifiable by smaller tolerances, greater experience and optimism, and a qualitative or subconscious application of the statistical method mentioned herein.

It is seen in Table 12 that all the factors are assumed to apply simultaneously at the hottest spot. It is true that some of them are interrelated, such as neutron flux, average fuel concentration, and warping of the fuel element as a result of high burnup. However, this method of design is bound to be overconservative if each hot-channel factor is the maximum possible effect of the corresponding uncertainty.

A sounder procedure, based on statistics, would be to determine or estimate the fractional standard deviation σ' for each independent uncertainty,* combine them to find the total σ of the limiting temperature, then design by the normal equations (without hot-channel factors) to an agreed-on number of σ s below the limiting temperature.^{98,105} The probability of a hot spot exceeding the limiting temperature is 16 per cent if the highest design temperature is σ lower, 2.3 per cent if 2σ lower, 0.13 per cent if 3σ lower, etc.

6.3 Heat Generation in Flowing Liquids and Slurries

Homogeneous reactors employing solutions of fuel plus moderator, such as the HRE, generate fission heat internally when the solution is in the enlarged vessel that constitutes the core. Reactors employing fuel slurries instead of solutions or dissolved or suspended fuel with separate moderator, such as the externally cooled LMFR, are similar cases. In these reactors there is usually no separate coolant in the core. Thus all the heat generated appears as temperature rise of the fuel fluid. This does not mean, however, that the outlet temperature t_2 is uniform even across any one channel. Apart from the radial variation of H , small for small channels and long neutron-diffusion lengths, and vice versa, there is a variation due to the nonuniformity of coolant velocity u and therefore residence time in the core. The consequent temperature nonuniformity is continually being decreased by radial molecular heat conduction in laminar flow and much more effectively by eddy conduction (Art. 4.23 of Sec. 9-2) in turbulent flow. However, radial temperature differentials may be of importance because of their effect on average density of the stream, because of thermal shock of surfaces on which the stream may impinge, etc. Accordingly, their evaluation is necessary in optimizing the design of such a reactor.

Volume heating of fuel solutions also occurs outside the reactor core because of the radioactive disintegration of fission products. Heating of both coolant and fuel solutions also takes place within the core as a result of γ absorption, fast-neutron slowing down, and neutron reactions. These other sources of heat within the core can usually (conservatively) be neglected (since they are much smaller than the fission-product plus β energy), being included with the fission heat generation. However, they can be important in evaluating behavior of the reactor in the event of coolant flow failure.

If it is necessary to consider the axial or radial variation in H , the calculation must generally be made by finite increments (Art. 7.2). In the case of uniform H , general mathematical solutions have been worked out for long tubes.^{99,100} This case gives the highest temperature differentials; thus it is somewhat conservative for design purposes.

From Eq. (5), the differential equation for a wide flat duct is

$$u \frac{\partial t}{\partial x} = \frac{\partial}{\partial y} \left[(\alpha + \epsilon_H) \frac{\partial t}{\partial y} \right] + \frac{H}{\rho c} \quad (82)$$

where x is measured along the length and y along the thickness. For streamline flow $\epsilon_H = 0$ and u is obtained from Table 1, Sec. 9-2. Equation (82) has been integrated for the conservative case of long ducts to give the transverse temperature distribution for the boundary conditions that both walls (at $y = 0$ and $y = L$) are at t_w and that the fraction of the heat generated that remains in the stream is F' ($F' = 0$ for isothermal walls and 1 for adiabatic walls). Substituting the position of the midplane gives the axial temperature t_{axial} . Integrating to the midplane gives the space mean temperature of the stream, or on weighting by the velocity the flow mean temperature

* σ' is the root-mean-square fractional deviation from the mean due to each uncertainty.

$$t_{\text{axial}} - t_w = \frac{HL^2}{4k} \left(\frac{1}{2} - \frac{5F'}{8} \right) \quad t_{\text{flow mean}} - t_w = \frac{HL^2}{4k} \left(\frac{2}{5} - \frac{17F'}{35} \right) \quad (83)$$

The integrations have also been carried out for turbulent flow, taking ϵ_H as equal to ϵ_F in Eq. (36), Sec. 9-2, and using a generalized velocity distribution similar to that of Eqs. (32) to (34), Sec. 9-2. Results for the principal conditions for flat plates and for tubes are given in Table 13.

Table 13. Values of $\frac{HL^2}{k(t - t_w)}$ for Liquid with Uniform Heating Density

Wall conditions	Velocity distribution	Value of t in $(t - t_w)$					
		Wide flat duct ($L = \text{wall spacing}$)			Round pipe ($L = \text{diameter}$)		
		t_{axial}^*	$t_{\text{flow mean}}^*$	$t_{\text{space mean}}$	t_{axial}^\dagger	$t_{\text{flow mean}}^\dagger$	$t_{\text{space mean}}$
Streamline							
Isothermal.....	Parabolic	8	10	12	16	24	32
Isothermal.....	Uniform	8	12	12	16	32	32
Adiabatic.....	Parabolic	-32	-46.7	-15	-32	-64	96
Adiabatic.....	Uniform	∞	∞	∞	∞	∞	∞
One wall isothermal and one adiabatic \ddagger ..	Parabolic	2	20/7	3			
One wall isothermal and one adiabatic \ddagger ..	Uniform	2	3	3			
Turbulent							
	Re	Pr					
Adiabatic.....	5,000	0.01	67	100	103	216	
Adiabatic.....	10,000	0.01	94	182	143	296	
Adiabatic.....	100,000	0.01	230	364	400	920	
Adiabatic.....	1,000,000	0.01	10,000	1,700	2,200	4,200	
Adiabatic.....	10,000	0.1		290		785	
Adiabatic.....	100,000	0.1		2,000		5,750	
Adiabatic.....	10,000	1		820		2,860	
Adiabatic.....	100,000	1		12,900		40,000	
Adiabatic.....	10,000	10		3,330		13,000	
Adiabatic.....	100,000	10		85,000		300,000	

* H. F. Poppendiek and L. D. Palmer, ORNL-1701, 1954.

† H. F. Poppendiek and L. D. Palmer, ORNL-1395, 1952; *Chem. Eng. Progr. Symposium Ser.*, No. 11, 1954.

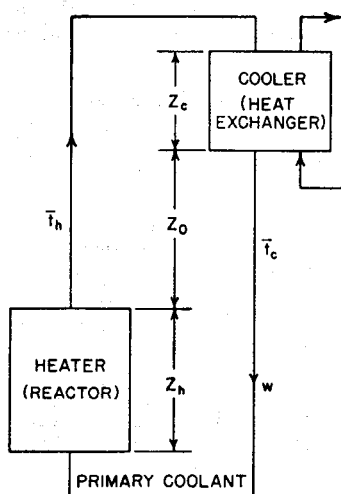
‡ t_w is at the isothermal wall, and t_{axial} at the adiabatic wall.

Experiments are lacking on laminar free convection in vertical fuel channels with uniform H , but theoretical analyses are available. They give conservatively high values of the maximum (axis-to-wall) temperature difference Δt_F across a horizontal section of the liquid fuel. For fuel sealed within channels of high height-breadth ratio Z/D , with an external coolant flowing upward which rises by Δt_c in height Z :¹⁰¹

$\frac{\Delta t_c \beta_0 D^4 c \rho^2}{Z k \mu}$	1	10	10 ²	10 ³	10 ⁴	10 ⁵
$\frac{D}{k \Delta t_F A}$ (flat channel).....	4	4	4.08	4.55	7.7	13.5
$\frac{D}{k \Delta t_F A}$ (pipe).....	4	4	4.02	4.4	7.85	25.5

6.4 Steady-state Thermal Circulation

Because of its simplicity and dependability, thermal circulation or gravity convection



of coolant or liquid fuel in a loop is frequently considered for the primary method of heat removal from a nuclear reactor. When forced circulation of the coolant is the normal method, thermal circulation is still of importance; by locating the heat exchanger higher than the reactor, partial flow is maintained in the event of pump failure.

The pertinent driving heads in a thermal-circulation loop are shown in Fig. 9. Usually there is little, if any, temperature change along the exterior piping, and it is convenient to express the buoyancy pressure ΔP_B over the loop in terms of the (average) temperature difference between the hot and cold legs and the effective driving head Z_e . Z_e evidently equals the minimum head Z_0 plus the effective values of Z_h and of Z_c . If Z_0 exceeds some five times Z_h and Z_c , one-dimensional flow and

$$Z_e = Z_0 + \frac{Z_h + Z_c}{2}$$

FIG. 9. Thermal circulation driving heads. (From C. F. Bonilla, Ref. 98.)

may be assumed without sensible error.

For convenience, the following explicit solutions for w and $t_h - t_c$ are given:

For streamline flow in a pipe loop,

$$w = \left(\frac{\pi}{128} \frac{\beta \rho^2 g Z_e D^4 q}{\mu L_e c} \right)^{1/2} \quad t_h - t_c = \left(\frac{128}{\pi} \frac{\mu L_e q}{\beta \rho^2 g Z_e D^4 c} \right)^{1/2} \quad (84)$$

For streamline flow in other cross sections, employing the ratio $\bar{u} \mu L / \Delta P g_c$ from Table 1, Sec. 9-2,

$$w = \left(\frac{\bar{u} \mu L}{\Delta P g_c} \frac{\beta \rho^2 g Z_e S q}{\mu L_e c} \right)^{1/2} \quad t_h - t_c = \left(\frac{\Delta P g_c}{\bar{u} \mu L} \frac{\mu L_e q}{\beta \rho^2 g Z_e S c} \right)^{1/2} \quad (85)$$

For turbulent flow,

$$w = \left(\frac{\beta \rho^2 g Z_e D_e S^2 q}{2 L_e f_{FC}} \right)^{1/3} \quad t_h - t_c = \left(\frac{2 L_e f_{FC} q^2}{\beta \rho^2 g Z_e D_e S^2 c^2} \right)^{1/3} \quad (86)$$

or, employing Eq. (27), Sec. 9-2, for f_F ,

$$w = \left(\frac{\beta \rho^2 g Z_e D_e^{1.2} S^{1.8} q}{0.092 L_e c \mu^{0.2}} \right)^{0.357} \quad t_h - t_c = \left(\frac{0.092 L_e \mu^{0.2} q^{1.8}}{\beta \rho^2 g Z_e D_e^{1.2} S^{1.8} c^{1.8}} \right)^{0.357} \quad (87)$$

The case of smaller Z_0 is covered elsewhere.⁹⁸

6.5 Comparison of Coolants

Many factors are involved in the selection of coolants, particularly primary coolants. These factors include cost, nuclear properties, hazards, and physical properties over the desired ranges of conditions.

In designing a nuclear power plant, any coolant should properly be considered only

in an optimized over-all design. If only a few factors are rigidly fixed, such as output and fuel, it is impossible to solve conveniently for the optimum values of all the other factors and thence the minimum cost. However, considerable guidance can be obtained by computing important derived quantities, pumping power in particular for power reactors. For a rough comparison of coolants, the ratio of their pumping powers for any desired fixed conditions is helpful. For a more thorough analysis, one or more of the conditions can be optimized for each coolant before computing the pumping power.

Employing Eq. (28), Sec. 9-2, for ΔP and Eq. (27), Sec. 9-2, for f_F , the pumping power in turbulent flow for substantially nonexpanding fluid is

$$P = \Delta P \frac{w}{\rho} = \frac{0.092 L_c}{g_c D_e^{1.2} S^{1.8}} \left[\frac{\mu^{0.2}}{\rho^2} \right] w^{2.8} \quad (88)$$

For streamline flow, using $(\bar{u}\mu L/\Delta P g_c)$ from Table 1, Sec. 9-2,

$$P = \frac{\Delta P g_c L}{\bar{u}\mu L g_c S} \left[\frac{\mu}{\rho^2} \right] w^2 \quad (89)$$

6.51 Coolant Temperature Rise Δt_c . If the coolant-film temperature difference $\Delta t_f \ll \Delta t_c$, as might particularly be true for large reactors with long or small diameter tubes and low q/A , the simplest basis of comparison is the pumping power required to give the same Δt_c . Replacing w in Eq. (88) by $q/(C \Delta t_c)$, for turbulent flow,

$$P = \frac{0.092}{g_c} \frac{L_c q^{2.8}}{D_e^{1.2} S^{1.8} (\Delta t_c)^{2.8}} \left[\frac{\mu^{0.2}}{\rho^2 c^{2.8}} \right] \quad (90)$$

Similarly, for streamline flow,

$$P = \frac{\Delta P g_c}{\bar{u}\mu L} \frac{L_c q^2}{g_c S (\Delta t_c)^2} \left[\frac{\mu}{\rho^2 c^2} \right] \quad (91)$$

Evidently, the smaller the physical-property groups in brackets in Eqs. (90) and (91), the better the coolant from this standpoint. Values for typical coolants are listed in Table 14. Water is by far the best at temperatures it (and the organics) can reach, and fused salts and metals above that. If in a comparison of coolants all are not in the same (streamline or turbulent) regime, P should be computed by the appropriate equation for each.

6.52 Coolant-film Temperature Difference Δt_f . If $\Delta t_f \gg \Delta t_c$, as might be approached in an enriched power reactor, the pumping power for turbulent flow of nonmetals to obtain the same Δt_f and thus h by Table 3, item a , is

$$P = \frac{49,850 L_c S h^{3.5}}{g_c D_e^{0.5}} \left[\frac{\mu^{1.835}}{\rho^2 c^{1.167} k^{2.333}} \right] \quad (92)$$

For liquid metals in turbulent flow in tubes, Table 4, item a , yields

$$P = \frac{49,850 L_c S h^{3.5}}{g_c D_e^{0.5}} \left[\frac{0.747 \mu^{0.2}}{\rho^2 c^{2.8} k^{0.7}} \left(1 - \frac{7}{Nu} \right)^{3.5} \right] \quad (93)$$

Similar relations can be derived for other channel shapes. A plot of h against pumping power per unit of area P/A also is convenient for comparing coolants on the constant Δt_f basis for a specific geometry.¹⁰²

For streamline flow in round pipes, Eq. (89) (increased by the ratio 4.36:3.66 from Table 6 for constant q/A) yields

$$P = \frac{5.66 L^3 D^2 h^6}{g_c} \left[\frac{\mu}{\rho^2 c^2 k^4} \right] \quad (94)$$

Table 14. Coolant Physical-property Groups*

Circulation Flow	Forced Turbulent	Forced Streamline	Forced Turbulent	Forced Turbulent	Forced Streamline	Forced Turbulent	Forced Streamline	Thermal Streamline	Thermal Turbulent
Constant.....	Δt_c	Δt_c	Δt_f	Δt_f	Δt_f	$\Delta t_c + \Delta t_f$	$\Delta t_c + \Delta t_f$	Δt_c	Δt_c
Equation.....	(90)	(91)	(92)	(93)	(94)	(95)	(96)	(84)	(87)
Coolant type.....	Any	Any	Nonmetal	Metal	Any	Nonmetal	Any	Any	Any
H ₂ O (saturated at 300°C).....	0.188	0.000922	19.79	3.44×10^8	0.721	0.721	0.753	5.03
Organic liquids:									
Dowtherm (300°C).....	1.582	0.01230	11,670	1.40×10^{12}	17.86	40.20	2.45	10.75
Cireo XXX oil (300°C).....	1.847	0.0339	130,800	8.97×10^{12}	36.2	136.8	5.51	14.10
Fused salts:									
NaOH (350°C).....	0.875	0.0416	2,160	1.258×10^9	7.11	17.35	9.12	14.35
HTS (300°C).....	2.95	0.0788	2.05×10^4	1.039×10^{11}	31.5	84.50	7.14	16.3
KCl-LiCl (400°C).....	4.54	0.1552	625	1.042×10^8	17.79	25.0	11.83	19.4
Liquid metals:									
Na (300°C).....	11.22	0.0479	1.188	43.6	0.262	7.30	28.9
Sn (300°C).....	25.2	0.0927	4.73	2,210	1.151	7.54	31.1
Hg (300°C).....	35.4	0.0532	13.89	85,100	1.898	3.08	22.6
Pb (500°C).....	41.9	0.1278	13.61	68,400	3.45	6.38	29.6
Bi (300°C).....	53.6	0.1413	15.39	37,300	3.21	2.83	39.8
K (300°C).....	56.1	0.1178	8.92	1,110	1.160	8.51	41.2
Gases:									
H ₂ (300°C, 10 atm abs).....	2.77×10^4	61.60	2.07×10^4	2.24×10^4	9.99×10^4	8.50×10^4	351	580
CO ₂ (300°C, 10 atm abs).....	0.990×10^4	44.90	3.38×10^7	5.55×10^7	5.50×10^8	4.74×10^8	82.4	358
He (300°C, 10 atm abs).....	1.47×10^8	268.0	1.47×10^7	2.86×10^{15}	5.64×10^8	4.84×10^8	438	730
Air (300°C, 10 atm abs).....	2.49×10^8	119.7	7.56×10^7	8.96×10^{17}	1.299×10^8	1.111×10^8	132.4	496

* The smaller the group, the better the coolant in that particular column. Units are centimeters, grams, seconds, and calories.

In streamline flow this comparison is less appropriate, since Δt_f and h are more dependent on D than on w and constant D would be inappropriate to compare fluids at constant Δt_f and h . Table 14 shows that sodium and then the other liquid metals are by far the best in this respect.

6.53 Hot-spot Temperature. When neither Δt_c nor Δt_f predominates, both should be considered. One comparison has been made¹⁰³ based on the same Δt_c , Δt_f , and total volume of cylindrical channels V_c , as well as channel length $2x_2$, and q . Different D , ΔP , and w are required for each coolant. For turbulent flow of nonmetals,

$$P = \frac{4}{Jg_c} \frac{q^2 x_2^2}{V_c^2 (\Delta t_c)^2 \Delta t_f} \left[\frac{\mu}{\rho^2 c^2 k} \text{Pr}^{-0.4} \right] \quad (95)$$

For streamline flow,¹⁰⁴

$$P = \frac{7.34}{Jg_c} \frac{q^2 x_2^2}{V_c^2 (\Delta t_c)^2 \Delta t_f} \left[\frac{\mu}{\rho^2 c^2 k} \right] \quad (96)$$

Dividing Eq. (96) by Eq. (95) yields $P_{\text{streamline}}/P_{\text{turbulent}} = 1.835 \text{Pr}^{0.4}$, which suggests that, if optimum design of a reactor yields coolant flow near the critical Re, it may be desirable to assure turbulent flow with nonmetallic coolants and streamline flow with metals. From Table 14 water is by far the best in turbulent flow, but in streamline flow sodium is better.

Comparison based on simultaneous constant Δt_c and Δt_f is unnecessarily restricted, since the permissible $\Delta t_c + \Delta t_f$ or $\Delta t_c + \Delta t_f + \Delta t_e$ is the important consideration. Comparison on this basis for a cosine distribution would be made by computing w in Eq. (81) by trial and error for each coolant, then substituting each w into Eq. (88) or (89). For this or any other flux distribution the relative ranking of the fluids will be intermediate between that for constant Δt_c and for constant Δt_f ; thus either water or sodium or NaOH might be best, depending on the design.

6.54 Thermal Circulation Δt_c . By Eq. (84), the efficiency of a coolant to dissipate heat with low coolant temperature rise is inversely proportional to the group $(\mu/\beta\rho^2c)^{1/2}$. If turbulent flow is attained, by Eq. (87) the pertinent group is $(\mu^{0.2}/\beta\rho^2c^{1.8})^{0.357}$. These groups are also given in Table 14 and show in this respect the moderate superiority of water. However, taking Δt_f into account, the liquid metals would generally be best, and certainly such would be the case at the high temperatures that might be reached in emergency cooling by this method.

6.55 General Evaluations. Considerations apart from those so far discussed cannot readily be made quantitative. However, a number of qualitative evaluations of coolants for various reactor designs have necessarily been made. For instance, Parkins¹⁰⁶ concludes that liquid metals are preferable for (nonboiling) heterogeneous power reactors because of the high temperatures and low decomposition obtainable. Those recommended are Na, Na + K, Pb, and Pb + 2.5 per cent Mg. Shimazaki,¹⁰⁷ from cost estimates for complete power plants using graphite-moderated solid-fuel reactors, finds Pb + 2.5 per cent Mg, Bi + 44.5 per cent Pb, Bi, Na, and HTS salt in that order of decreasing economy, though all are satisfactory. From the standpoint of current know-how, Na was believed best.

6.6 Comparison of Heat-transfer Surfaces

Different shapes or arrangements of strip, plate, gauze, or porous fuel elements or other heat-transfer surfaces can be compared and evaluated in a manner similar to that employed for coolants. This is best done in terms of the dimensionless correlations of f_F and Nu against Re. Details are available elsewhere.⁹³

7 SPECIAL STEADY- AND UNSTEADY-STATE CALCULATION AND TEST METHODS

7.1 Analytical Unsteady-state Thermal Analysis

The analytical solution of Eq. (5) has been extensively developed¹⁰⁸ for zero or constant heating density H , constant physical properties, simple shapes or initial

temperature distributions, and/or constant coolant h and \bar{t} . These idealized solutions do not closely fit most unsteady-state reactor thermal problems. However, they are frequently adapted to solve actual problems with adequate accuracy. Generally the maximum temperature of the solid vs. time (to estimate incipient mechanical failure), the maximum surface temperature vs. time (to estimate incipient coolant boiling), and the average temperature of the solid (to estimate thermal stress or heat storage) are the results sought.

The principal solutions with nuclear-power applications are as follows:*

1. Uniform initial temperature t_1 . Surface or coolant temperature suddenly changes to t_2 . $H = 0$.
 - a. Maximum, minimum, and average temperature of an infinite slab are obtainable as a function of time θ from Gurney-Lurie,²⁹ Groeber,⁵ Hottell,²⁹ or Bachmann¹⁰⁹ charts for constant h .
 - b. Same for an infinite cylinder.^{5,29,109}
 - c. Same for a solid sphere.^{5,29,109}
 - d. For an infinite bar, a parallelepiped, or a finite cylinder, the local or the over-all mean value of $(t - t_1)/(t_2 - t_1)$ is obtainable by multiplying together the values for the separate two or three dimensions.
 - e. Temperature in a semi-infinite solid.^{108,110}
2. Uniform initial temperature t_1 . Surface temperature changes linearly with time. $H = 0$.
 - a. Temperature in a semi-infinite solid.^{29,110}
 - b. Temperature change Δt in an infinite slab at distance x from the heated face can be computed by the "method of reflections"¹¹⁰ by summing terms $\Delta t'$ for a semi-infinite solid:

$$\Delta t_x = \Delta t'_x + \Delta t'_{2R-x} - \Delta t'_{2R+x} - \Delta t'_{4R-x} + \Delta t'_{4R+x} + \Delta t'_{6R-x} - \Delta t'_{6R+x} - \dots$$

- c. The maximum (at $\theta = \infty$) temperature difference across an infinite slab [obtainable by Eq. (9), since $dt/d\theta$ will be uniform]:

$$= (t_{\max} - t_{\min})_{\infty} = \frac{R^2}{2\alpha} \frac{dt}{d\theta} \quad (97)$$

- d. For a solid infinite cylinder, from Eq. (20):

$$(t_{\max} - t_{\min})_{\infty} = \frac{R^2}{4\alpha} \frac{dt}{d\theta} \quad (98)$$

- e. Cases *c* and *d* at shorter θ .¹¹¹
- f. For finite shapes, case *1d* above applies.
- g. An irregular variation of surface temperature with time can be fitted by a broken line of straight segments. At each change in slope, the change can be considered as a new $dt/d\theta$ starting then. The temperature changes at any location due to all previous straight segments are algebraically added.¹¹⁰
3. A definite q/A is forced into the body, initially at t_1 . $H = 0$.
 - a. At $\theta = 0$; a constant q/A starts to enter one face of an infinite slab of thickness R , the other being adiabatic. Reference 112 gives t_{\max} and t_{\min} :

$$t_{av} = t_1 + \frac{\theta q}{Ac\rho R}$$

- b. Same as case *a*, but q/A increases linearly with θ from $q/A = 0$ at $\theta = 0$ or decreases linearly with θ .¹¹²
- c. Same as case *a*, but the unheated face is in contact at constant h with a coolant maintained at t_1 .¹¹³

* Plots of most of these cases are given in Ref. 98.

- d. Same as case *a*, but the unheated face is in contact with a body of known heat capacity with h and $k = \infty$.¹¹⁴
- e. At $\theta = 0$ a constant q/A starts to enter the inner face of a concentric cylindrical shell.¹¹⁵
- f. An irregular variation of q/A with time can be handled as under case $2g$ above. For instance, an unheated "equalizing period" is analyzed by continuing the initial heating, later starting an additional equal negative heating period, and adding the two temperature changes anywhere algebraically.
- g. For an infinite bar, a parallelepiped, or a finite cylinder, the total local or mean temperature change is obtainable by adding the changes computed separately for each dimension.
- 4. The heating density throughout a body at t_1 suddenly changes from 0 to a constant value H . Heisler¹¹⁶ gives curves for the temperature distribution throughout infinite slabs, infinite solid cylinders, and solid spheres for the cases of constant surface temperature and constant coolant temperature and h .
- 5. The heating density H throughout the body varies with time.
 - a. For an infinite slab of thickness R , initial temperature t_1 , cooled face kept at t_1 , and linear uniform heating $H = \alpha\theta$. Letting $\alpha(\pi/2R)^2 = B$,

$$t = t_1 + \frac{2\alpha}{\pi c \rho B^2} \sum_{n=1}^{\infty} \left[\frac{1 - (-1)^n}{n^5} (e^{-n^2 B \theta} + n^2 B \theta - 1) \sin \frac{n\pi x}{2R} \right] \quad (99)$$

t_{\max} is at $x = R$, and on integrating to obtain t_{av} , $\sin n\pi x/2R$ is replaced by

$$\frac{2[1 - \cos(n\pi/2)]}{n\pi}$$

- b. Case *a*, except that $H = H_0 e^{b\theta}$.

$$t = t_1 + \frac{2H_0 \theta}{\pi c \rho} \sum_{n=1}^{\infty} \left[\frac{1 - (-1)^n}{n} \frac{e^{b\theta} - e^{n^2 B \theta}}{b\theta + n^2 B \theta} \sin \frac{n\pi x}{2R} \right] \quad (100)$$

t_{\max} and t_{av} are obtained as in case *a*.

- c. Same as case *b*, but cladding and stationary coolant layers without heat generation are added.¹¹⁷

The above solutions cover many reactor problems.* Where heating or temperature rise is stated, cooling or temperature fall can be read. Also, although uniform initial temperature t_1 is stated, the temperature change calculated can be added to a steady-state temperature distribution originally present (see Arts. 2.3 and 2.4) provided the heat source remains (if not, method 3f is also employed).

7.2 Numerical Design Methods

These methods subdivide the volume of each solid and fluid by a rectangular or a radial and circumferential grid, as fine as necessary for the desired accuracy, and assume that the mass of each subdivision is concentrated in a point, or "node."¹¹⁸ The thermal resistance between adjacent nodes is that between the sections of the subdivisions which pass through the nodes normal to the "bar" joining the nodes, namely, the distance between the nodes divided by k times the cross section (the average cross section if it varies). In the interior of a body, nodes are placed at the centers of the subdivisions. Along surfaces half-sized subdivisions are generally used, with the nodes at surface locations of known or desired temperature. The heat balance for each node of unknown temperature is then written in terms of the data

* For example, Ref. 110 combines methods 2b and 2g to obtain the temperature distribution and maximum thermal stress in a plate subjected to a complex temperature cycle of a reactor coolant.

and of the surrounding unknown temperatures, and the equations solved simultaneously or consecutively for the unknown temperatures. Suitable relations are given below for node 0 in a two-dimensional rectangular grid. If conditions are not uniform along z , it should also be subdivided. In all cases Δx is in the direction between the two nodes under consideration and Δy (and Δz) normal to that direction. In a square (or cubical) lattice they are, of course, equal and interchangeable.

7.21 Conduction. Heat conducted from adjacent node n at distance Δx is at a rate

$$\Delta q_{n,0} = \frac{(t_n - t_0) \Delta z \Delta y}{\Delta x_n/k_n + \Delta x_0/k_0} = K_{n,0} \Delta t_{n,0} \quad (101)$$

7.22 Convection and Radiation. Heating rate by convection from fluid at t_f passing a wall node is $\Delta q_{f,0} = (t_f - t_0)h \Delta z \Delta y = K_{f,0} \Delta t_{f,0}$. For a central node the conduction resistance is added:

$$\Delta q_{f,0} = \frac{\Delta t_{f,0} \Delta z \Delta y}{1/h + \Delta x/2k_0} = K_{f,0} \Delta t_{f,0} \quad (102)$$

Convective h by Arts. 3.2 to 5.4 and radiation h are directly additive if the same $\Delta t_{f,0}$ applies.

7.23 Forced Surface Heating. Heating rate at a given q/A is

$$\Delta q_{A,0} = \Delta z \Delta y \frac{q}{A} = q' \quad (103)$$

7.24 Volume Heating. Heating rate at a given H is

$$\Delta q_{v,0} = H \Delta z \Delta x \Delta y = H'$$

7.25 Transport. Heating rate by a fluid flowing into a subdivision is

$$\Delta q_{T,0} = (t_T - t_0)u\rho c \Delta z \Delta y = c \Delta w \Delta t_T = c'_T \Delta t_T$$

The outgoing stream is not of concern; thus this term changes on reversal of flow.

7.26 Accumulation. Heat accumulated by node 0 is at a rate

$$\Delta q_0 = (t'_0 - t_0)\rho c \Delta z \Delta x \frac{\Delta y}{\Delta \theta} = \frac{c'_0 \Delta t_0}{\Delta \theta} \quad (104)$$

where Δt_0 is the rise in temperature during time increment $\Delta \theta$.

The over-all balance of heat rates for node 0 is

$$\Delta q_0 = \Delta q_{n,0} + \Sigma(\Delta q_{n,0} + \Delta q_{f,0} + \Delta q_{A,0} + \Delta q_{T,0}) \quad (105)$$

7.27 Transient Problems. In these problems all the temperatures and other quantities in Eq. (105) are known, except t'_0 or Δt_0 in the accumulation term. Accordingly the equation can be written for each node in the problem, and each t' at the end of $\Delta \theta$ directly computed. The process is then repeated using the t' values in place of the t values, and t'' is computed for each node at $2 \Delta \theta$. This "iteration" process is continued until the desired total time interval is covered. For convenience, Eq. (105) is converted to

$$\begin{aligned} t'_0 &= (q' + H') \frac{\Delta \theta}{c'_0} + \left\{ 1 - \left[\frac{\Delta \theta}{c'_0} (\Sigma K_{n,0} + K_{f,0} + c'_T) \right] \right\} t_0 + \frac{\Delta \theta}{c'_0} \Sigma(K_{n,0} t_n) \\ &\quad + \frac{\Delta \theta}{c'_0} K_{f,0} t_f + \frac{\Delta \theta}{c'_0} c'_T t_T \\ &= B + B_0 t_0 + \Sigma B_n t_n + B_f t_f + B_T t_T \end{aligned} \quad (106)$$

The B coefficients defined above can be computed for each node, and the calculation of Eq. (106) carried out on a digital computer. If temperatures or flow vary sufficiently, the B values can be modified during the process.

The number of times that Eq. (106) must be employed to solve a given problem is proportional to $(\Delta\theta \Delta x \Delta y \Delta z)^{-1}$. Large increments favor speed and economy, and small increments favor accuracy. With a high-speed digital computer available, a single computation with a relatively fine grid is preferable; with hand calculation the use of two or three coarser grids and extrapolation to zero node spacing is preferable. If $\Delta\theta$ is selected too large, it will be found that successive values of t_0, t'_0, t''_0 , etc., oscillate more and more widely. To prevent this "instability," B_0 should not be negative at any node; thus $\Delta\theta$ should not exceed

$$\frac{c'_0}{\Sigma K_{n,0} + K_{f,0} + c'_T}$$

anywhere.

The "truncation error" due to the finite size of the time increments can be estimated by repeating the calculation with smaller increments; for any node 0 it cannot exceed a maximum of $\theta_{\text{total}}(\Delta t'_0 - \Delta t_0)/2 \Delta\theta$, where $(\Delta t'_0 - \Delta t_0)$ is the largest change in successive increments.¹¹⁹

Equation (106) simplifies considerably under some conditions. In particular, for a node in a square subdivision, completely surrounded by two, four, or six identical equidistant nodes, $K_{n,0}$ equals $k \Delta z$. If there is no heat convection or transport and the maximum stable $\Delta\theta$ ($\Delta\theta_{\text{max}}$) is employed, where

$$\Delta\theta_{\text{max}} = \frac{\text{(One-dimensional)} (\Delta x)^2}{2\alpha}, \quad \frac{\text{(Two-dimensional)} (\Delta x)^2}{4\alpha}, \quad \frac{\text{(Three-dimensional)} (\Delta x)^2}{6\alpha} \quad (107)$$

then B_0, B_f , and B_T all equal 0. If H' also equals 0, Eq. (106) yields

$$t'_0 = (t_n)_{\text{av}} \quad (108)$$

Thus, merely averaging the surrounding node temperatures t_n gives the central one $\Delta\theta_{\text{max}}$ later. Equation (107) is thus the most frequently used $\Delta\theta$, on account of speed. A somewhat more conservative procedure consists of averaging t_0 in equally with each of the m values of t_n . In this case

$$t'_0 = \frac{t_0 + \sum_1^m t_n}{m + 1} \quad (109)$$

and
$$\Delta\theta = \frac{(\Delta x)^2}{3\alpha}, \quad \frac{(\Delta x)^2}{5\alpha}, \quad \frac{(\Delta x)^2}{7\alpha} \quad (110)$$

An unknown *steady-state* temperature distribution or heat flow is obtainable with these numerical methods by carrying out the transient calculation at the given conditions until no further significant change with time occurs. While this generally requires many calculations, it may be the best method if the transient problem has already been set up on a high-speed computer.

At steady state, $t_0 = t'_0$ and Eq. (106) may be written

$$t_0 = \frac{q' + H'}{\Sigma K_{n,0} + K_{f,0} + c'_T} + \sum \frac{K_{n,0} t_n}{\Sigma K_{n,0} + K_{f,0} + c'_T} + \frac{K_{f,0} t_f}{\Sigma K_{n,0} + K_{f,0} + c'_T} + \frac{c'_T t_T}{\Sigma K_{n,0} + K_{f,0} + c'_T} \quad (111)$$

One such equation is obtained for each unknown temperature. A direct method to obtain the steady-state temperatures is to solve all the equations simultaneously. Though seldom used, this method is at times practical with a high-speed computer.

A more rapid solution is obtained by "relaxation," or balancing (or even over-

balancing) each time the most unbalanced node. The temperature unbalance of each node is recorded, as well as its temperature. When a node has been balanced by changing its temperature, the corresponding change in the balance or unbalance of each neighboring node is added to its previous unbalance. The node with the largest unbalance is always balanced next.¹¹⁸ Figure 10 shows the boundary fits obtainable for a specific case with coarse rectangular and cylindrical "square" grids.

For maximum speed it is desirable to solve the problem first on a coarse grid. The temperatures thus found around each square are averaged [or inserted in Eq. (111)], yielding a fairly reliable temperature for the center of the square. A grid containing twice as many points is obtained, diagonally to the first grid. This finer grid of temperatures is then improved by iteration or relaxation, and a still finer one drawn and improved as before, if desired.¹¹⁸ This procedure is faster than going at once to the finest grid, since it provides reliable estimates of the temperatures and fewer circuits of computation about the shape are needed. It is also more accurate, as additional

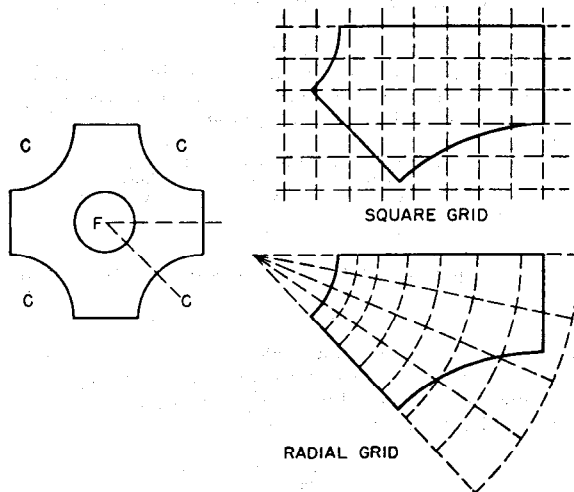


FIG. 10. Square grids for thermal analysis of LMFR fuel element. (From C. Williams, F. T. Miles, and O. E. Dwyer, *Nucleonics*, July, 1954.)

values of the desired temperatures and heat flows are provided at coarser grid sizes, permitting a graphical extrapolation to zero grid spacing.

Other variations of these methods are also employed, including heavier weighting of t_0 , balancing of whole groups of nodes in the early iterations, radial and triangular grids of nodes, etc.⁹⁸

7.3 Graphical Methods

For one-dimensional cases, such as thin or flat fuel elements or shields, Eq. (108) or (109) can be readily carried out graphically by the Binder or Schmidt method.²⁹ To obtain t'_b by averaging t_a and t_c as per Eq. (108), a straight line is drawn between t_a and t_c in Fig. 11a to intersect the position of node b , and $\Delta\theta = (\Delta x)^2/2\alpha$. If the surface temperature is held constant or varies in a known manner with time, one node would be placed at the surface. If the surface temperature depends on coolant temperature t_f and coefficient h , or on known heat velocity q/A , it is more convenient to place the surface between an inner "actual" and an outer "imaginary" node, as in Fig. 11b and c. If heat generation occurs, the additional temperature rise

$$t' - t = H \frac{\Delta\theta}{\rho c} = H \frac{(\Delta x)^2}{2k}$$

is added to each heated node at each time increment $\Delta\theta$. t_f , h , q/A , H , and even k at the surface may be varied as time or temperatures advance. If two materials A and B (i.e., fuel and cladding) are adjacent, the ratio $\Delta x_A/\Delta x_B$ may be set $= \sqrt{\alpha_A/\alpha_B}$ so as to maintain $\Delta\theta$ by Eq. (107) the same. If this gives inconvenient spacings, Δx may be kept constant and the design completed by weighting t_0 other than zero in one of the materials and using Eq. (106) for that material.²⁹

The solid or hollow cylinder and sphere with radial temperature and geometrical symmetry are also best treated as one-dimensional cases for either numerical or graphical solution. For the latter the same methods of Fig. 11 are employed, except that equally spaced nodes at r_a and r_b on the radius of a cylinder are spaced on the working plot¹²⁰ distances proportional to $(r_a + r_b)^{-1}$. For a sphere the spacing is as $(r_a + r_b)^{-2}$.

Comparable to Eqs. (109) and (110), smaller $\Delta\theta$ than $\Delta\theta_{max}$ can also be used graphically (method of Nessi and Nisolle⁵). However, the added effort is probably better

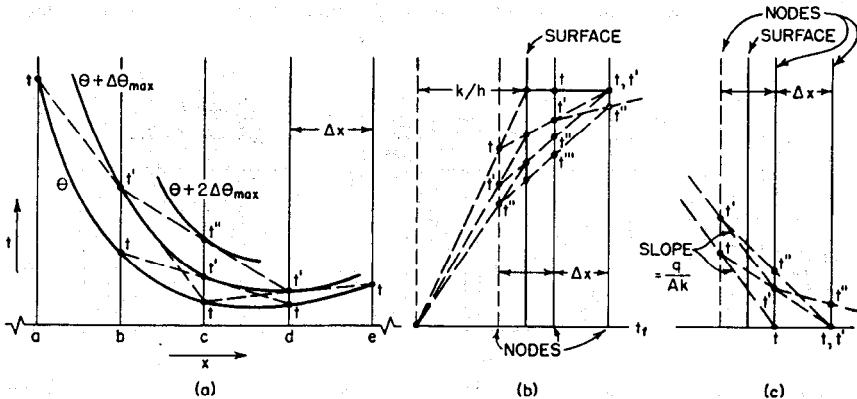


FIG. 11. Details of the Binder or Schmidt graphical method for one-dimensional heat conduction in a slab. (a) Central region with $H = 0$; (b) surface with convection cooling; (c) surface with known heat velocity. (From C. F. Bonilla, Ref. 98.)

expended into decreasing Δx . In general, if graphical analysis is carried out carefully and on a large scale, it can give satisfactory results for one-dimensional cases more rapidly than the other methods.

7.4 Homogeneous Electrical Analogues (Steady State)

As was done in Art. 3.12 of Sec. 9-2 for streamline flow, in heat conduction and convection design problems thermal resistance may be simulated by electrical resistance and temperature and heat flow by voltage and current. Merits of the electrical analogue over calculation, or performing a thermal experiment, are greater speed and economy, particularly in steady-state problems or when various similar cases are to be covered.

Two-dimensional steady-state problems with isothermal and insulated edges and one or more homogeneous thermal conductors can be solved most conveniently with Teledeltos paper,* though soft metal foil, brass shim stock, trays of conducting solution, and semiconducting plastic sheeting have been used. Teledeltos grades available are L (approximately 1,000 to 2,000 ohms per square) and H (approximately 10,000 to 20,000 ohms per square). Crosswise resistance is some 12 per cent higher than lengthwise resistance along the rolled sheet; this can be approximately corrected for by a corresponding difference in the x and y scales. The resistance R may be increased almost isotropically up to fivefold by punching out holes on a reasonably fine grid.

* Available from the Western Union Telegraph Company.

Equally spaced circles as follows are required (D/S is the ratio of diameter to center spacing):

Perforated R /unperforated R	1	1.25	1.5	2	3	4	5	∞
D/S (90° grid).....	0	0.39	0.51	0.65	0.79	0.86	0.90	1
D/S (60° grid).....	0	0.34	0.48	0.62	0.76	0.82	0.86	1

For conduction problems the shape is cut to scale out of the paper, allowing an extra $\frac{1}{4}$ in. at the isothermal edges to connect a good conductor. Du Pont 4922 silver lacquer is generally used; it has a lengthwise resistance of only several ohms per foot for a thin $\frac{1}{8}$ -in. strip and also negligible contact resistance (a fine copper wire can be incorporated to minimize the lengthwise resistance). Clean brass bars clamped against the paper, which is backed with rubber, are more convenient for making changes; contact resistance is about $\frac{1}{8}$ in. of the paper, negligible in large analogue sizes.

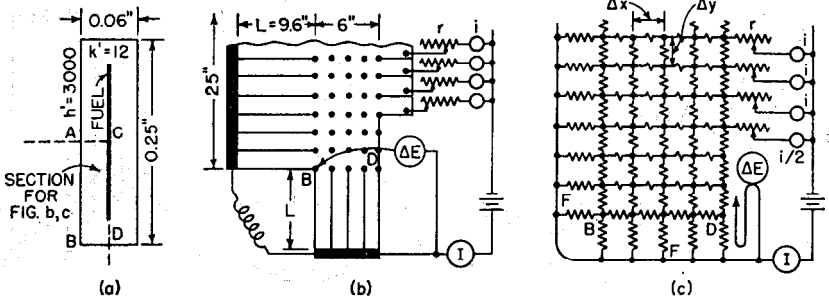


FIG. 12. Electrical analogues for two-dimensional steady-state heat conduction and convection study of a long thin-strip stainless-clad fuel element. (a) Actual size and thermal data; (b) possible homogeneous analogue arrangement [central dots apply to (c)]; (c) possible lumped analogue arrangement [nodes are at dots in (b), and $\Delta x = \Delta y$]. (From C. F. Bonilla, Ref. 98.)

Coolant film resistances are representable by additional paper slit into strips normal to the surface (strips of finite width, of course, depart from the true homogeneous analogue). To keep solid and film resistances in proportion, the strip length L is set equal to Sk/h , where S is the geometrical scale ratio of the analogue. For instance, in Fig. 12, an analogue for a very thin strip of U^{235} with stainless cladding, $L = (6/0.03)(12/3,000)$ ft = 9.6 in. If L is unreasonably long, additional resistors may be connected to each strip or some of the strips may be cut off at the base and the length of the rest shortened to give the same total resistance of the strips. Strips should be curled with string or small rubber bands to prevent contact at their edges. If different sheets of paper are attached together, a narrow strip of silver lacquer is used as glue. If the line of glue is nonisothermal, it should be frequently cut across with a razor to prevent conduction along it.

Unsteady-state problems require electrical capacity (see Art. 7.5). Uniformly distributed capacity could in principle be obtained with a large grounded plate covered with thin dielectric and a conducting sheet on top; actually uniformity would be poor, and the size would be very large or time very short. Large capacitors can be attached at small points, but the electrical connection resistance is high; large electrodes decrease the resistance of the main sheet. Thus "lumped" or "network" or "passive-network" analogues (Art. 7.5) are preferable for unsteady state.

Heat generation also requires electrodes as current lead-ins. Here connection resistance is not important, though points at which temperature (voltage) is sought should be roughly equidistant from two or more lead-ins rather than near one. In

Fig. 12b the fuel has been subdivided by short strips. Each rheostat r is adjusted until the currents i are distributed in proportion to the given heat-generation distribution (uniform for a small uniform strip fuel element such as this). If the resistances r are relatively high, the settings will not need trial-and-error readjustments to match the heat generation. Equal currents without repeated adjustment can also be obtained by using a constant-current ballast tube at rated current or a "beam-power" (6SJ7 or 6V6) vacuum tube, which is grid-controllable over a 10-fold range of current, roughly.

Points A and C are the hottest surface and interior points, and B is the coldest. To obtain the temperature rise Δt of any such points above the coolant temperature, the voltage difference ΔE above the end of the strips is read by a potentiometer or high-resistance voltmeter. Dividing the electrical (Ohm's) law into the thermal law, for any analogous locations,

$$\frac{\Delta t}{\Delta E} = \frac{q R_t}{I R_e} = \frac{q}{I} \frac{1}{kbR'}. \quad (112)$$

where R' is the ohms of a square of the paper used and b is the thickness (length of strip fuel element) of the section in Fig. 12b generating heat q . If the thickness of the U^{235} were significant, a larger analogue could be made with the fuel region of the proper resistance per square and a two-dimensional array of current inputs over it.

For two- and particularly three-dimensional problems, acidified strong CuSO_4 solution can be employed. The container has the desired shape to scale, and isothermal edges or surfaces are sheet-copper electrodes. Use of alternating current avoids electrode polarization. Solid electrolytes that can be cut and melted, such as gelatin in salted glycerin water, are also used. Fluid film resistances are more difficult to apply with these materials.

7.5 Lumped Component Electrical Analogues (Steady and Unsteady State)

Replacing the conducting paper of region $ABCD$ in Fig. 12 by a network of resistors is a further departure from the homogeneous thermal problem. However, this is outweighed by practical advantages in many cases, such as greater speed of setup if a resistor board is available, greater accuracy of resistors than sheets, and greater convenience for unsteady-state problems. Portions of the problem are usually "lumped" in any case, as in Fig. 12b, and added "lumping" is not detrimental unless fine local temperature distribution in this region is desired.

A resistor board for general use may have clips to hold cartridge resistors or a linear or tapered rheostat permanently at each resistor position. Up to three decades are also available in single plug-in resistor assemblies (Goodyear). Many nodes are provided, only the desired ones for any problem being connected. For single problems the network can be put together more quickly and economically by soldering the proper resistors together and mounting them on plywood. Good linear wire-wound rheostats (General Radio) are everywhere within 1 per cent of their scale value. In fixed resistors the lathe-cut carbon-film type (Aerovox) gives a good combination of cost, stability, and uniformity (± 1 per cent).

In setting up a lumped-component analogue with constant fluid temperatures (i.e., small changes in stream temperatures or for a cross section normal to the stream or streams) the general methods of Art. 7.2, illustrated in Fig. 12c, are employed for the resistances. For convenience in obtaining surface temperatures, nodes are usually located along all surfaces. As many of the nodes as possible inside the conduction region are usually placed on a square grid, so the same size resistor can be used between them.

If each central resistor in the square grid in Fig. 12c is arbitrarily selected as 100 ohms, each edge resistor, between surface nodes, is 200 ohms. To maintain the proportion

$$\left(\frac{R_t}{R_e}\right)_{\text{solid}} = \left(\frac{R'_t}{R'_e}\right)_{\text{square}} = \left(\frac{R_t}{R_e}\right)_{\text{film}}$$

each full surface film resistor equals $R'_e k/h \Delta x$, or

$$\frac{100 \times 12}{3,000 \times (0.0075/12)} = 640 \text{ ohms}$$

in this case. At corners B and D , 1,280-ohm resistors are used, except that the two at B can evidently be replaced by one 640-ohm resistor. Equation (112) gives any desired Δt , as before.

For unsteady-state analyses, a condenser* is attached to each node with an electrical capacity proportional to the thermal capacity represented by the node. Thus, the capacitor for a central node would be proportional to $bc\rho \Delta x \Delta y$, or $bc\rho(\Delta x)^2$ with a square grid. A side node has half this capacity, and a corner node (B and D) one-quarter. The other terminal of each capacitor is connected to the reference voltage, wire F in this case. Capacitors up to 20 μf are frequently employed. The dielectric must be good to keep self-discharge low over the time of operation; leakage time constants RC of 20,000 and 100,000 ohm-farads (seconds) at 25°C—still higher at lower temperatures—are available (i.e., Sprague). Mylar dielectric (Good-All) yields even higher RC .

The scale of resistances and capacitors may be independently selected, but they then control the ratio of thermal time to equivalent time in the electrical analogue. The time-scale ratio is obtainable by dividing the heat-conduction equation [Eq. (5) with H and the parenthesis = 0] by the comparable relation $dE/d\theta = \nabla^2 E/C''_e R''_e$, where C''_e and R''_e are the farads and ohms per unit length. The product $C''_e R''_e$ can be computed for any cross section (such as one transverse increment of the grid), because C_e and R_e vary inversely. They can also be C'''_e and R'''_e for one length-wise increment of the grid if the distance variables in $\nabla^2 E$ are changed to grid steps. Thus

$$\frac{\alpha\theta_i}{(\Delta x)^2} = \frac{\theta_e}{C'''_e(R'''_e)} \quad (113)$$

For an estimated desired range of θ_i , θ_e can be calculated. If θ_e is impractically short or long, Δx , C'''_e , and/or R'''_e , may be altered as desired or convenient. The capability of such an unsteady-state analogue to subdivide space is proportional to the number n of the largest capacitors $(C'''_e)_{\max}$ available. Its capability to subdivide time is, for practical purposes, proportional to $n(C'''_e)_{\max}(R'''_e)_{\max}/(\theta_e)_{\min}$, where $(R'''_e)_{\max}$ is the highest resistor size available allowing sufficient sensitivity and $(\theta_e)_{\min}$ is the minimum reliable response time of the electrical recorder, or indicator plus observer. †

Study of a transient in heat generation or in coolant temperature may be illustrated by the case of Fig. 12. Considered as a slab,

$$\frac{hR}{k} = \frac{3000 \times 0.03}{12 \times 12} = 0.625$$

From a chart for case 1a, Art. 7.1, $h^2\theta/kc\rho = 0.010$ for 90 per cent of the surface temperature change uncompleted and 1.7 for 10 per cent of the midplane change uncompleted, or a maximum reasonable range of θ_i of 0.0036 to 0.60 sec. Taking C'''_e as 20 μf and R'''_e as 100 ohms yields $\theta_e = 0.0082$ to 1.37 sec. While this range would be feasible with fast instrumentation, it would be simpler to increase R'''_e , to say 10^5 to 10^6 ohms, and θ_e proportionally. Voltage could be increased as desired. Rheostats r might need adjustment during the experiment to keep the currents constant. Indi-

* A purely resistive network¹²¹ can instead be used and step-wise subdivision of time, but the solution is more time-consuming. This process amounts to solving Eq. (106) simultaneously for all nodes for one $\Delta\theta$, then repeating as many times as necessary.

† In large complicated shapes the temperature may be desired at many points, for thermal-stress calculations. This may be accomplished with a reasonable number of condensers by first setting nodes over the whole object up to the available number of condensers and finding their temperature history. Then subdivisions are set up in turn with finer grids, and the boundary temperatures made to vary as previously found.

cating or recording instruments should be of high enough resistance not to alter the currents appreciably.

Lumped-component electrical analogue circuits can also be devised for steady-state and even transient analysis of complete systems, such as a reactor, pump, heat exchanger, turbine, and condenser. Such methods have not yet been developed in general terms.

7.6 Mass Transfer and Mass-transfer Analogues

Mass transfer is the passage of molecules of a dissolved or vaporized constituent from one phase to another, by diffusion and convection in the direction toward equilibrium. Normally the phases are insoluble or only slightly soluble in each other, and the substance being transferred may be the only, the major, or a minor constituent of one of the phases. Nuclear applications include the dissolving of fuel or fertile elements by liquid-fuel or breeder-blanket solutions; the removal of converted fertile elements, residual fuel, or fission products by evaporation, sparging, or extraction of their solution by a second liquid or a solid; the dissolving or differential thermal solubility corrosion of pipes and vessels; etc. In fact, a principal advantage of liquid-fuel and homogeneous reactors is that by mass transfer the fission-product concentration can be kept low for safety and neutron economy and the fuel, fertile, and converted elements can be maintained at their most economical concentrations.

Most nuclear mass-transfer processes employ at least one dilute solution. This makes mass transfer analogous to heat transfer with constant properties, since the molecular and eddy diffusion in the laminar boundary layer and core are comparable to the corresponding conductions and the physical properties of the dilute phase or phases (the main resistance to mass transfer) are substantially constant at the values for the pure phase or phases. Theoretical approaches can be based on velocity distribution such as Eqs. (31) to (33) of Sec. 9-2, Eq. (35) of Sec. 9-2 to yield ϵ , and finally integration of Eq. (37) of Sec. 9-2. Agreement is good at the same Re between the analogous heat- and mass-transfer expressions over the whole practical range of Schmidt number Sc , $\mu/D\nu\rho$, or 0.5 to 3,000. Deissler has obtained theoretically,¹²² for flow in a smooth pipe with Sc above about 50,

$$St_H = 0.079f_F^{1/2} Pr^{-3/4} \quad St_M = 0.079f_F^{1/2} Sc^{-3/4} \quad (114)$$

which is adequate for diffusion-controlled thermal corrosion of pipes by most liquid metals and fused salts. Also, Chilton and Colburn's empirical analysis has shown that j_D and j_H [see Table 3, Sec. 9-2, and Eq. (116)] are roughly equal for any given shape and Re value.¹²⁴ Thus both analyses indicate that Tables 3 and 8 for nonmetals would hold for mass transfer in metals or nonmetals on replacing Nu by Sh (Sherwood number F'/u ; see below) and Pr by Sc . At Re above about 10,000, j_H is also roughly equal to $\frac{1}{2}j_F$. Thus the average mass-transfer coefficient F' can be estimated from pressure-drop as well as from heat-transfer data.

Laminar mass transfer is evidently analogous to laminar heat transfer. Tables 5 to 7 can be applied by further substituting $D\nu\rho$ for k/c in Gz and Gz' . Also free-convection Table 9 applies; $\beta \Delta t$ should be computed¹²⁵ as $\Delta\rho/\bar{\rho}$.

In all cases, the total rate of mass transfer w_M is obtained by

$$w_M = F'A(\Delta c)_m = \frac{F'A}{R'T} (\Delta p) \quad (115)$$

where A = surface area through which mass transfer occurs

$(\Delta c)_m$ = average concentration difference causing mass transfer, mass per unit volume

F' = film mass-transfer coefficient, velocity units, i.e.,
 $lb/(sec)(ft^2)(lb/ft^3) = fps$

For a volatile solute, partial pressure p is more convenient. If one phase flows parallel or countercurrent to the other or has a constant concentration at its surface,

the log mean Δc would apply. In other cases the mean Δc integrated over the area would be used.

Because of the similarity in the correlations for heat and mass transfer, the latter can be utilized as an analogue to yield information on the former. In particular, heat-transfer coefficients for fuel elements or other objects of special shape can be obtained by casting or machining the object of a material that will vaporize or dissolve slowly. The object, with all pertinent surroundings to scale, is placed in a nonrecirculating stream of an appropriate fluid at a temperature yielding a suitable mass-transfer rate and at a velocity yielding the desired Re .

The average coefficient* \bar{h} for the test fluid or, more importantly, for the reactor fluid, if it is a different fluid, can be computed from the loss in weight of the object or from the gain in concentration in the mixed stream. Even more simply, the ratio between the local h (based on approach temperature) at different positions, or between h and \bar{h} , is the ratio of the rate of vaporization or solution at those positions as measured mechanically. For gases at 0 to about 50°C naphthalene is reliable and convenient;⁵ such a study was made of the STR fuel-element assembly.¹²⁶ Camphor, acetamide, and other solids that sublime are also suitable.¹²⁷ For cold water as the fluid, β -naphthol, benzoic acid, and cinnamic acid are useful.¹²⁴ Heat-transfer information for liquid metals is not obtainable in this way, since the electronic contribution is absent in mass transfer and Sc values are not possible as low as the Pr values of liquid metals.

The Chilton-Colburn relation yields

$$j = \frac{F'}{u'} (Sc')^{2/3} = \frac{h}{c\rho u} (Pr)^{2/3} \quad (116)$$

$$\frac{h}{F'} = \frac{c\rho u}{u'} \left(\frac{Sc'}{Pr}\right)^{2/3} = c\rho' \frac{\mu}{\mu'} \frac{D'}{D} \left(\frac{Sc'}{Pr}\right)^{2/3}$$

The mass-transfer quantities in Eq. (116) are primed, and the heat-transfer quantities are not primed. For air and naphthalene $Sc' = 2.5$. Expressing T' in degrees Rankine, evaporation rate w' in mils (0.001 in.) of naphthalene per hour, and naphthalene partial pressure driving force $\Delta p'$ in millimeters of Hg, $F' = 0.02574w'T'/\Delta p'$ fph. Using fresh air and basing F' (and h) on inlet-stream concentration (or temperature), $\Delta p'$ is the vapor tension p'_s of naphthalene in millimeters, where

$$\log p'_s = 11.450 - \frac{6712.7}{T'} \quad (117)$$

If true local F' and h are desired, $\Delta p'$ is set equal to $p'_s - p'_b$, where p'_b is the local average partial pressure in the stream as calculated from upstream total vaporization rate. p'_b in millimeters is given by the ideal-gas law as

$$\frac{553.6W'T'}{Q'M'}$$

where W' = upstream rate of evaporation, lb/sec

Q' = gas flow rate, cfs

M' = molecular weight (128.2 for naphthalene)

T' = temperature, °R

7.7 Similitude Tests

For new and complicated shapes or assemblies of fuel elements, coolant channels, etc., heat-transfer coefficients and temperature and flow distributions can be approximately estimated by methods in this and the previous chapter. For best results,

* These mass- and heat-transfer coefficients must be based on analogous driving forces. The difference between the surface and the approach concentrations or temperatures is the most convenient, but the surface to local-mean driving force is common.

full-scale tests at working conditions are indicated. However, in many cases this would be quite difficult, expensive, and/or time-consuming. But fluid-flow or heat-transfer characteristics for any given shape have regularly been expressed as relations among a certain number of dimensionless ratios. Thus, if it is possible in a test to control all but one of the dimensionless ratios to the working-condition values, the remaining ratio in the test will also have the same value as it would at working conditions. The desired ratio can be computed from the test data, and the unknown quantity therein computed for the working conditions.

The deviations from working conditions that are of interest are size, velocity, and fluid properties (different fluid and/or temperature). The following cases are most encountered. Arbitrarily, the primed quantities will refer to the test and unprimed to the working conditions. D is any characteristic length.

7.71 Flow Distribution, Type of Flow, Pressure Drop. In a scale model at the same Re as the working unit, the values of N/D , f_F , c_D , and any other such size and flow dimensionless ratios are the same as in the working unit. Then from Eq. (60), Sec. 9-2, the ratio $\Delta P/\Delta P'$ for streamline or turbulent flow in a pipe, and also for flow through an orifice, is obtained as $(w/w')^2(\rho'/\rho)(D'/D)^4$. Since the ratio $\Delta P/\Delta P'$ is the same for all such standard cases, it is necessary and sufficient also for complex shapes to keep Re the same in the scale model as in the working unit to obtain similar flows.

$$Re = \frac{D\bar{u}\rho}{\mu} = \frac{D'\bar{u}'\rho'}{\mu'} \quad \frac{Q\rho}{D\mu} = \frac{Q'\rho'}{D'\mu'} \quad (118)$$

ΔP can then be computed from $\Delta P'$ by the above ratio. Alternatively, the f versus Re curve found with one liquid holds for all other liquids.

For example, the pressure vs. sodium flow rate curve of an SIR fuel-element assembly was obtained as f versus Re much more conveniently with water than with sodium. A full-scale model was used, and (as a precaution, though not apparently required) actual velocity \bar{u} by employing hot water so that $\mu'/\rho' = \mu/\rho$. The necessary water temperatures for sodium at 600 and 900°F are 171.5 and 211°F, respectively. Similarly, flow distribution in the STR core at high Re was studied with a full-scale model and air (instead of hot water). Also, a 1.5 scale model of the PWR thermal shield¹²² was tested with air.*

7.72 Turbulent h . In general, to obtain the correct Nu or St under any conditions, the problem is to obtain in the test the same Re and Pr as in the working unit. However, for nonmetallic fluids in turbulent flow it is experimentally well established (e.g., Table 3, item a) that

$$j_H = St Pr^{3/4} = \phi(Re)$$

Thus only Re need be kept the same [Eq. (118)], in which case

$$\frac{h}{h'} = \left(\frac{c}{c'}\right)^{1/4} \frac{\bar{u}}{\bar{u}'} \frac{\rho}{\rho'} \left(\frac{\mu'}{\mu} \frac{k}{k'}\right)^{3/4} \quad (119)$$

For instance, average or local h may be desired over a fuel element too small for the installation of thermocouples and heating elements; in that case, a model several times larger than the working unit can be tested. A large model may also be used to permit testing at lower than actual working velocity. Most frequently tests at lower temperatures or with more convenient fluids are desired; the product $D'\bar{u}'$ is set at $D\bar{u}\rho\mu'/\rho'\mu$.

With metallic fluids, Table 4 indicates that it is adequate to keep Pe the same for Nu to be the same in the test as in actual operation. Because of the low values of Pr for liquid metals, no other fluids can replace them in similitude tests, however.

* A one-fourth-size model of the PWR core yielded useful flow-distribution data with air,¹²² even though only one-sixty-seventh of the PWR Re was obtained. However, for accurate results the same Re is needed. This is difficult to achieve in a full-scale or smaller model because of the high pressures and/or velocities and powers required. For instance, CO_2 at 1,200 psi has been used (to test the LSR core design). Much denser gases, such as Freon C-318 (C_4F_8 , $M' = 200$), UF_6 ($M' = 352$), or very cold air, might perhaps be employed at atmospheric pressure.

7.73 Streamline h . Table 5 shows that Nu in simple streamline flow is the same if Gz is the same. Since in a scale model L'/D' is the same as L/D ,

$$\frac{c\bar{u}\rho D}{k} = \frac{c'\bar{u}'\rho'D'}{k'} \quad \text{and} \quad \frac{h}{h'} = \frac{D'k}{Dk'} \quad (120)$$

7.74 Conduction and Convection. If conduction is to be simulated as well as turbulent convection, it is necessary for h and k_s/D to be proportional in the test and the working conditions, where k_s is for the solid or every one of several solids. Thus, besides Eq. (118) there is the requirement that $Nu_s = h'D'/k_s = hD/k_s$. As before, Eq. (119) will hold for nonmetals. Eliminating \bar{u}/\bar{u}' and h/h' among the three equations,

$$\frac{k'_s}{k_s} = \left(\frac{\mu'c'k'^2}{\mu ck^2} \right)^{1/4} \quad (121)$$

Thus to simulate conduction and convection in a scale model of an irregular fuel element or assembly it is first necessary to pick the solid, fluid, and test temperature range such that Eq. (121) holds. A convenient procedure is to plot the left-hand side of Eq. (121) against temperature for each solid under consideration and the right-hand side for each fluid. Every solid-fluid intersection yields a feasible pair of materials and test temperature.

When the test temperature and materials have been selected, any D' and \bar{u}' can be used that obey Eq. (118). Actual temperature differences Δt from fluid to solid at any position are obtained from the corresponding $\Delta t'$ by

$$\frac{\Delta t}{\Delta t'} = \frac{qk'_sD'}{q'k_sD} \quad (122)$$

7.75 Forced Plus Free Convection of Nonmetals. In a forced-convection film coefficient, free convection may be significant, as for a fuel element during low flow or pump failure (see Table 10). Setting the $Gr \times Pr$ products equal and solving with Eqs. (118), (119), and (122) gives the requirement for q' :

$$\frac{q'}{q} = \frac{\beta}{\beta'} \left(\frac{\rho}{\rho'} \right)^2 \left(\frac{\mu'}{\mu} \right)^{3/8} \left(\frac{k'}{k} \right)^{1/8} \left(\frac{c}{c'} \right)^{3/8} \quad (123)$$

D' and \bar{u}' must satisfy Eq. (118), and any Δt can be obtained from the corresponding $\Delta t'$ by

$$\frac{\Delta t}{\Delta t'} = \frac{q}{q'} \left(\frac{D'}{D} \right)^3 \left(\frac{c\mu}{c'\mu'} \right)^{1/8} \left(\frac{k}{k'} \right)^{3/8} \quad (124)$$

7.76 Unsteady State. If steady-state conditions are properly simulated for the cooling of a solid as above described, the unsteady state is also simulated if $\theta\alpha_s/D^2$ is the same. The unsteady-state fractional temperature change at θ is thus the same as that in the test at $\theta' = \theta\alpha_s D'^2/\alpha'_s D^2$.

REFERENCES

1. Lane, J. A.: *Proc. Univ. Reactors Conf.*, Oak Ridge Institute for Nuclear Science, 1954.
2. NBS-NACA Tables, National Bureau of Standards, Washington, D.C., 1954; Hilsenrath, J., and Y. S. Touloukian, *Trans. ASME*, **76**: 967-985 (1954).
3. Bromley, L. A.: *Univ. Calif. Radn. Lab. Rept.* UCRL-1852.
4. Lindsay, A. L., and L. A. Bromley: *Ind. Eng. Chem.*, **42**: 1508-1511 (1950).
5. Jakob, M.: "Heat Transfer," vol. 1, John Wiley & Sons, Inc., New York, 1949.
6. Orr, C.: Ph.D. dissertation, Georgia Institute of Technology, 1952.
7. Deissler, R. G., and C. S. Eian: NACA, RME52C05, 1952, and RME53G03, 1953.
8. Hougen, J. O., and E. L. Piret: *Chem. Eng. Progr.*, **47**: 295-304 (1951).

9. Perry, J. H. (ed.): "Chemical Engineers' Handbook," 3d ed., McGraw-Hill Book Company, Inc., New York, 1950.
10. Aladev, I. T.: *Bull. USSR Acad. Sci., Tech. Sci. Div.*, **11**: 1669 (1951).
11. Monrad, C. C., and J. F. Pelton: *Trans. Am. Inst. Chem. Engrs.*, **38**: 593 (1942).
12. Stein, R. P., and W. Begell: *Jour. Am. Inst. Chem. Engrs.*, **4** (March, 1958).
13. Verschoor, H., and S. Stemerding: "General Discussion on Heat Transfer," pp. 201-203, Institute of Mechanical Engineers, London, 1951.
14. Deissler, R. G.: *ASME Paper* 53-S-41, 1953.
15. Dingee, D. A., et al.: *Battelle Memorial Inst. Rept.* 1026, 1955.
16. Miller, P., et al.: *Nuclear Eng. Sci. Congr. Preprint* 25, Cleveland, 1955.
17. Jackson, C. B.: "Liquid Metals Handbook," 3d ed., Government Printing Office, 1955.
18. Lubarsky, B., and S. J. Kaufman: NACA TN 3336, Washington, D.C., 1955.
19. Poppendiek, H., and W. B. Harrison: *Chem. Eng. Progr. Symposium Ser.*, **9**: 93 (1954).
20. U.S. Atomic Energy Commission: "Reactor Handbook," vol. 2, pp. 277-286, by R. D. Brooks and S. K. Freidlander, McGraw-Hill Book Company, Inc., New York, 1955.
21. Sleicher, C. A., Jr., and M. Tribus: *Proc. Heat Transfer of Fluid Mech. Inst.*, 1956, pp. 59-78.
22. Stein, R. P.: *AEC Reactor Heat Transfer Conference*, New York, Nov. 1, 1956.
23. Norris, R. H., and D. D. Streid: *Trans. ASME*, **62**: 525 (1940).
24. Kays, W. M.: *ASME Paper* 54-A-151, 1954.
25. Deissler, R. G.: NACA, TN-2410, 1951.
26. Rickard, C. K., et al.: *AEC Reactor Heat Transfer Conference*, New York, Nov. 1, 1956.
27. MacDonald, W. C., and R. C. Quittenton: *Chem. Eng. Progr. Symposium Ser.*, **9**: 59-67 (1954).
28. Douglas, W. J. M., and S. W. Churchill: *Chem. Eng. Progr. Symposium Ser. Preprint* 16, Louisville Meeting, 1955.
29. McAdams, W. H.: "Heat Transmission," 3d ed., McGraw-Hill Book Company, Inc., New York, 1954.
30. Dwyer, O. E., et al.: *Proc. 1953 Conf. on Nuclear Eng.*, p. F-73, University of California, Berkeley, 1953.
31. McGoff, M. J., and J. W. Mausteller: *MSA Memo Rept.* 87, 1955.
32. Tidball, R. A.: *Chem. Eng. Progr. Symposium Ser.*, **5**, 1953.
33. Norris, R. H., and W. A. Spofford: *Trans. ASME*, **64**: 489-496 (1942).
34. Kays, W. M., et al.: "Gas Turbine Plant Heat Exchangers," American Society of Mechanical Engineers, 1951.
35. Wilke, C. R., and O. A. Hougen: *Trans. Am. Inst. Chem. Engrs.*, **41**: 445-451 (1945).
36. Leva, M.: *Ind. Eng. Chem.*, **39**: 857 (1947).
37. Donohue, D. A.: *Ind. Eng. Chem.*, **41**: 2499-2511 (1949).
38. Eckert, E. R. G.: "Introduction to the Transfer of Heat and Mass," McGraw-Hill Book Company, Inc., New York, 1950.
39. U.S. Atomic Energy Commission: "Reactor Handbook," vol. 2, chap. 1, sec. 3.7, by A. F. Lietzke, T. M. Hallman, and E. M. Sparrow, McGraw-Hill Book Company, Inc., New York, 2d ed., 1958.
40. Kyte, J. R., et al.: *Chem. Eng. Progr.*, **49**: 653 (1953).
41. Moscicki, I., and J. Broder: *Roczniki Chem.*, **6**: 321 (1926).
42. Hyman, S. C., C. F. Bonilla, and S. W. Ehrlich: NYO-564, 1951.
43. Isakoff, L., and F. W. DeVries: M.S. thesis in chemical engineering, Columbia University, New York, 1951.
44. Eckert, E. R. G., and A. J. Diaguila: *Trans. ASME*, **76**: 497-504 (1954).
45. Pigford, R. L.: *Chem. Eng. Progr. Symposium Ser.*, **17**: 79-92 (1955).
46. Sanders, A.: M.S. thesis in chemical engineering, Columbia University, New York, 1954.
47. Misra, B.: Ph.D. thesis in chemical engineering, Columbia University, 1955; *Chem. Eng. Progr. Symposium Ser.*, **18**: 7-21 (1956).
48. Carpenter, F. G., and A. P. Colburn: "General Discussion on Heat Transfer," pp. 20-26, Institution of Mechanical Engineers, London, 1951.
49. Seban, R. A.: *Trans. ASME*, **76**: 299-303 (1954).
50. Rohsenow, W. M., et al.: *ASME Papers* 54-A-144 and 54-A-145, 1954.
51. Untermeyer, S.: *Nucleonics*, **12**(7): 43-47 (July, 1954).
52. Nakagawa, Y., and T. Yoshida: *Chem. Eng. (Japan)*, **16**: 74-82, 104-110 (1952).
53. Paschkis, V., and G. Stolz: Quenching Program, Columbia University, Mechanical Engineering Department, Mar. 1, 1955.
54. Ellion, M. E.: Memo 20-88, Jet Propulsion Laboratory, California Institute of Technology, 1954.

55. Pike, F. R., P. D. Miller, Jr., and K. O. Beatty, Jr.: *Chem. Eng. Progr. Symposium Ser.*, **17**: 13-19 (1955).
56. Bonilla, C. F., and C. W. Perry: *Trans. Am. Inst. Chem. Engrs.*, **37**: 685-705 (1941).
57. Kutateladze, S. S.: *Otdelenie Tekhnicheskikh Nauk*, **4**: 529-536 (1951).
58. Cichelli, M. T., and C. F. Bonilla: *Trans. Am. Inst. Chem. Engrs.*, **41**: 755-787 (1945).
59. Robinson, D. B., and D. L. Katz: *Chem. Eng. Progr.*, **47**: 317-324 (1951).
60. Styuschchin, N. G., and L. S. Sterman: *J. Tech. Phys. (USSR)*, **21**: 448 (1951).
61. Grady, J. J.: M.S. thesis in chemical engineering, Columbia University, New York, 1950.
62. Rohsenow, W. H.: *Trans. ASME*, **74**: 969-975 (1952).
63. Hayworth, H. C., and N. Nicholas: M.S. thesis in chemical engineering, Columbia University, New York, 1951.
64. Pramuk, F. S., and J. W. Westwater: *Chem. Eng. Progr. Symposium Ser.*, **18**: 79-83 (1956).
65. Rohsenow, W., and P. Griffith: *Chem. Eng. Progr. Symposium Ser.*, **18**: 47-49 (1956).
66. Gessler, J. L.: M.S. thesis in chemical engineering, Johns Hopkins University, Baltimore, 1948.
67. Bromley, L. A.: *Chem. Eng. Progr.*, **46**: 221-227 (1950).
68. Bancharo, J. T., et al.: *Chem. Eng. Progr. Symposium Ser.*, **17**: 21 (1955).
69. Lottes, P. A.: *Proc. 1955 Conf. Nuclear Eng.*, p. A-1, University of California, Los Angeles.
70. Bailey, R. V.: at Tulane University.
71. Cook, W. H.: ANL, 1954.
72. Armacost, W. H., et al.: *Trans. ASME*, **76**: 715-748 (1954).
73. Lyon, R. E., et al.: *Chem. Eng. Progr. Symposium Ser.*, **17**: 41-47 (1955).
74. Bonilla, C. F., et al.: NYO-7638, 1956.
75. Piret, E. L., and H. S. Isbin: *Chem. Eng. Progr.*, **50**: 305-311 (1954).
76. Goldmann, K.: *NDA Rept.* 10-68, 1953.
77. Greenfield, M. L., et al.: Report 54-77, Department of Engineering, University of California, Los Angeles, 1954.
78. McAdams, W. H., et al.: *Ind. Eng. Chem.*, **41**: 1945 (1949).
79. Clark, J. A., and W. M. Rohsenow: *Trans. ASME*, **76**: 553 (1954).
80. Jens, W. H., and P. A. Lottes: ANL-4915, 1952.
81. Buchberg, H., et al.: *Proc. Heat Transfer and Fluid Mechanics Inst.*, pp. 177-191, Stanford University, Stanford, Calif., 1951.
82. Gunther, F. C.: *Trans. ASME*, **73**: 115 (1951).
83. Bernath, L.: Du Pont Memo DPW-54-526, 1954; *Chem. Eng. Progr. Symposium Ser.*, **18**: 1-6 (1956).
84. Weatherhead, R. T.: ANL, 1955.
85. Jeffery, R. W.: B.S. thesis in mechanical engineering, Massachusetts Institute of Technology, Cambridge, Mass., 1952.
86. Motte, E. I., and L. A. Bromley: UCRL-2511, 1954.
87. Carter, J. C.: ANL-4766, 1952.
88. Beighley, C. M., and L. E. Dean: *Jet Propulsion*, May-June, 1954, pp. 180-186.
89. Mumm, J. F.: ANL, 1954.
90. Jens, W. H.: *Mech. Eng.*, **76**: 981-986 (1954).
91. Roy, G. M., and C. A. Pursel: General Electric Company, 1954.
92. Armacost, W. H., et al.: *Trans. ASME*, **76**: 715-748 (1954).
93. Nerad, A. J., and A. Howard: unpublished reports, General Electric Company, 1936.
94. Bromley, L. A., et al.: UCRL-1894, 1952.
95. Martin, W., et al.: AECU-2169, 1952.
96. Rosenthal, M. W., and R. L. Miller: ORNL-2294 (1957).
97. LeTourneau, B. W., and R. E. Grimble: *Nuclear Sci. Eng.*, **1**: 359-369 (1956).
98. Bonilla, C. F. (ed.): "Nuclear Engineering," McGraw-Hill Book Company, Inc., New York, 1957.
99. Poppendiek, H. F., and L. D. Palmer: ORNL-1395, 1952; *Chem. Eng. Progr. Symposium Ser.*, No. 11, 1954.
100. Poppendiek, H. F., and L. D. Palmer: ORNL-1701, 1954.
101. Hamilton, D. C., et al.: ORNL-1769, 1954.
102. Carberry, J. J.: *Chem. Eng.*, **60**: 225-227 (June, 1953).
103. Goodman, C., et al.: "The Science and Engineering of Nuclear Power," vol. 2, pp. 120-176, Addison-Wesley Publishing Company, Reading, Mass., 1949.
104. Bonilla, C. F.: *AEC Rept.* M-4476, 1949.
105. Buckley, P. S.: *Chem. Eng.*, **57**: 112-114 (September, 1950).

106. Parkins, W. E.: F55-71, *Proc. 1953 Conf. on Nuclear Eng.*, University of California, Berkeley, 1953.
107. Shimazaki, T. T.: *Chem. Eng. Progr. Symposium Ser.*, **12**: 113-119 (1954).
108. Carslaw, H. S., and J. C. Jaeger: "Conduction of Heat in Solids," Oxford University Press, New York, 1947.
109. Bachmann, H.: "Tafeln über Abkühlungsvorgänge einfacher Körper," Springer-Verlag OHG, Berlin, 1938.
110. Fritz, R. J.: *Trans. ASME*, **76**: 913-921 (1954).
111. Russell, T. F.: First Report, pp. 149-187, Alloy Steels Research Committee, England.
112. Newman, A. B.: *Trans. Am. Inst. Chem. Engrs.*, **30**: 598-612 (1934).
113. Newman, A. B., and L. Green: *Trans. Electrochem. Soc.*, **66**: 345-358 (1934).
114. Beatty, K. O., et al.: *Ind. Eng. Chem.*, **42**: 1527-1532 (1950).
115. Rubin, T.: *AEC Rept. Y-F-10-28*, 1950.
116. Heisler, M. P.: *Trans. ASME*, **78**: 1187-1192 (1956).
117. U.S. Atomic Energy Commission: "Reactor Handbook," vol. 2, Engineering, AEC-D-3646, McGraw-Hill Book Company, Inc., New York, 1955.
118. Dusenberre, G. M.: "Numerical Analysis of Heat Flow," McGraw-Hill Book Company, Inc., New York, 1949.
119. Hellman, S. K., et al.: *Trans. ASME*, **78**: 1155-1161 (1956).
120. Patton, T. C.: *Ind. Eng. Chem.*, **36**: 990 (1944).
121. Liebmann, G.: *Trans. ASME*, **78**: 655-665 (1956).
122. Hazard, H. R., and J. M. Allen: BMI-1141, 1956.
123. Deissler, R. G.: NACA TN-3145, 1954.
124. Sherwood, T. K., and R. L. Pigford: "Absorption and Extraction," McGraw-Hill Book Company, Inc., New York, 1952.
125. Bonilla, C. F.: *Paper 122*, vol. 9, p. 331, UN Conference on Atomic Energy, Geneva, 1955.
126. DeBortoli, R. A., et al.: *Nuclear Sci. Eng.*, **1**: 239-251 (1956).
127. Plewes, A. C., et al.: *Chem. Eng. Progr.*, **50**: 77-80 (1954).

9-4 THERMAL STRESS AND DISTORTION

BY

Robert Daane

Thermal stresses are prevalent in reactors as a result of the nonuniform temperatures associated with the removal of heat generated in both the fissionable materials and other materials in the presence of irradiation. Sudden changes in the heat-generation rate or the coolant temperature or flow rate may give rise to large temperature differences and correspondingly large thermal stresses. In many reactor designs, it is necessary, in consideration of nuclear characteristics, strength, and corrosion resistance, to have a conjunction of various materials with unmatched thermal-expansion coefficients which may lead to large thermal stresses at operating temperature.

In addition to the thermal stresses, which may lead to fractures, the above thermal conditions will usually give rise to distortions of reactor parts. For example, fuel-element distortions may interfere with coolant flow or cause changes in reactivity. Distortions of control rods and other moving parts may interfere with their operation.

NOMENCLATURE AND UNITS

- C = curvature of a bar resulting from uneven heating
- E = modulus of elasticity, psi
- h = surface heat-transfer coefficient (heat-transfer rate per unit surface area per unit temperature difference between the surface and the bulk of the surrounding medium), Btu/(hr)(in.²)(°F)
- k = thermal conductivity, Btu/(hr)(°F)(in.)
- N = number of cycles of repeated thermal strain
- q = heat generation per unit volume, Btu/(hr)(in.³)
- T = temperature at a point, °F
- x, y, z = rectangular coordinates, in.
- α = coefficient of linear thermal expansion, (°F)⁻¹
- ϵ = unit strain
- $\Delta\epsilon_p$ = inelastic strain per half cycle of repeated thermal strain
- ν = Poisson's ratio
- σ = unit normal stress, tension when positive, psi
- a, b, d, t = characteristic dimensions of various thermally stressed objects, in.

1 THERMAL STRESS AND DISTORTION BY ELASTICITY THEORY

The theory of elasticity, based primarily on the assumption that stress is proportional to strain, makes possible the calculation of thermal stresses in many important problems. Although elastic thermal stresses are of very limited significance, they are usually of some interest in view of the intractability, in most cases, of any more realistic analysis.

1.1 Order of Magnitude of Thermal Stress

The largest thermal strain that can occur in an unrestrained part having a fairly regular shape (i.e., without relatively thin sections or protrusions or sharply reentrant boundary surfaces in which stress concentrations may occur) is generally